

**PREDICTION OF MASS TRANSFER COEFFICIENT
UNDER TWO PHASE FLOW CONDITIONS USING
TURBULENT DIFFUSION MODELS**

A Thesis

Submitted to the College of Engineering of

Nahrain University in Partial Fulfillment

of the Requirements for the Degree of

Master of Science

in

Chemical Engineering

by

ISHTAR ZAKI SADIQ

(B. Sc. In Chemical Engineering 2004)

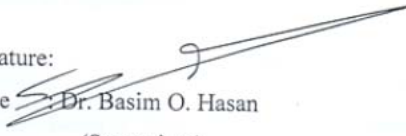
**Thul-Hijjah
January**

**1428
2008**

Certification

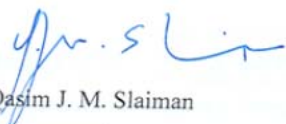
I certify that this thesis entitled "**Prediction of Mass Transfer Coefficient under Two Phase Flow Conditions Using Turbulent Diffusion Models**" was prepared by **Ishtar Zaki Sadiq** under my supervision at Nahrain University/College of Engineering in partial fulfillment of the requirements for the degree of Master of Science in Chemical Engineering.

Signature:

Name :  Dr. Basim O. Hasan
(Supervisor)

Date : 17 / 2 / 2008

Signature:

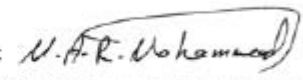
Name :  Prof. Dr. Qasim J. M. Slaiman
(Head of Department)

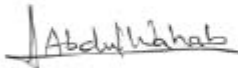
Date : 20 / 4 / 2008

Certificate

We certify, as an examining committee, that we have read this thesis entitled " **Prediction of Mass Transfer Coefficient under Two Phase Flow Conditions Using Turbulent Diffusion Models** " , examined the student **Ishtar Zaki Sadiq** in its content and found it meets the standard of thesis for the degree of master of Science in Chemical Engineering.

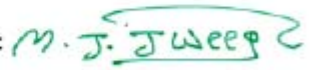
Signature: 
Name: **Dr. Basim O. Hasan**
(Supervisor)
Date: 17 / 2 / 2008

Signature: 
Name: **Ass.Prof.Dr. Muhanned A.R. Mohammed**
(Member)
Date: 16 / 3 / 2008

Signature: 
Name: **Dr. Majid I. Abdulwahab**
(Member)
Date: 11 / 2 / 2008

Signature: 
Name: **Prof. Dr. Abbas H. Sulaymon**
(Chairman)
Date: 17 / 2 / 2008

Approval of the College of Engineering

Signature: 
Name: **Prof. Dr. Muhsin J. Jweeg**
(Acting Dean)
Date: 27 / 5 / 2008

Abstract

A theoretical study has been performed to analyze the mass transfer and shear stress in co-current annular, two phase gas-liquid (air-water), turbulent flow conditions in a horizontal pipe using eddy diffusivity concept. The mass transfer coefficient has been predicted and discussed for a wide range of liquid superficial Reynolds number ($Re_{sL}=2000$ to 40000), gas superficial Reynolds number ($Re_{sg}=10000$ to 80000), liquid Schmidt number ($Sc_L=100$ to 3000), and liquid temperatures (25 °C - 60 °C). For the same ranges, the wall and interfacial shear stresses and friction factors are estimated using experimental and theoretical correlations proposed for two phase flow. The variation of eddy diffusivity is divided into two main regions, one in the liquid phase and the other in the gas phase. A new expression for eddy diffusivity is developed using three resistances in series. Using this expression an equation for calculating the mass transfer coefficient for a wide range of Re , Sc , and void fractions (or liquid layer thickness) is derived. Numerous previously proposed correlations are used to calculate the void fraction from fluids (air and water) velocities and their physical properties.

The influence of liquid Re_{sg} , gas Re_{sg} , liquid Sc , and void fraction on the mass transfer coefficient, shear stresses, and friction factors is studied and discussed. In addition, the theoretical analysis included the estimation of shear stress and friction factor for stratified flow. The analytical results are verified by comparison with the empirical mass transfer correlations obtained from diffusion controlled corrosion studies under two phase flow conditions by other workers. The results showed that the eddy diffusivity is an efficient way to predict the mass transfer coefficient under annular two phase flow conditions. Also increasing Re_{sL} and Re_{sg} leads to increase of mass transfer coefficient but the influence of Re_{sL} is higher than that of Re_{sg} . The liquid Sc has a major effect on mass transfer coefficient while gas Sc has a minor effect.

The Re_{sL} , Re_{sg} , and temperature affect the wall and interfacial shear stress and friction factor. Applying statistical analysis to the results, a correlation is obtained to predict mass transfer coefficient for the investigated range of Re and Sc .

List of Contents

Contents	Page
Abstract	I
List of Contents	III
Nomenclature	VI
List of Tables	VIII
List of Figures	VIII
Chapter One: Introduction	1
Chapter Two: Turbulent Diffusion and Eddy Diffusivity	
2.1 Introduction	4
2.2 Turbulence and Eddy Diffusion	6
2.2.1 Prandtl – Mixing Length Theory	8
2.2.2 Laminar Sub-Layer	10
2.2.3 Reynolds Stresses	12
2.2.4 Eddy Diffusivity Theory	14
2.3 Friction Factor	16
2.4 Eddy Diffusivity Models	18
2.5 Review of Mass Transfer Models Concerning Single Phase	21
Chapter Three: Two Phase Flow and Turbulent Diffusion	26
3.1 Introduction	27
3.2 Analysis for Two-Phase Flow	31
3.3 Holdup in Horizontal Two-Phase Gas-liquid Flow	38
3.4 Flow Pattern Mapping	38
3.4.1 Bubble to slug pattern	39
3.4.2 Slug to annular pattern	41
3.5 Two Phase Flow Mass Transfer Models	44
3.6 Mass Transfer Coefficient Correlation in Two Phase Flow	
Chapter Four: Theoretical Analysis	

4.1 Single Phase	48
4.1.1 Lin et. al. Model	48
4.1.2 Johansen Model	49
4.1.3 Rosen and Tragardh Model	49
4.1.4 Slaiman et. al. Model	49
4.2 Two Phase Flow	50
4.2.1 Void Fraction	50
4.2.1.1 Zivi Model	50
4.2.1.2 Chisholm Model	51
4.2.1.3 Hart et. al. Model	51
4.2.1.4 Chen and Spedding	51
4.2.2 Friction Factor	52
4.2.3 Definition of Superficial Velocities	53
4.2.4.1 Stratified Flow	53
4.2.4.2 Annular Flow	55
4.2.5 Mass Transfer Coefficient in Annular Flow	56
4.2.6 Concentration Profile in Liquid Layer	62
4.2.7 Mass Transfer Coefficient from Eddy Diffusivity in Two Phase	64
4.2.7.1 Wang and Nesic Model	64
4.2.7.2 Sato et al-Welle	64
4.2.7.3 Sato et al	65
Chapter Five: Results and Discussion	
5.1 Single Phase	67
5.2 Results of Two Phase	72
5.2.1 Void Fraction for Annular Flow	72
5.2.1.1 Effect of Re	72
5.2.1.2 Effect of Liquid Temperature	75

	77
5.2.2 Friction Factors	77
5.2.2.1 Effect of Liquid and Gas Reynolds Numbers	79
5.2.2.2 Effect of Temperature	79
5.2.3 Shear Stress	79
5.2.3.1 Effect of Liquid and Gas Reynolds Numbers	81
5.2.3.2 Effect of Temperature	83
5.2.4 Mass Transfer Coefficient	83
5.2.4.1 Comparison of Present Results with the Experimental Correlations	86
5.2.4.2 Effect of Liquid Superficial Re	88
5.2.4.3 Effect of Gas Superficial Re	89
5.2.4.4 Effect of Liquid Schmidt Number and Temperature	89
5.2.4.5 Effect of Void Fraction	93
5.2.5 Mass Transfer Coefficient from Eddy Diffusivity in Two Phase	94
5. 2. 6 Concentration Profile	94
5. 2. 6. 1 Effect of Liquid Superficial Re	95
5. 2.6. 2 Effect of Gas Superficial Re	97
5. 2.6.3 Effect of Liquid Schmidt Number	
Chapter Six: Conclusions and Recommendations	99
6.1 Conclusions	100
6.2 Recommendations	101
References	
Appendices	A-1
Appendix A	B-1
Appendix B	C-1
Appendix C	D-1
Appendix D	

Nomenclature

A	Area, m ²
C	Concentration, mol/m ³
C*	Dimensionless concentration
C _{A,s}	Concentration of species A at the surface
C _{A,b}	Concentration of species A at the bulk
D _{AB}	Molecular diffusivity, m ² /s
d	Pipe diameter, m
\overline{D}	Hydraulic diameter, m
d _B	Bubble size, m
d _{hL}	Hydraulic diameter of liquid, m
dp/dL	Pressure gradient, N/m ³
e	Roughness
f	Friction factor
f _{TP}	Two phase fraction factor
h _L	Height of liquid layer, m
K	Mass transfer coefficient
L	Prandtl mixing length
N _A	Molar flux of component A, mol/m ² .s
ΔP	Pressure drop, N/m ²
Pr	Prandtl number
P ₀	Initial pressure, N/m ²
p _L	Pressure of liquid, N/m ²
Q	Volumetric flow rate, m ³ /s
R	Pipe radius, m
R ⁺	Dimensionless radius
Re	Reynolds number, ρdu/μ
Re _{TP}	Reynolds number for two phase
Re _{sg}	Reynolds number based on gas superficial velocity
Re _{sL}	Reynolds number based on liquid superficial velocity
r _w	Radius at the wall, m
R _t	Total resistance
S	Length in cross section, m
Sc _t	Turbulent Schmidt Number
Sc	Schmidt number
Sh	Sherwood number
T	Temperature, °C
t	Time, s
u	Velocity, m/s
u'	Fluctuating velocity in axial direction
u	Local velocity
u ⁺	Dimensionless velocity

u^*	Friction velocity, m/s
u_B	Bubble velocity, m/s
u_δ	Velocity at the outer edge of a laminar sublayer, m/s
\overline{u}_x	Time-smoothed velocity, m/s
u_z	Velocity in direction Z, m/s
v'	Fluctuating velocity in radial direction
v_g	Gas volume, m ³
v_L	liquid volume, m ³
x	Dryness fraction
y	Distance from the wall, m
y^+	Dimensionless distance from the wall
Z	Ratio y/R

Greek Letters

ϵ_m	Eddy viscosity, kg/m.s
α	Void fraction
δ	Diffusion layer thickness, m
δ_b	Thickness of a laminar sublayer, m
δ_d	Thickness of diffusion sublayer, m
δ_f	Thickness of buffer layer, m
ϵ_d	Mass eddy diffusivity, m ² /s
ϵ_h	Thermal eddy diffusivity at interface, m ² /s
ϵ_m	Momentum eddy diffusivity, m ² /s
ϵ_{mi}, ϵ	Momentum eddy diffusivity at interface, m ² /s
μ	Kinetic viscosity, kg/m. s
μ_L	Kinetic viscosity of liquid, kg/m. s
μ_G	Kinetic viscosity of gas, kg/m. s
ν	Kinematic viscosity, m ² /s
ρ	Density, kg/m ³
ρ_m	mixture density, kg/m ³
τ	Shear stress, N/m ²
τ_i	Interfacial shear stress
τ_w	Wall shear stress, N/m ²

Subscripts

b	Bulk
g	Gas
i	Interface
L	Liquid
TP	Two phase
w	Wall

List of Tables

Table	Title	page
2.1	Commen Selected Eddy Diffusivity Models	21

List of Figures

Figures	Title	Page
2.1	Fluid Movement as Thin Layer	5
2.2	Different Types of Velocity [Ibrahim,1984]	8
2.3	A Schematic Diagram of Ideal Stratified Flow	32
	A Schematic Diagram of Annular Flow	32
3.1	A Typical Flow Regime Map For Gas/Liquid Two –Phase Flow	41
3.2	in Horizontal Pipes Reproduced with Premission of The	
3.3	International Society of Shore and Polar Engineers [Wang et al, 2004]	
4.1	Interfacial Area in Stratified Flow	53
4.2	Liquid and Gas Areas in Stratified Flow	53
4.3	Gas-Liquid Annular Flow	55
4.4	Diffused Species Concentration Variation From Gas Bulk to	56
	The Wall	
5.1	Variation of Eddy Diffusivity with y^+ from Various Authors	67
5.2	Comparison of Sh obtained from Various Eddy Diffusivity Models for Sc=100	68

5.3	Comparison of Sh obtained from Various Eddy Diffusivity Model for Sc=500	69
5.4	Comparison of Sh obtained from Various Eddy Diffusivity Model for Sc=3000	70
5.5	Comparison between Single Phase Sh and Two phase Sh	71
5.6	Comparison between Single Phase Sh and Two phase Sh	71
5.7	Comparison between Single Phase Sh and Two phase Sh	72
5.8	Variation of Void Fraction with Re_{sL} at $Re_{sg} = 80000$ and $T=25$ °C as Obtained from Various Authors	73
5.9	Variation of Void Fraction with Re_{sL} at $Re_{sg} = 20000$ and $T=25$ °C as Obtained from Various Authors	73
5.10	Variation of Void Fraction with Re_{sL} at $Re_{sg} = 40000$ and $T=40$ °C as Obtained from Various Authors	74
5.11	Variation of Void Fraction with Re_{sL} at $Re_{sg} = 80000$ and $T=40$ °C as Obtained from Various Authors	74
5.12	Variation of Void Fraction with Re_{sL} at $Re_{sg} = 20000$ and $T=40$ °C as Obtained from Various Authors	75
5.13	Variation of Void Fraction with Re_{sL} at $Re_{sg} = 80000$ and $T=60$ °C as Obtained from Various Authors	76
5.14	Variation of Void Fraction with Re_{sg} at $Re_{sL} = 20000$ and $T=25$ °C as Obtained From Various	76
5.15	Variation of Void Fraction with Re_{sL} for $Re_{sg} = 80000$	76
5.16	at Various Temperature	
5.17	Effect of Re_{sL} on the Friction Factor at the Wall	77
5.18	Effect of Re_{sL} on the Interfacial Friction Factor at Different Re_{sg}	78
	Effect of Re_{sL} on the Interfacial Friction Factor at Different Temperatures	79

5.19	Variation of τ_{wL} with Re_{sL} at various Re_{sg} and $T=25$ C	80
5.20	Variation of τ_i with Re_{sL} at various Re_{sg} and $T=25$ C	81
5.21	Variation of τ_i with Re_{sL} at Different Temperatures	82
5.22	Shows the Variation of τ_{wL} with Re_{sL} at Different Temperatures	82
5.23	Comparison of Sh of Present Analysis with Proposed Experimental Correlations at $Sc_L=490$	83
5.24	Comparison of Sh of Present Analysis with Proposed Experimental Correlations at $Sc_L=216$	84
5.25	Comparison of Sh of Present Analysis with Proposed Experimental Correlations at $Sc_L=98$	84
5.26	Comparison of Sh of Present Analysis with Proposed Experimental Correlations at $Sc_L=490$.	
5.27	Comparison of Sh of Present Analysis with Proposed Experimental Correlations at $Sc_L=490$.	85
5.28	Variation of Sh with Re_{sL} at Various Re_{sg} for $Sc_L=490$	85
5.29	Variation of Sh with Re_{sL} at Various Re_{sg} for $Sc_L=216$	
5.30	Variation of Sh with Re_{sL} at Various Re_{sg} for $Sc_L=98$	86
5.31	Variation of Sh with Re_{sg} as Compared with Langsholt et al	87
5.32	Variation of Sh with Sc_L at Various Values of Re_{sL}	87
5.33	Variation of f_{wL} with Reg at Various α	88
5.34	Variation of f_{wB} with Reg at Various α	89
5.35	Variation of Sh with Re_{sL} at Various α Values	90
5.36	Variation of Sh with Re_{sL} at Various α Values	90
5.37	Comparison of Sh Obtained from Eddy Diffusivity Models Proposed by Various Authors	91
5.38	Comparison of Sh Obtained from Eddy Diffusivity Models Proposed by Various Authors	92
		93
		94

5.39	Concentration Profile in the Liquid Layer and The Effect of Re_{sL}	96
5.40	Concentration Profile in the Liquid Layer and The Effect of Re_{sL}	96
5.41	Concentration Profile in the Liquid Layer and the Effect of Re_{sg}	97
5.42	Effect of Sc_L on the Concentration Profile in the Liquid Layer	98

Chapter One

Introduction

In oil and gas industry, various flow regimes in two-phase flow pipeline are encountered depending upon pipeline diameter, the composition of phases, and their velocities [Wang 2005]. Because of the complex nature of two phase flow, the problem was first approached by through empirical models. The trend has shifted to the modeling approach. The fundamental postulate of the modeling approach is the existence of flow patterns or flow configuration [Ansari et al 1994].

Eddy diffusion plays important role in the momentum and mass transfer from one phase to another or between phase and pipe wall. Practically all engineering processes involving fluid depend on the interaction of a fluid with a phase boundary. Fluid friction over extended surfaces, heat and mass transfer to fluids in evaporation, distillation and gas absorption are some of the processes involving the transport of momentum, heat, and mass from a phase boundary to a fluid in turbulent flow. Also in many industrial processes mass, heat, and momentum transfer occurs from one phase to another. In two phase mass transfer the solute may diffuse through a gas phase and then diffuse through and be absorbed in an adjacent and immiscible liquid phase [Welty et. al. 2001]. The understanding of turbulent transport mechanism and the subsequent ability to predict the relevant transport rates are essential to the development of rational design procedures for various processes [Slaiman et.al, 2007].

In mass transfer the two phases are usually in direct contact and the interfacial area is not well defined. In mass transfer there will exist a concentration gradient in each phase causing diffusion to occur [Geancoplis 1984]. Despite many years of intensive research in turbulent diffusion it is

still poorly understood and can only be rather crudely predicted in many cases [Robert and Webster, 2003]. Because of highly complex turbulent flow mechanism, the prediction of the transport rates necessarily involves the formulation of conceptual models which embody many simplifying assumptions. Various models proposed in literature constitute the framework predictive theory and may be broadly divided into three general classes [Gulfinger 1975], a) models based on film theory , b) models based on eddy or turbulent diffusivity, and c) models based on the surface renewal concept [Danckwerts, 1951] .

The development of the theory of transfer of mass between a solid surface and a turbulent fluid has been handicapped by the lack of data on the manner in which the eddy diffusivities vary with distance from the surface. Data on eddy diffusivity very close to the surface are particularly important in order to understand the mechanism of transfer at high Prandtl and Schmidt numbers [Slaiman et al 2007].

The eddy diffusivity for mass may be obtained from concentration profiles and measured mass fluxes. Data very near the wall are difficult to obtain by either of these procedures, since the pitot tubes and thermocouples employed affect the nature of the flow being studied [Sherwood et. al. 1968]. Interferometric techniques have been used giving values of eddy diffusivity at y^+ as low as 0.5 – 1. The various empirical constants introduced in the formulation of the turbulence models must be evaluated through comparison with experimental data [Gutfinger 1975, Gurniki et.al. 2000]. The eddy diffusivity behavior in the viscous sub-layer, damped turbulence layer, and turbulent core affect greatly the rate of mass transport between the wall and bulk. Over the years there were many models proposed for eddy diffusivity. Most of these models need to be examined against the experimental or theoretical results.

Many of the two phase flow transportation processes found in industrial applications occur in the annular flow regimes. Annular two – phase flow is one of the most important flow regimes and is characterized by a phase interface separating a thin liquid film from the gas flow in the core region. Two – phase annular flow occurs widely in film heating and cooling processes, particularly in power generation and especially in nuclear power reactors. The configuration or flow pattern taken up by mixing gas and liquid streams depends up on the flow rates of the two phases, on the physical properties, and on pipe geometry. Annular flow is one of the most important flow patterns, because it occurs frequently in industrial equipment. Despite its apparent simplicity with respect to other flow regimes, the annular configuration is very complicated in detail, which is reflected in great uncertainties in the prediction of the performances of annular two-phase systems [Wongwises and Naphon, 2000].

In present study it is aimed to predict the mass transfer coefficient between solid wall and two phase fluid (gas –liquid) flowing turbulently in annular flow using eddy diffusivity concept for wide range of liquid superficial Reynolds number (Re_{sL}), gas superficial Reynolds number (Re_{sg}), liquid Schmidt number (Sc), and void fraction (or liquid holdup). Also it is aimed to investigate the effect of liquid and gas Re , void fraction (or liquid holdup), and liquid Schmidt number (Sc_L) on the two phase mass transfer coefficient.

Chapter Two

Turbulent Diffusion and Eddy Diffusivity

2.1 Introduction

The understanding of turbulent transport mechanism and the subsequent ability to predict the relevant transport rates are essential to the development of rational design procedures for various processes. Despite many years of intensive research in turbulent diffusion, it is still poorly understood and can only be rather crudely predicted in many cases [Robert and Webster, 2003]. Because of highly complex turbulent flow mechanism, the prediction of the transport rates necessarily involves the formulation of conceptual models which embody many simplifying assumptions [Gutfinger, 1975]. A quantitative knowledge of turbulence is necessary for the study of turbulent mass transfer. Attempts have been made, since the time of Reynold's classical experiment on flow visualization, and the consequent classification of laminar and turbulent regime of flow behavior, to quantitatively describe the turbulence. The chaotic nature of fluid motion during turbulent flow has made the exact quantitative description of it difficult. This chaotic behavior arises out of irregular momentum exchange [Lin et. al. 1951].

The flow of a fluid in a tube can be conceived as a unit composed of several parallel layers of fluid, Fig. (2.1) , each layer will be traveling with different velocity. A lump of fluid in a slow moving layer will be dragged by an adjacent fast moving lump in the nearby layer, or the slow moving fluid will hinder the movement of the fast moving fluid. In this process the bigger eddy becomes smaller and smaller, breaking into two or more smaller eddies. This creates a chaotic momentum exchange, which in turn gives rise to resistance to flow. The net result is

the creation of a disturbed situation which is called turbulence [Lin et.al. 1951].

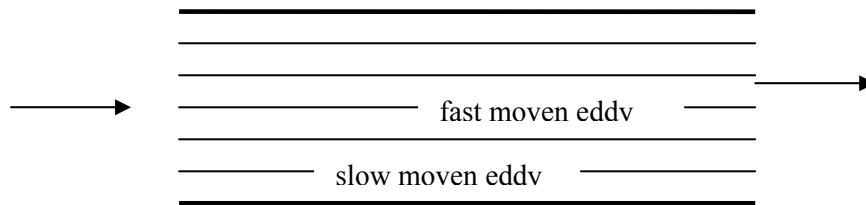


Fig. 2.1. Fluid Movement as Thin Layer

Because of the very nature of this irregular creation, one finds it difficult to give a quantitative and measurable explanation to this phenomena. Interphase transfer of material is a process of considerable engineering importance, as illustrated by the unit operations of drying, gas absorption, and humidification. In some cases of mass transfer between a solid or liquid and a fluid moving in turbulent motion much of the resistance to diffusion is encountered in a region very near the boundary between phases. According to the simple film concept the entire resistance to inter phase transfer of material is represented by a stagnant fluid film at the inter-face, through which the diffusing substance must pass the slow process of molecular diffusion [Sherwood and Woertz, 1939].

It is generally recognized that the concept of a single stagnant film constituting the entire resistance is an over-simplification of the situation and that much of the resistance may be in the eddy zone or "core" of turbulent stream. Any analytical treatment of the whole process may be subject to serious error if it does not allow for the resistance to eddy diffusion which is a process fundamentally different in character from molecular diffusion [Sherwood and Woertz ,1939].

Sherwood and Woertz [1939] reported a study of eddy diffusion of carbon dioxide and hydrogen in a turbulent air stream. The results showed that the rate of eddy diffusion is proportional to the concentration gradient, and that the proportionality constant, or "eddy diffusivity", is independent of the nature of the diffusing gas. The study was made in the central third of a large round duct, and shed no light on the nature of eddy diffusion in the vicinity of the wall.

2.2 Turbulence and Eddy Diffusion

Turbulent diffusion is a complex process and despite many years of research it is still poorly understood and can only be predicted in many cases [Philip et.al. 2002]. In a majority of practical applications the flow in the main stream is turbulent rather than laminar. Although many investigators contributed considerably to the understanding of turbulent flow, so far no one has succeeded in predicting convective transfer coefficient or friction factors by direct analysis. This is not too surprising because the flow of any point is subject to irregular fluctuations in direction and velocity. The science of fluid mechanics has been developed very materially in recent years. The nature of turbulence has received special attention and many of the concepts and theories proposed bear directly or indirectly on the question of mass transfer in a turbulent fluid [Sherwood and Woertz, 1939].

Turbulent motion is characterized by the random motion of the particles constituting the fluid stream. Individual particles move irregularly in all directions with respect to mean flow, and it is convenient to think of a fluid in turbulent flow as having a mean velocity u in a direction x , with a superimposed random motion resulting in instantaneous deviations from u at any point. The irregular motion of the turbulent stream results in swirls or eddies, which are small masses of

fluid moving temporarily as units . An eddy has a short life, soon breaking up in to fragments which then form new eddies. Mixing and diffusion within an eddy may be quite slow, but material may diffuse rapidly by the process of eddy transfer and disintegration.

Turbulence is difficult to define exactly, nevertheless, there are several important characteristics that all turbulence flow posses. These characteristics include unpredictability, rapid diffusivity, high levels of fluctuating vorticity, and dissipation of kinetic energy. The velocity fluctuations act to efficiently transport momentum, mass and heat. This turbulent transport is significantly more effective than molecular diffusion. At any instant eddies are present in the flow and these eddies range in size from the largest scales of the flow down to small scales where molecular diffusion dominates.

A particle of the fluid undergoes a series of random movements, superimposed on the main flow. These eddy movements bring about mixing throughout the turbulent core. This process is often referred to as "eddy diffusivity". The value of the eddy mass diffusivity will be very much larger than the molecular diffusivity in the turbulent core. In an effort to characterize this type of motion, Prandtl proposed mixing length velocity fluctuation hypothesis, that any velocity fluctuation u'_x is due to the y-directional motion of an eddy through a distance equals to the mixing length, L.

The Prandtl mixing length theory finds wide application in turbulent transfer processes where only the temporal mean of the flow quantities are known . In an attempt to understand quantitatively this turbulence phenomena , different types of velocities are now considered which would occur when a fluid flows through a circular tube or any other geometry [Ibrahim 1984].When velocity in one direction (u_x) is plotted

against time (t) , on gets Fig . (2.2) , which shows the time – smoothed velocity , (\bar{u}_x) . This time – smoothed velocity is comprised of a fluctuating velocity (u'_x) and an instantaneous velocity (u_x) [Ibrahim, 1984] , i.e. ,

$$u_x = \bar{u}_x + u'_x \quad (2-1)$$

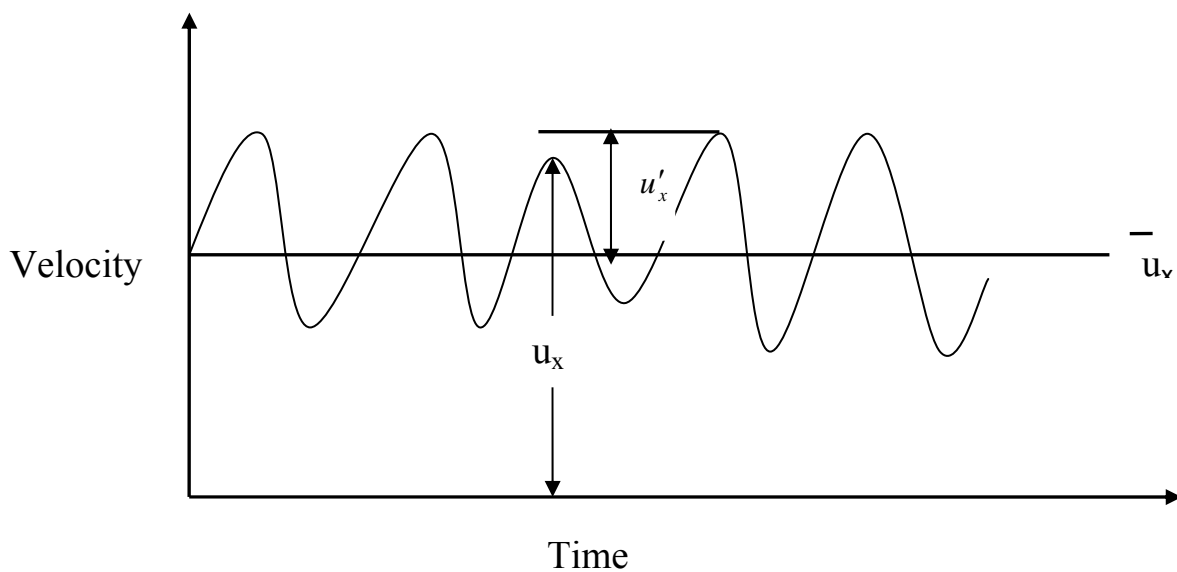


Fig.2.2- Different Types Of Velocity [Ibrahim, 1984]

2.2.1 Prandtl – Mixing Length Theory

Prandtl conceived the velocity fluctuation as being due to the y – directional movement of an eddy , a lump of fluid , transverse to the direction of flow , through a distance (L) [Ibrahim, 1984] .

To explain this distance (L), consider a portion of the momentum boundary layer as show in Fig. (2.3). The distance (L) , as conceived by Prandtl, is the mixing length, which he described physically as a distance travelled by an eddy, transverse to the direction of flow . When this eddy

reaches its destination, it loses its identity and mingles with the bulk fluid. In undergoing this transformation the lump of fluid retains its mean velocity from its point of origin. Upon reaching its destination, i.e., a distance of (L) from the point of origin. This lump of fluid will differ in mean velocity from that of an adjacent fluid by an amount equivalent to the fluctuating velocity [Welty et. al. 2001].

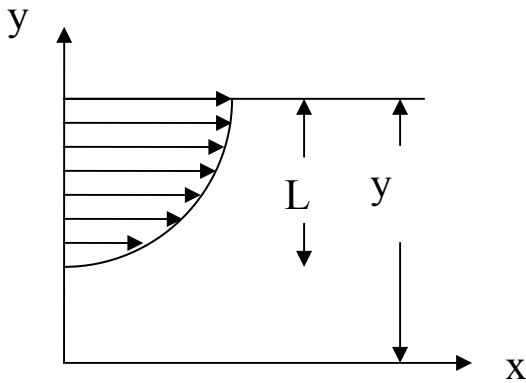


Fig.2-3–Momentum Boundary Layer And Mixing Length [Ibrahim, 1984].

Where

$$\overline{u_x}ly + L - \overline{u_x}ly = u_x' \quad (2-2)$$

Since the mixing length itself is small, one can write

$$\overline{u_x}ly + L - \overline{u_x}ly = L \frac{d\overline{u_x}}{dy} \quad (2-3)$$

From which it can be deduced that

$$u_x' = \pm L \frac{d\overline{u_x}}{dy} \quad (2-4)$$

Hence

$$u_x' = \overline{u_x}ly + L - \overline{u_x}ly = \pm L \frac{d\overline{u_x}}{dy} \quad (2-5)$$

Thus, the fluctuating velocity can be expressed in terms of mixing length

2.2.2 Laminar Sub-Layer

The viscous (laminar) sub-layer is the region which is of most importance in heat and mass transfer calculations since it constitutes the major part of the resistance to transfer [Gufinger, 1975]. In the laminar sub-layer, turbulence has died out and momentum transfer is attributable solely to viscous shear. Because the layer is thin, the velocity gradient is approximately linear and equal to u_δ / δ_b where u_δ is the velocity at the outer edge of a laminar sub-layer of thickness δ_b . Hence

$$\tau_w = \mu \frac{u_\delta}{\delta_b} \quad (2-6)$$

then, $(u^*)^2 = \frac{\tau_w}{\rho} = \frac{\mu u}{\rho y}$ (2-7)

hence, $\frac{u_x}{u^*} = \frac{y u^* \rho}{\mu}$ (2-8)

or $u^+ = y^+$ (2-9)

This relation holds reasonably well for values of y^+ up to about 5 and it applies to both rough and smooth surfaces [Coulson and Richardson 1998].

The thickness of laminar sub-layer can be estimated from the universal velocity profile, since the laminar sub-layer extends from $y^+ = 0$ to $y^+ = 5$. From the definition of y^+

$$\frac{u^* y \rho}{\mu} = y^+ \quad (2-10)$$

thus $y = y^+ \frac{\mu}{u^* \rho}$ (2-11)

since,
$$\frac{u}{u^*} = \sqrt{\frac{2}{f}} \quad (2-12)$$

and at the outer edge $y = \delta_b$, hence

$$\frac{\delta_b}{d} = \frac{5}{\text{Re}} \sqrt{\frac{2}{f}} \quad (2-13)$$

Since the buffer layer extends to $y^+ = 30$, therefore the thickness of buffer layer (δ_f) is [Coulson and Richardson 1998, Hinze 1975],

$$\frac{\delta_f}{d} = \frac{30}{\text{Re}} \sqrt{\frac{2}{f}} \quad (2-14)$$

The velocity of the fluid at the edge of the laminar sub-layer can be calculated from Eq.(2.16) at $u^+ = 5$ [Knudsen and Katz,1958], i.e.,

$$u^+ = \frac{u_\delta}{u^*} = 5 \quad (2-15)$$

hence,
$$u_\delta = 5u^* = 5u \sqrt{\frac{f}{2}} \quad (2-16)$$

According to Eqs. (2.13) and (2.16) the increase in surface roughness or friction factor decreases the thickness of viscous sub-layer and increases the velocity at its outer edge. The results indicated that for turbulent flow in tubes δ_b is less than 1 percent of the tube diameter at Reynolds number of 10,000 and decreases rapidly as the Reynolds number increases. The actual thickness of the viscous sub-layer is very small except for very large pipes and low Reynolds numbers, and it is extremely difficult to measure a detailed velocity profile in this small distance. It is reasonable to expect that the thickness of the viscous sub-layer would in some instances be nearly zero ($y^+ < 1$) or relatively larger (y^+ up to 10). The instantaneous thickness is probably a function of time in the same way that turbulent velocity fluctuations are a function of time. From this point

of view, the viscous sub-layer is not an entity apart from the turbulent core but exists in conjunction within it, and a continuous transition from one to other occurs [Knudsen and Katz, 1958].

2.2.3 Reynolds Stresses

Any particle of the fluid undergoes a series of random movements, superimposed on the main flow. These eddy movements bring about mixing throughout the turbulent core. This process is often referred to as "eddy diffusion". The value of the eddy mass diffusivity will be very much larger than the molecular diffusivity in the turbulent core. In an effort to characterize this type of motion, Prandtl proposed mixing length hypothesis, that any velocity fluctuation u'_x is due to the y-directional motion of an eddy through a distance equals to the mixing length, L. Referring to Fig. (2.3) the fluid eddy possessing a mean velocity \bar{u}'_y is displaced into a stream where adjacent fluid has mean velocity, \bar{u}'_{y+L} . The velocity fluctuation is related to the mean velocity gradient by

$$u'_x = \bar{u}_x|_{y+L} - \bar{u}_x|_y = \mp L \frac{du}{dy} \quad (2-5)$$

The total shear stress in a fluid was defined by the expression

$$\tau = \mu \frac{d\bar{u}_x}{dy} - \rho \overline{u'_x u'_y} \quad (2-17)$$

The substitution of Eq. (2.5) into Eq. (2.17) gives

$$\tau = \rho(v + Lu'_y) \frac{d\bar{u}_x}{dy} \quad (2-18)$$

or,

$$\tau = \rho(\nu + \varepsilon_M) \frac{d\bar{u}_x}{dy} \quad (2-19)$$

where $\varepsilon_M = Lu'$ is designated the eddy momentum diffusivity. It is analogous to the molecular momentum diffusivity ν [Gutfinger 1975, Brodkey and Hershey 1989].

Similar analysis can be made for mass transfer in turbulent flow since this transport mechanism is also due to the presence of the fluctuation or eddies. The instantaneous rate of transfer of component A in the y-direction is

$$N_{A,y} = C'_A u'_y \quad (2-20)$$

where $C_A = \bar{C}_A + C'_A$, the temporal average plus the instantaneous fluctuation in the concentration of component A. Again the concept of mixing length can be used to define the concentration fluctuation by the following relation:

$$C'_A = \bar{C}_A|_{y+L} - \bar{C}_A|_y = L \frac{d\bar{C}_A}{dy} \quad (2-21)$$

Inserting Eq. (2.21) into Eq. (2.20), an expression of turbulent mass transfer by eddy transport is obtained. The total mass transfer normal to the direction of flow is:

$$N_{A,y} = -D_{AB} \frac{d\bar{C}_A}{dy} - \overline{u'_y L} \frac{d\bar{C}_A}{dy} \quad (2-22)$$

or,

$$N_{A,y} = -(D_{AB} + \varepsilon_D) \frac{d\bar{C}_A}{dy} \quad (2-23)$$

where $\varepsilon_D = \overline{Lu'_y}$ is designated as the eddy mass diffusivity.

2.2.4 Eddy Diffusivity Theory

The concentration profile can be obtained from eddy diffusivity expression . The mass flux from the wall can be presented as

$$N_A = -(D + \varepsilon_D) \frac{dC_A}{dy} \quad (2-23)$$

By including the kinematic viscosity and defining for Schmidt number , the above equation becomes :

$$N_A = -u^* \left(\frac{1}{Sc} + \frac{\varepsilon_D}{\nu} \right) \frac{dC_A}{dy^+} \quad (2-24)$$

$$N_A = K(C_b - C_w) = u^* \left(\frac{1}{Sc} + \frac{\varepsilon_D}{\nu} \right) \frac{dC_A}{dy^+} \quad (2-25)$$

Equation (2.25) can be intergrated from the wall ($y^+=0$ and $C=C_w$) to the center of turbulent core ($y^+=R^+$ and $C=C_b$) . The following equation is obtained:

$$K(C_b - C_w) \int_0^{R^+} \frac{dy^+}{\left(\frac{1}{Sc} + \frac{\varepsilon_D}{\nu} \right)} = u^* \int_{C_w}^{C_b} dC_A \quad (2.26)$$

Eq. (2.26) becomes:

$$K \int_0^{R^+} \frac{dy^+}{\left(\frac{1}{Sc} + \frac{\varepsilon_D}{\nu} \right)} = u^* \quad (2.27)$$

$$\frac{K}{u^*} = \frac{1}{\int_0^{R^+} \frac{dy^+}{\left(\frac{1}{Sc} + \frac{\varepsilon_D}{\nu} \right)}} \quad (2-28)$$

$$Sh = \frac{Kd}{D} \quad (2.29)$$

By substituting Eq. (2.29) in to Eq. (2-28):

$$\frac{sh.D}{d.u^*} = \frac{1}{\int_0^{R^+} \frac{dy^+}{\left(\frac{1}{Sc} + \frac{\epsilon D}{\nu}\right)}} \quad (2-30)$$

Since $Sc = \frac{\nu}{D}$, hence

$$u^* = \bar{u} \sqrt{\frac{f}{2}} \quad (2-12)$$

$$\frac{Sh.D}{d.u.\sqrt{f/2}} = \frac{1}{\int_0^{R^+} \frac{dy^+}{\left(\frac{1}{Sc} + \frac{\epsilon D}{\nu}\right)}} \quad (2-31)$$

Hence the Sh in single phase flow is obtained from Eq (2.29) by substituting the expression of eddy diffusivity for each value of Re and Sc

$$Re = \frac{\rho du}{\mu} = \frac{du}{\nu} \quad (2-32)$$

Rearranging in terms of Sh , the following expression is generated:

$$\frac{Sh.D}{d.Re.\nu\sqrt{f/2}} = \frac{1}{\int_0^{R^+} \frac{dy^+}{\left(\frac{1}{Sc} + \frac{\epsilon D}{\nu}\right)}} \quad (2-33)$$

or

$$Sh = \frac{\sqrt{f/2} Re Sc}{\int_0^{R^+} \frac{dy^+}{\frac{1}{Sc} + \frac{\epsilon}{\nu}}} \quad (2-34)$$

2.3 Friction Factor

The Fanning friction factor is the relation between the wall shear stress and kinetic energy of flow and is defined as

$$f = \frac{\tau_w}{\frac{1}{2}\rho u^2} \quad (2-35)$$

Friction factor can be expressed in terms of the pressure drop in pipe (which is easily measured) by recalling that in fully developed flow, there is a static force balance between the accelerating pressure difference and relating forces at the the wall. Appyling force balance over a length of pipe, L , which has a radius R , then,

$$(P_o - P_L)\pi R_o^2 = \tau_w 2\pi R_o L \quad (2-36)$$

Solving for τ_w in Eq. (2.36) and substituting into Eq. (2.35) to obtain

$$f = \frac{d\Delta P}{2\rho u^2 L} \quad (2-37)$$

Eq.(2.37) only applies to a straight, cylindrical pipe or to regular shape (i.e, constant cross section area) but non circular ducts [Thomson, 2000].

Nikuradse [1932] from experimental data obtained the following equation

$$\frac{1}{\sqrt{f}} = 4 \log(\text{Re} \sqrt{f}) - 0.4 \quad (2-38)$$

This equation is valid to Re up to 3200000 for turbulent flow of fluids in smooth tubes. It is superior to any other correlation now in existence, although simpler correlations such as Blasius [1913] have been proposed:

$$f = 0.079 \text{Re}^{-1/4} \quad (2-39)$$

which is used to predict friction factor for smooth pipe for Re 3000 to 100000 [Brodkey and Hershey, 1989 and Welty et al., 2001]. Also, an empirical equation relating friction factor and Re was presented by Drew et al. [1932],

$$f = 0.0014 + 0.125\text{Re}^{-0.32} \quad (2-40)$$

This equation holds for Re of 3000 to 3000000. Similar relationship between Re and f is given by Eq.(2.41). This equation is used in heat transfer calculations which makes use of the analogy between the transfer of momentum and the transfer of heat [Kundsen and Katz, 1958],

$$f = 0.046 \text{Re}^{-0.2} \quad (2-41)$$

From universal velocity profile, Von Karman [1931] developed the following equation for turbulent flow in rough tubes

$$\frac{1}{\sqrt{f}} = 4.06 \log \frac{d}{e} + 2.16 \quad (2-42)$$

which compares very well with the equation obtained by Nikuradse from experimental data

$$\frac{1}{\sqrt{f}} = 4.0 \log \frac{d}{e} + 2.28 \quad (2-43a)$$

For commercial pipes the following correlation is recommended [Knudsen and Katz, 1958]

$$1/\sqrt{f} = 3.2 \log ((\text{Re} \sqrt{f}) + 1.2) \quad (2-43b)$$

Haaland [1983] showed that over the range $4000 \leq \text{Re} \leq 10^8$ and $0 \leq e/d \leq 0.05$, the friction factor may be expressed (within $\pm 1.5\%$) as

$$\frac{1}{\sqrt{f}} = -3.6 \log \left[\frac{6.9}{\text{Re}} + \left(\frac{e}{3.7d} \right)^{10/9} \right] \quad (2-44a)$$

This expression allows explicit calculation of the friction factor [Welty et al 2001].

Chen [1985] has developed an explicit friction factor equation which is valid for all regions of turbulent flow with an accuracy of within about $\pm 8\%$

$$f = 0.0791 \left[\frac{1}{\text{Re}^{0.83}} + 0.11 \left(\frac{e}{d} \right) \right]^{0.3} \quad (2-44b)$$

It is found experimentally that for commercial steel pipe $e=4.572 \times 10^{-2}$ mm and for cast iron pipe $e=0.2591$ mm [Brodkey and Hershey 1989].

2.4 Eddy Diffusivity Models

The eddy diffusivity of momentum may be calculated from shear stress Eq.(2.19) [Brodkey and Hershey, 1989]. The shear stress at any point y is related to the shear stress at the wall by

$$\tau = \frac{r}{r_w} \tau_w \quad (2-45)$$

and since $r = r_w - y$ (2-46)

Substitution in Eq. (2.19) yields

$$\frac{\tau_w}{\rho} \left(1 - \frac{y}{r_w} \right) = (v + \epsilon_M) \frac{du}{dy} \quad (2-47)$$

Solving for ϵ_M and introducing the relation $(u^*)^2 = \tau_w / \rho$

$$\epsilon_M = \frac{u^{*2} (1 - y/r_w)}{du/dy} - v \quad (2-48a)$$

from the relations

$$y^+ = \frac{yu^*}{v} = \frac{y}{r_o} \frac{\text{Re}}{2} \sqrt{f/2} \quad \text{and} \quad u^+ = \frac{u}{u^*} \quad (2-15)$$

one obtains $dy^+ = \frac{u^* dy}{\nu}$ and $du^+ = \frac{du}{u^*}$

$$\text{from which } \frac{du^+}{dy^+} = \frac{\nu}{u^{*2}} \frac{du}{dy} \quad (2-48b)$$

Combining Eqs. (2.48a) and (2.48b)

$$\frac{\varepsilon_M}{\nu} = \frac{(1 - y^+ / [(Re/2)\sqrt{f/2}]) - 1}{du^+/dy^+} \quad (2-49)$$

The eddy diffusivity of momentum may be calculated using Eq. (2.49) from universal velocity distribution [Brodkey and Hershey, 1989]

In the viscous sub-layer the viscous effect are significant and a special treatment is required to describe the simultaneous action of both viscous and turbulent forces. The exact description of this region is of great importance since this region is characterized by very steep gradients of velocity, temperature and concentration particularly at high Pr and Sc [Gutfinger, 1975]. The concept of eddy diffusivity is a mean for calculating mass or heat transfer rates from momentum transfer rate [Notter and Sliacher, 1972].

Numerous formulas have been proposed to describe the eddy viscosity distribution. Predictions of heat and mass transfer rates based on various models exhibit considerable agreement at high Pr and Sc. Since the region of interest at high Pr and Sc is very close to the wall (i.e., $y^+ < 1$ for Pr or Sc $> 10^4$), the importance of difference between the various expressions restricted to the behavior of the predicted ε_M as $y^+ \rightarrow 0$. This is the region where the uncertainties associated with experimental measurement are greatest. The expression of Van Driest [1956], Deissler [1955], and Son and Hanraty [1967] result in $\varepsilon_M \sim (y^+)^4$ as $y^+ \rightarrow 0$ while Reichard [1943] expression leads to $\varepsilon_M \sim (y^+)^3$. The expression of

Spalding [1961] is flexible with ε_M related either to $(y^+)^3$ or $\sim(y^+)^4$. Several attempts have been made to provide theoretical basis for either a $(y^+)^3$ or $\sim(y^+)^4$ variation of ε_M . Townsend [1961] and Wasan et. al. [1964], concluded that ε_M varies with $(y^+)^3$ as y^+ goes to zero. This conclusion is supported by many investigators [Hughmark 1969, Shaw and Hanratty 1964, Sirker and Hanratty 1969].

The equations making use of the analogy between momentum and mass (or heat) transfer require the relation between ε_D or ε_H and ε_M to be known if the results are to be accurate. To simplify the calculations, $\varepsilon_D/\varepsilon_M$ is taken to be unity. The ratio $\varepsilon_M/\varepsilon_H$ is called turbulent Prandtl number (Pr_t) and the ratio $\varepsilon_M/\varepsilon_D$ is called turbulent Schmidt number (Sc_t). These ratios parallel the molecular Prandtl number (ν/α) and molecular Schmidt number (ν/D) [Hubbard and Lightfoot 1966].

Isakoff and Drew [1951], Page et. al. [1932], and Slicher et. al. [1952] determined experimentally the values of ε_H . Their results showed that $\varepsilon_H/\varepsilon_M$ is function not only of Re but also of the position in the cross section.

Rosén and Tragardh [1993], studied the phenomena of high-Schmidt-number mass transfer in the concentration polarization boundary layer during ultrafiltration. Rosén and Tragardh [1995], derived the turbulent Schmidt number relationship from spatially resolved measurements of the Reynolds stress and measurements of mass transfer coefficients for high Schmidt number solutes.

Aravinth [2000] obtained modified eddy diffusivity expression for the turbulent boundary layer near a smooth wall has from earlier models and used this eddy diffusivity expression to predict radial temperature or concentration profile.

Slaiman et al [2007] examined various previously proposed models of eddy diffusivity against experimental data. They found that some models exhibit considerable deviation from experimental results and proposed new eddy diffusivity models based on three resistances in series concept taking in account the resistance of turbulent core and buffer zone. Table 1 summarizes many models for eddy diffusivity.

2.5 Review of Mass Transfer Models Concerning Single Phase

The earliest study is that of Gilliland and Sherwood [1934], who measured the rate of vaporization of nine liquids into air flowing in a wetted wall column. Tests were made at total pressures from 0.1 to 3 atm. They correlated their results by the following equation for $0.6 \leq Sc \leq 2.26$ and $3000 \leq Re \leq 38000$.

$$Sh = 0.023Re^{0.83}Sc^{0.44} \quad (2-50)$$

Lin and Sherwood [1950] studied the effect of Sc on mass transfer in laminar and turbulent flow of water over cast tubes, cylinders, plates, and spheres of benzoic acid, cinnamic acid, and beta-naphthol. For $1000 < Sc < 3000$ and $230 < Re < 6500$ for tubes. The results showed that the mass transfer coefficient becomes constant for L/D of 6 or greater. There were appreciable differences of mass transfer coefficient of three solutes.

Table 2.1: Common Selected Eddy Diffusivity Models

Author	ε/v	y^+ range
Von Karman (1939)	$\varepsilon_m / v = 0$ $\varepsilon_m / v = 0.2y^+ - 1$ $\varepsilon_m / v = 0.4y^+ - 1$	$0 < y^+ < 5$ $5 < y^+ < 30$ $y^+ > 30$
Lin, Moulton, and Putnam (1953)	$\varepsilon_m / v = (y^+ / 14.5)^3$ $\varepsilon_m / v = 0.2y^+ - 0.949$	$0 < y^+ < 5$ $5 < y^+ < 33$

Deissler (1955)	$\varepsilon_m / \nu = n^2 u^+ y^+ [1 - \exp(-n^2 u^+ y^+)]$ $\varepsilon_m / \nu = \frac{y^+}{2.78} - 1 \quad n = 0.124$	$0 < y^+ < 26$ $y^+ > 26$
Van Driest (1956)	$\varepsilon_m / \nu = 1/2 [1 + 4n^2 y^{+2} (1 - \exp(-y/26)) - 1/2]$ $n = 0.41$	all y^+
Wasan and Wilke (1964)	$\frac{\varepsilon_m}{\nu} = \frac{4.16 \times 10^{-4} y^{+3} - 15.15 \times 10^{-6} y^{+4}}{1 - 4.16 \times 10^{-4} y^{+3} - 15.15 \times 10^{-6} y^{+4}}$	$y^+ < 20$
Mizushima et. al. [1971]	$\varepsilon_m / \nu = a y^{+3}$ $\varepsilon_m / \nu = 0.4 y^+ (1 - y^+ / R^+) - 1$ $\varepsilon_m / \nu = 0.07 R^+$ $a = f(\text{Re}), R^+ = (f/8)^{0.5} \text{Re}$	$0 < y^+ < 26$ $26 < y^+ < 0.23 R^+$ $0.23 R^+ < y^+ < R^+$
Rosen and Tragardh (1995)	$\varepsilon_m / \nu = 0.0012 S_c^{-0.112} y^{+3}$	$0 < y^+ < 26$
Aravinth [2000]	$\varepsilon / \nu = \frac{0.0007 y^{+3}}{1 + 0.00405 y^{+3}}$	$0 < y^+ < 30$
Slaiman et. al [2007]	$\varepsilon / \nu = 0.001 S_c^{-0.0116} y^{+3}$ $\varepsilon / \nu = 0.5 y^+$ $\varepsilon / \nu = 0.07 R^+$	$0 < y^+ < 22.4 S_c^{-0.017}$ $22.4 S_c^{-0.017}$ $< y^+ < 0.14 R^+$ $y^+ > 0.14 R^+$

Lin et. al. [1953] presented theoretical analysis of mass transfer between turbulent fluid stream and wall. In their paper the authors stated that the concept of the existence viscous sub-layer of diffusion may not be true according to the ultramicroscopic observations of fluid particles adjacent to the wall by Fage and Townend [1932], where they noticed that the velocity fluctuations vertical to the wall do not cease to exist until they reach the wall, therefore the transfer of matter in region of $\delta_d < y < \delta_b$ is by turbulence, although the momentum is transferred by viscous

mechanism. They based their analysis on the presence of small amount of eddy in the viscous sub-layer and verified this experimentally by means of light interference technique [Lin et al 1953]. They recommend the Levich [1962] relation for the ratio of thickness of viscous and diffusion sub-layers,

$$\frac{\delta_b}{\delta_d} = Sc^{1/3} \quad (2-51)$$

Meyereink and Friedlander [1962] reported experimental data for mass transfer from the pipe wall made of benzoic acid, cinnamic acid, and aspirin dissolving in water or aqueous solution of sodium hydroxide. The following correlation was obtained for fully developed Sh,

$$Sh=0.070 Re^{0.94} \quad (2-52)$$

Harriot and Hamlton [1965] measured mass transfer rates for smooth pipe sections of benzoic acid dissolving in glycerin-water solutions. They reported experimental data for wide range of Schmidt number, $Sc=430-100000$ and $Re=10000-100000$. The data were correlated with an average deviation of 5.4 per cent by the equation

$$Sh=0.0096 Re^{0.913} Sc^{0.346} \quad (2-53)$$

The results indicated that the exponent of Sc may vary with Re and the exponent of Re may vary with Sc.

Lin et. al. [1951] made a systematic study of the transfer rate of ions and other reacting species in electrochemical reactions in several kinds of mixtures and measured the mass transfer coefficients in laminar and turbulent flow by this method. Mitchell and Hanratty [1966] developed the shear-stress meter and used this for a study of turbulence at a wall.

The meter was used to steady the turbulence in the

intermediate vicinity of a pipe. The surface shear stress was obtained from measuring the current flowing in the circuit.

Shaw and Hanraty [1964] measured the fully developed mass transfer rate at $Sc=2400$ and $Re=8000-50000$ and found that K^+ is independent of Re .

Hubbard and Lightfoot [1966] studied the turbulent mass transfer in rectangular duct using diffusion-controlled reduction. Experiments were made at $Sc=1700-30000$ and $Re=7000-60000$. They found that the Sh dependence on Sc varies from 0.367 at $Re=60000$ to 0.300 at $Re=7000$; and Sh dependence on f varies from 0.8 at $Sc=1700$ to 0.3 at $Sc=30000$.

Mizushima et. al. [1971] obtained mass transfer data using (LCDT) at a nickel cathode. Experimental results showed that Sh varies with $1/3$ power of Sc and about 0.9 power of Re at $Sc=800-15000$ and $Re=3000-80000$ for $Sc>1000$, they approximated their results to

$$Sh = 0.827\sqrt{f/2A} Re Sc^{1/3} \quad (2-54)$$

where A is function of Re .

Dawson and Trass [1972] studied the effect of surface roughness on the mass transfer rate using electrochemical technique. For smooth surface the following correlation was obtained

$$Sh = 0.0153 Re^{0.88} Sc^{0.32} \quad (2-55)$$

Shaw and Hanraty [1977] studied the influence of Sc on the rate of mass transfer between turbulently flowing fluid and pipe wall using electrochemical method.

Berger and Hau [1977], made electrochemical measurements to obtain mass transfer data for fluid flowing turbulently in circular pipe. Mass transfer coefficient was measured in fully developed and entrance

region (developing concentration boundary layer). For $Sc < 10^4$ and $Re=10^4-10^6$. The following correlation was proposed for fully developed turbulent flow:

$$Sh=0.0165Re^{0.86}Sc^{0.33} \quad (2-56)$$

Poulson and Robinson [1986] used the corrosion process (weight loss) to determine the overall and local mass transfer coefficients for different geometers. The method involved corroding copper specimens in dilute hydrochloric acid containing ferric ions. Data for fully developed flow in circular pipe, were found to be correlated by the following equation

$$Sh=0.026Re^{0.82}Sc^{0.35} \quad (2-57) \quad \text{with correlation}$$

coefficient of 0.982. The authors stated that developing roughness is less than in chemical dissolution technique, and it is function to Re and rate of mass transfer.

Znad [1996] analyzed the mass transfer coefficient using experimental data of other investigators [Eisenberg et al 1954, Jaralla 1984, Samh 1994]. He obtained the following relation for mass transfer coefficient by assuming that the eddy diffusivity of mass is proportional to the cube of distance from the wall (i.e., $D \propto y^3$),

$$Sh = 0.38073\sqrt{f/2} Re^{0.834} Sc^{0.334} \quad (2-58)$$

Aravinth [2000] investigated theoretical mass and heat transfer in pipe flow and proposed the following correlation:

$$Sh = \frac{\frac{f}{2} Re Sc}{1 + \sqrt{\frac{f}{2}} (14Sc^{2/3} - 13.2)} \quad (2-59)$$

Chapter Three

Two Phase Flow and Turbulent Diffusion

3.1 Introduction

When gas and liquid flow simultaneously in a pipe, various flow regimes may form, depending on the flow rate and physical properties of the phases and also on the geometry and inclination of the configuration. Determination of the flow pattern is the first step for developing two phase flow model. It is well known that the rates of transfer of mass, heat and momentum between a solid wall and a fluid in turbulent flow near the wall can under suitable conditions, be characterized by an eddy diffusion coefficient (eddy diffusivity for mass or heat, eddy viscosity for momentum). In some cases of mass transfer between a solid or liquid and a fluid moving in turbulent motion much of the resistance to diffusion is encountered in a region very near the boundary between phases [Sherwood and Woertz ,1939].

Two-phase flows are encountered in a wide range of industrial applications, such as chemical plants, nuclear reactors, oil wells, pipelines, evaporators and condensers [Kreith and Bohem, 1988]. The flow pattern taken up by mixing gas and liquid streams depends upon the flow rates of the two phases, on the physical properties and on pipe geometry.

In the design and analysis of two-phase systems, little attention has been paid to the inherent discreteness of the flow field. Analyses have usually considered only the two extremes of fully mixed homogeneous flow or fully separated flow. While such analyses are important in defining limiting behavior or in qualitatively predicting system performance, they usually fall short of general design utility. The

heterogeneous nature of two-phase flow could be important, a measurement of the flow rates of individual components through an orifice could be calculated from a measurement of the fluctuating pressure drop. The inherent unsteadiness of these flows has been adequately demonstrated by a number of workers and is readily testified to by an experimenter who has tried to measure differential pressures along a duct carrying two-phase flow [Sato et al 1981].

The major problem lies in the fact that in general, two-phase flow is a macroscopic conglomeration and may not be treated on the whole as a single fluid. Hence, point differentials are not adequate in themselves to completely describe the system behavior because, at one instant one phase exists and one set of reations would hold, where as, at the next instant the fluid would change and the alternate set of equations would govern [Owen and Novak ,1974].

3.2 Analysis for Two-Phase Flow

In accordance with Sato et al [1981] the averaging procedure of Reynolds for single-phase flow, to be also applicable to two-phase flows, where the liquid phase is incompressible and the gas phase behaves only as avoidage. Hence only the shear stress in the liquid phase will be considered. It is further assumed that the turbulent fluctuations can be divided into two components, caused by the movement of the liquid and by phase interaction, respectively. Thus

$$u = \bar{u} + (\dot{u})_m + (\dot{u})_i \quad (3-1)$$

where the indices denote (liquid) momentum and phase interaction, respectively, leading to the following expression for the shear stress in two-phase flow:

$$\tau_{rz} = (1 - \alpha) \left(\frac{\mu du_{Lz}}{dr} - \rho l \overline{(\dot{u}_r \dot{u}_z)_m} - \rho l \overline{(\dot{u}_r \dot{u}_z)_i} \right) \quad (3-2)$$

with the hypothesis of Boissinesq:

$$\tau_{rz} = (1 - \alpha) \mu l \left(1 + \frac{\varepsilon_m}{\nu L} + \frac{\varepsilon_i}{\nu L} \right) \frac{du_{Lz}}{dr} \quad (3-3)$$

where $\overline{\varepsilon}$ represents the turbulent viscosity due to phase interaction. The frictional pressure drop is given by the following equation

$$\left(\frac{dp}{dz} \right)_{fr} = \frac{4}{D} \tau_w \quad (3-4)$$

Where τ_w is obtained from equation (3.3), for this purpose the following assumptions must be made :

The liquid velocity distribution is similar to that in single phase flow, as was found by Sato et. al. [1981] and Serizawa et. al, [1975] the power law of equation (3.5)

$$u_z = u_{z \max} \left(1 - \frac{2r}{D} \right)^{1/n} \quad (3-5)$$

Both ε_m and ε_i are almost constant in the core region of the pipe, as validated by Sato et.al [1981].

Correlations for $\overline{\varepsilon}$ and Friction factor are obtained by slightly modifying the single phase expressions equations.

$$\frac{\varepsilon_m}{\nu} = \frac{\text{Re}_D}{30} \sqrt{\frac{f}{8}} \quad (3-6)$$

and

$$\text{Re}_D = \frac{\rho(u_z)D}{\mu} \quad (3-7)$$

and

$$f = 0.0056 + \frac{0.5}{\text{Re}_D^{0.22}} \quad (3-8)$$

Hence

$$\frac{\varepsilon m}{\nu L} = \frac{\text{Re}_{Dtp}}{30} \sqrt{\frac{ftp}{8}} \quad (3-9)$$

And in the same sence

$$ftp = 0.0056 + \frac{0.5}{\text{Re}_{Dtp}^{0.22}} \quad (3-10)$$

The definition of Re_{Dtp} in literature appear to vary. Sato et.al. [1981] proposed the following Eq. for Re in two phase flow :-

$$\text{Re}_{tp} = \frac{\alpha \rho_G u_G^2 + (1-\alpha) \rho_L u^2 L}{\mu_L \frac{u_L}{D}} \quad (3-11)$$

As $\rho_G \ll \rho_L$ this may further be simplified to

$$\text{Re}_{tp} = \frac{(1-\alpha) \rho_L u^2 L}{\mu_L \frac{u_L}{D}}$$

$$\text{Re}_{tp} = \frac{\alpha \rho_G u_G^2 + (1-\alpha) \rho_L u_L^2}{\mu_L} \quad (3-12)$$

Till 1981, no correlations for turbulent viscosity in two phase gas-liquid flow exist [Welle 1981]. Sato et al [1981] developed the following model for momentum eddy diffusivity in two phase flow in the wall vicinity by modifying Van Driest [1956] models for single phase:

$$\varepsilon_m / \nu_L = 0.4 y^+ \{1 - \exp(-y^+ / A^+)\}^2 \left\{1 - \frac{11}{6} \left(\frac{y^+}{R^+}\right) + \frac{4}{3} \left(\frac{y^+}{R^+}\right)^2 - \frac{1}{3} \left(\frac{y^+}{R^+}\right)^3\right\} \quad (3.13)$$

$$R^+ = Ru^* / \nu_L, A^+ = 16, y^+ = y u^* / \nu_L \text{ and } u^* = \sqrt{w / L}$$

For bubble flow they proposed the following model at the liquid-gas interface

$$\varepsilon_m / \nu_L = 0.4 (1 - \exp(-y^+ / A^+))^2 \left(\frac{d_B}{2}\right) U_B \quad (3-14)$$

where U_B bubble velocity and d_B = bubble size. Welle [1981] proposed the following eddy diffusivity model in the turbulent core of pipe flow:

$$\varepsilon_m / \nu = \frac{Re_{tp}}{30} \sqrt{f_{tp} / 8} \quad (3-15)$$

They developed the eddy diffusivity expression in the liquid layer

$$\varepsilon / \nu_L = \frac{0.4}{6} Ru_L^* (1 - (1 - z)^2)(1 + 2(1 - z)^2) \quad (3-16)$$

where $Z = y/R$

At the interface, Sato et. al. [1981] developed the following expression for eddy diffusivity:

$$\varepsilon / \nu_L = 0.0029 \alpha u_g \rho_L D / \mu_L \quad (3-17)$$

Sato et al [1981] stated that better approximation of the values ($\overline{\varepsilon}$) can be obtained by a relationship of the form

$$\frac{\varepsilon_i}{\nu} = +b \alpha u_G \rho_L D / \mu_L \quad (3-18a)$$

In which a and b are constants. This correlation does not yield a smooth transition to single phase liquid flow, as it is clear that ($\frac{\varepsilon_i}{v}$) should be zero in case of finding a correlation of the form :-

$$\frac{\varepsilon_i}{v} = \alpha \left(a + b \alpha u_G \rho_L \frac{D}{\mu_L} \right) \quad (3-18b)$$

Sato et al [1981], from experimental data, showed that

$$\frac{\varepsilon_i}{v} = \alpha \left(100 + 0.0024 u_G \rho_L \frac{D}{\mu_L} \right) \quad (3-19)$$

Sato et al proposed the following expression based on the liquid later over entire cross section

$$\frac{\varepsilon}{v_L} = [1 - \exp(\frac{-y^+}{A^+})]^2 \left\{ 1 - \frac{11}{6} \left(\frac{y^+}{R^+} \right) + \frac{4}{3} \left(\frac{y^+}{R^+} \right)^2 - \frac{1}{3} \left(\frac{y^+}{R^+} \right)^3 \right\} 0.4 y^+ \quad (3-20)$$

3.3 Holdup in Horizontal Two-Phase Gas-liquid Flow

Butler [1975] surveyed the literature on two-phase holdup and suggested by intuitive reasoning that a number of the more commonly used holdup prediction equations may be represented by the relation,

$$\left[\frac{1-\alpha}{\varepsilon} \right] = A \left[\frac{1-x}{x} \right]^p \left[\frac{\rho_G}{\rho_L} \right]^q \left[\frac{\mu_L}{\mu_G} \right]^r \quad (3-21)$$

where α is the gas void fraction, x the dryness fraction, ρ the density and μ the absolute viscosity, and the subscripts L and G refer to the liquid phase and gas phase respectively. The factors A, P, q and r, were shown to assume varying numerical values depending on which particular model was under consideration. Thus equation (3.21) provided a link for the various suggested holdup relations which, in their original forms, not only appeared unrelated, but sometimes gave conflicting results. However,

what was lacking was some theoretical basis for the form of equation given by (3-21), and some rational explanation as to why there existed such a wide variation in the numerical values of the factors A,P,q and r with the various models that have been proposed.

Spedding and Chen [1979a and 1979b] in deriving holdup equations for the cases of ideal stratified and ideal annular horizontal flow, have shown that the form of equation (3-21) may in fact be analytically derived for certain situations. In these cases, it was found that the values of A,P,q and r varied with the ideal flow patterns considered. The flow regimes, namely laminar or turbulent, and also with the range of the holdup values.

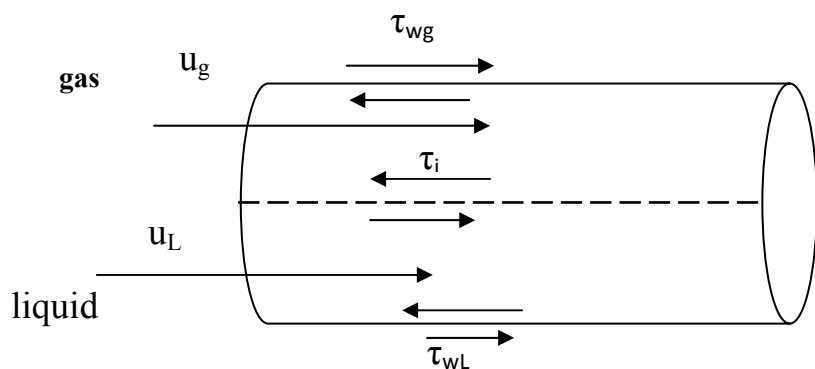


Fig.(3.1)- A Schematic diagram of ideal stratified flow.

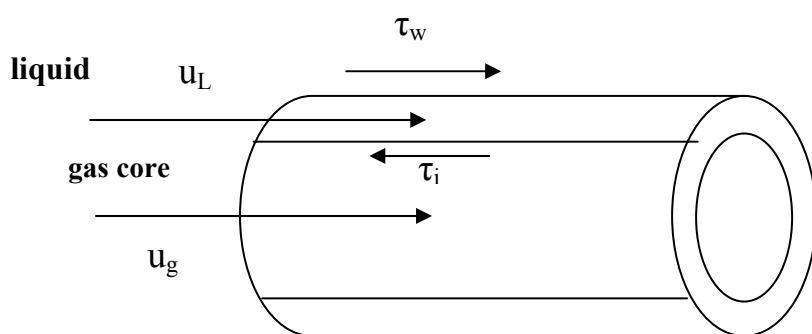


Fig.(3-2)- A Schematic diagram of ideal annular flow.

Ideal equilibrium stratified flow and annular flow are depicted schematically in figures (3.1) and (3.2) respectively. For stratified flow, by taking a force balance in the liquid phase and in the gas phase separately, it is possible to write [Chen and Spedding, 1982].

$$-A_L \left[\frac{dp}{dl} \right]_{LF} - \tau_{WL} S_L + \tau_i S_i = 0 \quad (3-22)$$

$$-A_G \left[\frac{dp}{dl} \right]_{GF} - \tau_{WG} S_G + \tau_i S_i = 0 \quad (3-23)$$

And for annular flow [Chen and Spedding, 1982],

$$-A_G \left[\frac{dp}{dl} \right]_{GF} - \tau_i S_i = 0 \quad (3-24)$$

$$-A_L \left[\frac{dp}{dl} \right]_{LF} + \tau_i S_i - \tau_{WL} S_L = 0 \quad (3-25)$$

where A is the flow area of the particular phase, (dp/dL) the pressure gradient, τ the shear stress and S the length in across section where shear forces are experienced. The subscript F refers to the frictional component, while G and L refer to the gas and liquid phases, i refers to the interface, and W refers to the wall. It is assumed that the pressure gradients in the liquid and the gas phases are equal.

$$\left[\frac{dp}{dl} \right]_{LF} = \left[\frac{dp}{dl} \right]_{GF} \quad (3-26)$$

The shear stresses may be evaluated as in the case of single phase flow,[Tail and Dukler , 1976, Wongwises et. al. 2000]

$$\tau_{WL} = f_L \frac{\rho_L u_L^2}{2} \quad (3-27)$$

$$\tau_{WG} = f_L \frac{\rho_G \bar{u}_G^2}{2} \quad (3-28)$$

$$\tau_i = f_i \rho_G \frac{(\bar{u}_G - \bar{u}_i)^2}{2} \quad (3-29)$$

where \bar{u} is the actual average velocity, and f the friction factor which may be expressed in the Blasius form for smooth pipes.

$$f_L = C_L \left[\frac{\bar{D}_L \bar{u}_L \rho_L}{\mu_G} \right]^{-m_L} \quad (3-30)$$

$$f_G = C_G \left[\frac{\bar{D}_G \bar{u}_G \rho_G}{\mu_G} \right]^{-m_G} \quad (3-31)$$

By combining equations (3-23) and (3-24)

$$\frac{\tau_i S_i}{A_G} = \frac{\tau_{WL} S_L}{A_L} - \frac{\tau_i S_i}{A_L} \quad (3-32)$$

where $S_i = \pi D_i$ and $S_L = \pi D$

where, for a smooth pipe, C is numerical constant, assuming the value of 16 or 0.046 depending on whether the flow is laminar or turbulent, and m also assuming the values of 1 or 0.2 correspondingly. \bar{D} is the hydraulic diameter for the phase, being four times the actual flow area over the wetted perimeter.

However, in the case of annular flow the assumption of $f_i = f_G$ is well-known to be inappropriate. The annular liquid film is supported by a rather complicated system of forces and the liquid surface is always covered with various types of waves [Butter Worth, 1972].

Various models are proposed to estimate the interfacial friction factor, f_i . The interfacial friction factor f_i results from drag exerted by the gas phase

on a rough surface, i.e. the rippling liquid phase, and is given by Eck [1973].

$$f_i = \frac{0.0625}{\left[10 \lg 10 \left(\frac{15}{ReG} + \left(\frac{K}{3.715} \right) \right) \right]^2} \quad (3-33)$$

where

K/D is the relative sand roughness of the inner tube wall.

Wallis [1970] has shown that the interfacial friction factor may be approximated by:

$$f_i = 0.0050(1 + 75R_L) \quad (3-34)$$

Dukler et. al [1989] proposed the following relation for annular flow

$$\frac{f_i}{f_g} = 1 + 150(1 - \varepsilon^{1/2}) \quad (3-35)$$

Fossa [1995] in his analysis of annular flow used the relation proposed by Whalley and Hewitt [1978]:

$$\frac{f_i}{f_w} = 1 + 24(\rho_L / \rho_g)^{0.5} \frac{h_L}{D} \quad (3-36)$$

Hart et. al [1989] found that there is a pronounced correlation between the ratio f_L/f_i , and the superficial Reynolds number of the liquid phase Re_{sL}

$$\frac{f_L}{f_i} = 108 R_{esL}^{-0.726} \quad (3-37)$$

In which 108 and -0.726 are empirical constants this equation is much simpler than correlations obtained by using the friction factors f_L and f_i , an approach which is generally accepted in the literature [Lockhart and Martinelli, 1949, Taitel and Dukler, 1976, Chen and Spedding, 1983 ; Oliemans, 1987].

Sripattrapan and Wongwises [2005] adopted:

$$f_i = fg(1 + 12(\rho_L / \rho_g)^{1/3}(1 - \varepsilon^{1/2})) \quad (3-38)$$

Chun and Kim [1995] carried out experimental work on two phase stratified flow (air-water) and determined experimentally the interfacial friction factor and the gas side friction factor for different values of flow velocity and wall roughness. They obtained semi-empirical correlation for friction factor.

Butter worth [1975] found that most of the liquid or gas void fraction correlations in the literature can be rewritten in to the following equation:

$$\frac{1-\alpha}{\alpha} = a \left(\frac{u_L}{u_G} \right)^b \left(\frac{\rho_L}{\rho_G} \right)^c \left(\frac{\mu_L}{\mu_G} \right)^d \quad (3-21)$$

where μ_G and μ_L are the dynamic viscosities of gas and liquid, respectively. The values of a, b, c and d in equation (3-21) appear to be constant for a limiting range of values of the superficial velocities u_{SG} and u_{SL} and the transport properties. From the force balance under steady-state conditions Hart. et. al. [1989] derived the following equation describing the liquid holdup in the stratified, wavy and annular flow regimes:

$$\frac{1-\alpha}{\alpha} = \frac{u_L}{u_G} \left[1 + \left(\frac{f_L \rho_G}{f_i \rho_G} \right)^{\frac{1}{2}} \right] \text{ for } \alpha \leq 0.06 \quad (3-39)$$

where f_L is the friction factor referring to the shear stress between the liquid film and tube wall. The value of the liquid holdup in horizontal gas-liquid pipe flow can be obtained from equation (3-39), rearranging equation (3-39), we obtain

$$\frac{f_L}{f_i} = \left(\frac{u_G}{u_L} \cdot \frac{1-\alpha}{\alpha} - 1 \right)^2 \cdot \frac{\rho_G}{\rho_L} \quad (3-40)$$

Substitution of equation (3.36) in to equation (3.39) gives the following correlation containing two empirical constants:

$$\frac{1-\alpha}{\alpha} = \frac{u_L}{u_G} \left(1 + \left[108 R_{esL}^{-0.363} \left(\frac{\rho_L}{\rho_G} \right)^{\frac{1}{2}} \right] \right) \quad (3-41)$$

Zivi [1968] proposed the following relation for void fraction

$$\alpha = \left\{ 1 + \left(\frac{1-x_f}{x_f} \right) \left(\frac{\rho_g}{\rho_L} \right)^{2/3} \right\}^{-1} \quad (3.42)$$

where $x_f = \frac{\dot{m}_g}{\dot{m}_g + \dot{m}_L}$

This relation is adopted by Sripattapan and Wongwises [2005] in their analysis of separated two phase flow.

Chisholm [1983] presented the following relation to predict void fraction

$$\alpha = \left[1 + \left(\frac{1-x_f}{x_f} \right) \left(\frac{\rho_g}{\rho_L} \right) \left(\frac{\rho_L}{\rho_m} \right)^{0.5} \right]^{-1} \quad (3-43)$$

This relation is adopted by Kim and Ghajar [2006] for different two phase flow patterns.

3.4 Flow Pattern Mapping

In general, tube diameter can be expected to have an effect on the location of the transition boundaries in these coordinates of superficial velocity, u_{SL} and u_{SG} . However, in two test section diameters are not drastically different. Furthermore, the drop tower data include only the patterns of bubbly and slug flow and models show that the transition between bubbly and slug flow is relatively insensitive to diameter. At this time there is debate as to whether the bubble and slug flow regions should be considered as separate patterns or whether this series of runs simply represents a continuum of bubble sizes. Physical models have been developed which suggest that the mechanism by which the flow takes place changes drastically between these two patterns. However, preliminary analysis for microgravity indicates that these two regions may represent a continuum of the same physical process. If that proves to be the case only two patterns can be considered to characterize the flow, bubbly and annular. Modeling of the flow pattern transitions is in its earliest stages, however it is possible to suggest some simple ideas by which the location of transition boundaries can be estimated

3.4.1 Bubble to slug pattern

The linear velocities and the superficial velocities are related by

$$u_L = \frac{u_{SL}}{1-\alpha} \quad \text{and} \quad u_G = \frac{u_{SG}}{\alpha} \quad (3-44)$$

where the superficial velocities are computed as if that phase was flowing alone in the tube. The transition from bubble to slug flow is thought to

take place when the bubble concentration and size is such that adjacent bubbles come into contact. Then coalescence can be expected and surface tension causes the two coalescing bubbles to form one larger one characteristic of slug flow. Thus, one need only estimate the average voids at this condition to obtain an equation relating the superficial velocities at transition. Small bubbles in a cubic array can achieve, at most a void fraction of 0.52. However, large bubbles, with diameter approaching that of the tube, will generate a holdup before touching which depends on their shape and orientation. For large spherical bubbles this can be shown to be approx. $\epsilon=0.5$. Because one observes various alignments, it is speculated that the average void fraction at contact -and thus at transition- is approx. $\epsilon=0.45$. The resulting equation is then [Welle 1981].

$$u_{SL} = 1.22 u_{SG} \quad (3-45)$$

3.4.2 Slug to annular pattern

The following mechanism is hypothesized to take place and cause this transition. During slug flow there is a large axial variation in void fraction between the slugs and the Taylor bubbles. As the gas rate is increased, the lengths of the bubbles increase. When these slugs become short enough, slight variation in the local velocity or adjacent film thickness can cause the slug to momentarily rupture. Then surface tension forces draw the liquid around the wall of the pipe to establish annular flow and the slug can not be reformed. In order to estimate the flow conditions at which this change will take place equations are developed relating the axial average voids and the superficial flow rates for slug flow. A similar relation is developed for annular flow. It is speculated that the transition between slug and annular flow takes place when the void fraction, as dictated by the former two models, becomes equal. That is, at lower gas velocities,

the slug flow model always predicts higher average voids than does the annular flow model at the same flow rates. However, at the transition velocity, the voids predicted by the two models are equal. At still higher gas flow rates the slug flow model predicts lower voids than does the annular flow model, and thus the flow pattern becomes one of annular flow since surface tension will cause the liquid to warp around the wall instead of existing in discrete slugs.

The flow visualization shows that the slug and bubble velocities are equal.

For annular flow; where all of the liquid flows as a smooth film along the wall and the gas flows in the core. A force balance on a control volume bounded by the pipe walls and two planes normal to the axis separated by an axial distance ΔZ , gives [Sato et al 1981]

$$\frac{\Delta p}{\Delta z} = \frac{4\tau_w}{d} \quad (3-4)$$

Figure 3.3 shows typical flow regime map for gas/liquid two-phase flow in horizontal pipes.

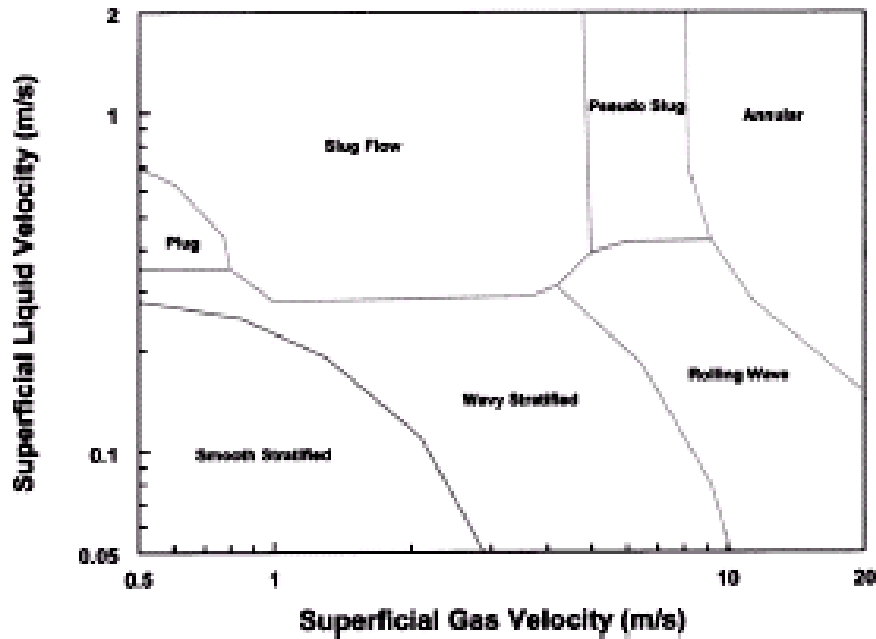


Fig.3.3: A Typical flow regime map for gas/liquid two-phase flow in horizontal pipes.1 Reproduced with permission of The International Society of Offshore and Polar Engineers [Wang et al 2004].

3.5 Two Phase Flow Mass Transfer Models

Mass transfer prediction is of great importance, particularly for the transport based models, and is also the key for the implementing the two or multiphase flow models.

Conventional tools for mass transfer predictions in fully developed single-phase pipe flow have a dimensionless form:

$$Sh = a \cdot Re^b \cdot Sc^c \quad (3-46)$$

Where a,b and c are the constants determined by experiments, Sh is the Sherwood number Kd/D , Re is Reynolds number Ud/v , and Sc is Schmidt number v/D . A number of empirical mass transfer correlations have been developed in the past for single-phase flow starting with the well-known Chilton and Colburn [1934] correlation:

$$Sh = 0.023 Re^{0.8} .S_c^{0.33} \quad (3-47)$$

The most recent and widely used correlation proposed by Berger and Hau [1977] for mass transfer in smooth pipes is given as

$$Sh = 0.0165 Re^{0.86} .S_c^{0.33} \quad (2-56)$$

However, there are no studies on mass transfer correlations valid in multiphase flow [Wang and Nestic 2003]. Langsholt et.al. [1997] and Wang [2001] measured wall stress and mass transfer coefficients in a two-phase gas-liquid flow.

The mass transport of species in the diffusion boundary layer is described locally by using a much more detailed method. Thus, the mass flux, N_A , of species A throughout the boundary layer can be expressed as:

$$N_A = -(D_A + \varepsilon_D) \frac{dC_A}{dy} \quad (3-23)$$

where D_A is the molecular diffusion coefficient of species A, ε_D is the turbulent diffusion coefficient, C_A is the concentration of species y and A is the distance from the wall.

In the model, ε_D is obtained from Davies [1972] correlation, which is based on a semi-empirical turbulent mass transfer theory.

$$\frac{\varepsilon_D}{\nu} = 0.18 \left(\frac{y}{\delta} \right)^3 \quad (3-48)$$

where δ is the thickness of the laminar boundary layer and ν is the Kinematic viscosity. The coefficient 0.18 was derived on the basis of several assumptions. For pipe flow, δ can be expressed as a function of Reynolds number

$$\delta = 25 \text{Re}^{-7/8} d \quad (3-49)$$

where d is the pipe diameter. Lin et.al. [1953] presented a similar correlation:

$$\frac{\varepsilon_D}{\nu} = 0.041 \left(\frac{y}{\delta} \right)^3 \quad (3-50)$$

Yet another semi-empirical correlation was reported by Rosen and Tragardh [1995], which contains a Schmidt number dependence:

$$\frac{\varepsilon_D}{\nu} = 0.155 S c^{-0.112} \left(\frac{y}{\delta} \right)^3 \quad (3-51)$$

Both methods for calculating mass transfer rates by using Sherwood number or locally by using ε_D must yield similar results to be considered as valid. Since all the expressions shown above were developed for single-phase pipe flow, applying them to the multiphase flow without any modification is uncertain [Wang and Nestic ,2003].

The global equation defining a turbulent mass transfer of species A is [Langsholt et. al. 1997, Wang and Nestic 2003]

$$N_A = +K_A(C_{A,S} - C_{A,b}) \quad (3-25)$$

Where N_A is flux of species A, $C_{A,S}$ and $C_{A,b}$ are the concentrations of species A at the surface and bulk respectively. Here, k depends markedly on flow conditions, which are represented by a dimensionless Reynolds number (Re). Also, it is complicated function of fluid properties which is conveniently related to the dimensionless Schmidt number (Sc). Sherwood number, which can be determined by equation such as (2-29),

relates the turbulent mass transfer coefficient K to the molecular diffusion rate D , where d is to a characteristic dimension such as a pipe diameter.

In turbulent flow, the mass flux N_A of species A can also be expressed by equation (2.23), which describes in more detail the mass transport through the boundary layer and can be rewritten as :

$$\frac{N_A}{D_A + \varepsilon_D} dy = -dC_A \quad (2-23)$$

Integrating equation (2-23) across the boundary layer, one has

$$\int_0^\delta \frac{N_A}{D_A + \varepsilon_D} = C_{A,b} - C_{A,s} \quad (3-52)$$

Substitution of equation (3-25) into equation (3-52) yields a relationship between the mass transfer coefficient and turbulent diffusivity:

$$\int_0^\delta \frac{dy}{D_A + \varepsilon_D} = \frac{1}{K_A} \quad (3-53)$$

Multiplying equation (3.53) by the kinematic viscosity ν , one has

$$\frac{u}{K_A} = \int_0^\delta \frac{dy}{\frac{1}{Sc} + \frac{\varepsilon_D}{\nu}} \quad (3-54)$$

Given a mass transfer coefficient correlation, the corresponding turbulent diffusivity correlation can be obtained, vice versa.

3.6 Mass Transfer Coefficient Correlation in Two Phase Flow

Since no explicit mass transfer correlations for multiphase flow can be found in the open literature, Wang and Nesic [2003] used single-phase Berger and Hau [1977] correlation to predict mass transfer in two phase flow by replacing the pipe diameter in equation (2.56) with a hydraulic

diameter [Pots, 1995]. They found that the Berger and Hau [1977] correlation can't be directly applied to predict mass transfer in multiphase flow. Wang and Nesic [2003] stated that a modified mass transfer coefficient correlation for two phase flow regimes needs to be developed. Also they concluded that the use of turbulent diffusivity correlations, such as Davies [1972], Lin et.al. [1953], Rosen and Tragardh, [1995], for two or multiphase flow is also uncertain. Therefore, a modified turbulent diffusivity correlation for multiphase flow regimes is needed.

The mass transfer coefficient experimentally obtained in a fully developed stratified two-phase gas-liquid flow by Langsholt et. al. [1997]. The exponent on the Schmidt number remains 0.33, which is based on an assumption that the eddy diffusivity near the pipe wall is proportional to $(y^+)^3$ as proposed by several researchers [Wang and Nesic 2003].

Wang and Nesic [2003] carefully analyzed the stratified flow data of Langsholt et.al [1997], and obtained a modified mass transfer correlation for stratified flow was identified:

$$Sh = 0.64R_e^{0.59} S_c^{0.33} \quad (3-55)$$

They used the liquid film height to compute Sherwood number and the pipe diameter is used to compute Reynolds number.

Wongwises and Naphon [2000] performed experimental and theoretical heat and mass transfer characteristics for the counter flow of air and water in vertical circular pipe. They used turbulence model (k-ε) characteristics to analyze the high Reynolds number flow and solved the momentum equations to determine the turbulence viscosity. They

obtained the following mass model to estimate the mass transfer rate of water to air:

$$Sh = aRe_g Sc^{0.33} \quad (3-56)$$

where Re_g is the air Reynolds number and a is constant obtained from plot given in their study. They found that their results are similar to that proposed by Chilton and Coulburn [1934]:

$$Sh = 0.023Re_g^{0.83} Sc^{0.33} \quad (3-57)$$

Hu and Zhang [2006] developed a modified k- ϵ turbulence model to simulate the gas liquid two phase flow heat transfer in steam surface condenser. They found that their results agree well with the experimental results of other authors.

For stratified flow, Wang and Nesic [2003] proposed the following eddy diffusivity model

$$\frac{\epsilon_D}{\nu} = 0.06 \left(\frac{y}{\delta} \right)^3 \quad (3-58)$$

and

$$\delta = 25R_{ed}^{-7/8} h \quad (3-49)$$

where h is liquid film height, pipe diameter d is used to calculate Reynolds number.

Since the mass transfer in slug flow is very different from that in full pipe flow, the extrapolations of the mass transfer correlation developed in single-phase flow to multiphase flow will cause a large error in the corrosion mechanistic modeling [Wang 2005].

Wang et al [2002] proposed the following correlation for average mass transfer coefficient in a superficial gas velocity of 4.8 m/s, different superficial liquid velocities, and effective pipe diameter is used:

$$Sh = 0.544 Re^{0.61} Sc^{0.33} \quad (3.59)$$

Chapter Four

Theoretical Analysis

This chapter presents the analysis of the problem variables and development of models to estimate the mass transfer coefficient, friction factor, and shear stresses for the investigated range of Re_{sg} , Re_{sL} , Sc_L , liquid temperature, and void fraction. In the present analysis the assumption of unity turbulent Schmidt number (Sc_t) is adopted which is good first approximation for most theoretical studies [Gutfinger 1995].

4.1 Single Phase

Various models of the eddy diffusivity presented in Table 2.1 for single phase are used to calculate the mass transfer coefficient for wide range of Re and Sc . The various models are substituted in Eq. (2.34) to find Sh :

$$Sh = \frac{\sqrt{f/2} Re Sc}{\int_0^{R^+} \frac{dy^+}{\frac{1}{Sc} + \frac{\varepsilon}{\nu}}} \quad (2-34)$$

4.1.1 Lin et. al. Model

Lin et.al. model [1953] is substituted in equation (2.34) and the integration is performed using MathCAD program

$$Sh = \frac{\sqrt{f/2} Re Sc}{\int_0^5 \frac{dy^+}{\frac{1}{Sc} + \left(\frac{y^+}{14.5}\right)^3} + \int_5^{33} \frac{dy^+}{\frac{1}{Sc} + \left(\frac{y^+}{5} - 0.949\right)}} \quad (4-1)$$

4.1.2 Johansen Model

Johansen model [1991] is substituted in equation (2.34) and the integration is performed to given

$$Sh = \frac{\sqrt{f/2} \operatorname{Re} Sc}{\int_0^5 \frac{dy^+}{\frac{1}{Sc} + \left(\frac{y^+}{11.15}\right)^3} + \int_5^{30} \frac{dy^+}{\frac{1}{Sc} + \left(\left(\frac{y^+}{11.4}\right)^2 - 0.1923\right)} + \int_{30}^{R^+} \frac{dy^+}{\frac{1}{Sc} + 0.4y^+}} \quad (4-2)$$

4.1.3 Rosen and Tragardh Model

Rosen and Tragardh model [1995] is substituted in equation (2.34) and the integration is performed to given

$$Sh = \frac{\sqrt{f/2} \operatorname{Re} Sc}{\int_0^{26} \frac{dy^+}{\frac{1}{Sc} + 0.0012Sc^{-0.112}y^{+3}}} \quad (4-3)$$

4.1.4 Slaiman et. al. Model

Slaiman et. al. model [2007] is substituted in equation (2.34) and the integration is performed to given

$$Sh = \frac{\sqrt{f/2} \operatorname{Re} Sc}{\int_0^{22.36Sc^{-0.006}} \frac{dy^+}{\frac{1}{Sc} + 0.001Sc^{-0.0116}y^{+3}} + \int_{22.36Sc^{-0.006}}^{0.14R^+} \frac{dy^+}{\frac{1}{Sc} + 0.5y^+} + \int_{0.14R^+}^{R^+} \frac{dy^+}{0.07R^+}} \quad (4-4) \quad \text{where}$$

$$R^+ = \frac{Ru^*}{v} \quad (4-5)$$

$$\text{Since } u^* = \bar{u} \sqrt{f/2} \quad (2-12)$$

Substituting equation (2.12) in to equation (4.5), yields

$$R^+ = \frac{R\bar{u}\sqrt{f/2}}{\nu} \quad (4-6)$$

Since $Re = \frac{\rho u d}{\mu} = \frac{du}{\nu}$, or $u = \frac{Re \nu}{d}$ (2-32)

By substituting for u in Eq. (4.6)

$$R^+ = \frac{R\sqrt{f/2}}{\nu} \frac{Re \nu}{d} \quad (4-7)$$

then

$$R^+ = \sqrt{f/8} Re \quad (4-8)$$

where friction factor is obtained from Blasius correlation for smooth pipe:

$$f = 0.079 Re^{-0.25} \quad (2-39)$$

The shear stress is given by

$$\tau_w = \frac{1}{2} f_w \rho u^2 \quad (2-35)$$

4.2 Two Phase Flow

4.2.1 Void fraction

The void fraction is calculated using four models for various values of Re_{sL} , Re_{sg} , and temperature.

Void fraction (α) is defined as [Taitel and Dukler 1976, Ghajar 2004, Stripntrapan and Wongwises 2005]:

$$\alpha = \frac{V_g}{V_g + V_L} \quad (4-9)$$

4.2.1.1 Zivi Model [1968]

Zivi [1968] developed the following relation for void fraction in annular flow:

$$\alpha = \left[1 + \left(\frac{1-x}{x} \right) \left(\frac{\rho_g}{\rho_L} \right)^{2/3} \right]^{-1} \quad (3-42)$$

4.2.1.2 Chisholm Model [1983]

Chisholm [1983] proposed the following model to predict the void fraction for annular flow:

$$\alpha = \left[1 + \left(\frac{1-x}{x} \right) \left(\frac{\rho_g}{\rho_L} \right) \left(\frac{\rho_L}{\rho_m} \right)^{0.5} \right]^{-1} \quad (3-43)$$

$$\rho_m = \frac{1}{\frac{1-x}{\rho_L} + \frac{x}{\rho_g}} \quad (4-10)$$

And $x = \frac{\rho_g u_{sg}}{\rho_g u_{sg} + \rho_L u_{sl}} \quad (4-11)$

4.2.1.3 Hart et al Model [1989]

Hart et al [1989] proposed the following void fraction model

$$\frac{1-\alpha}{\alpha} = \frac{u_L}{u_g} \left[1 + \left(10.4 \text{Re}_{sL}^{-0.363} \left(\frac{\rho_L}{\rho_g} \right)^{0.5} \right) \right] \quad (3-41)$$

4.2.1.4 Chen and Spedding [1980]

Chen and Spedding [1980] analyzed the annular flow and obtained:

$$1-\alpha = \frac{1}{1 + \left(\frac{0.005(1+75(1-\alpha))}{f_L(1-(1-\alpha)^{0.5})} \right)^{0.5} \left[\frac{\rho_g}{\rho_L} \right]^{0.5} \left[\frac{Q_g}{Q_L} \right]^{0.5}} \quad (4-12)$$

$$\frac{Q_g}{Q_L} = \frac{u_g A_g}{u_L A_L} = \frac{u_g \alpha A}{u_L (1-\alpha) A} = \frac{u_{sg}}{u_{sL}} \quad (4-13)$$

For particular values of velocity and gas and liquid densities Eq. (4.12) is solved by trial and error procedure to obtain α .

4.2.2 Friction Factor

In two phase flow three types of friction factor are encountered, liquid side friction factor, gas side friction factor, and the friction factor at gas liquid inter phase. The liquid side friction factor is obtained from [Hart et al 1989, Wongwises et al 1998], as

$$f_{wL} = 0.046 \left(\frac{\rho_L du_{sL}}{\mu_L} \right)^{-0.2} = 0.046 \text{Re}_{sL}^{-0.2} \quad (4-14)$$

while the gas side friction factor

$$f_{wg} = 0.046 \left(\frac{\rho_g du_{sg}}{\mu_g} \right)^{-0.2} = 0.046 \text{Re}_{sg}^{-0.2} \quad (4-15)$$

The interfacial friction factor is obtained from

$$f_i = f_{wg} \left(1 + 150 \left(1 - \alpha^{1/2} \right) \right) \quad (3-35)$$

which is strongly recommended for annular flow [Dukler et. al. 1989].

The liquid side shear stress is calculated via

$$\tau_{wL} = \frac{1}{2} f_{wL} \rho_L u_L^2 \quad (3-27)$$

The gas side

$$\tau_{wg} = \frac{1}{2} f_{wg} \rho_g u_g^2 \quad (3-28)$$

The interfacial shear stress

$$\tau_i = \frac{1}{2} f_i \rho_g (u_g - u_L)^2 \quad (4-16)$$

$$\tau_i = \tau_{wL} \frac{S_L}{S_i} \alpha - \tau_{wg} \frac{S_g}{S_i} (1 - \alpha) \quad (4-17)$$

4.2.3 Definition of Superficial Velocities

The gas superficial velocity is given by [Hart et al 1989 Wongwises et al 1998]

$$u_{sg} = \alpha u_g \quad (3-44)$$

and the liquid superficial velocity

$$u_{sL} = (1 - \alpha) u_L \quad (3-44)$$

The gas superficial Reynolds number is therefore

$$Re_{sg} = \frac{\rho_g u_{sg} D}{\mu_g} = \alpha Re_g \quad (4-18)$$

Hence

$$Re_{sL} = \frac{\rho_L u_{sL} D}{\mu_L} = (1 - \alpha) Re_L \quad (4-19)$$

4.2.4.1 Stratified Flow

For Stratified Flow

$$A_T = \left[\int_0^R 2\pi r dr = 2\pi \frac{r^2}{2} \right]_0^R$$

$$A_T = \pi R^2 = \frac{\pi}{4} D^2 \quad (4.20)$$

and

$$A_L = R^2 \cos^{-1} \frac{R-h_L}{R} - (R-h_L) \sqrt{2Rh_L - h_L^2} \quad (4-21)$$

$$A_g = \left[\int_{h_L}^D \frac{\pi}{2} D dD = \frac{\pi}{4} D^2 \right]_{h_L}^D = \frac{\pi}{4} (D^2 - h_L^2) \quad (4-22)$$

or

$$A_g = A_T - A_L = \frac{\pi}{4} D^2 - \frac{\pi}{4} h_L^2 = \frac{\pi}{4} (D^2 - h_L^2)$$

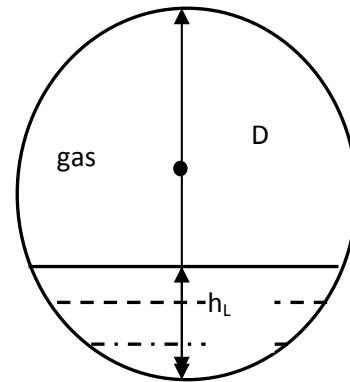


Fig. 4.1 Interfacial Area in Stratified Flow

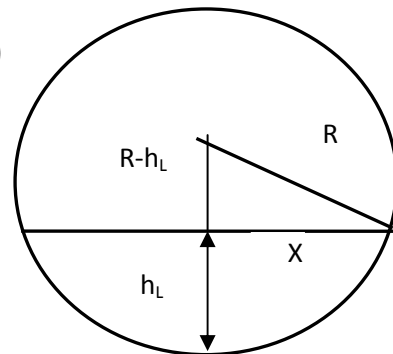


Fig. 4.2 Liquid and Gas Areas in Stratified Flow

$$\alpha = \frac{V_g}{V_g + V_L} = \frac{A_g L}{A_g L + A_L L} \quad (4-9)$$

$$\alpha = \frac{A_g}{A_g + A_L}$$

(4-23)

$$\alpha = \frac{\pi/4(D^2 - h_L^2)}{\pi/4D^2} = \frac{(D^2 - h_L^2)}{D^2}$$

$$D^2 - h_L^2 = \alpha D^2$$

$$h_L^2 = D^2 - \alpha D^2$$

$$h_L^2 = D^2(1 - \alpha)$$

Hence the liquid height is

$$h_L = \sqrt{(1 - \alpha)D} \quad (4-24)$$

The gas height

$$h_g = D - h_L \quad (4-25)$$

To find the interfacial and surface areas

$$R^2 = X^2 + (R - h_L)^2 \quad (4-26)$$

$$X^2 = R^2 - (R - h_L)^2$$

$$X = \sqrt{R^2 - (R - h_L)^2} \quad (4-27)$$

$$2X = 2\sqrt{R^2 - (R - h_L)^2}$$

$$S_i = 2XL = 2L\sqrt{R^2 - (R - h_L)^2} \quad (4-28)$$

The liquid side surface area is given by

$$S_L = \pi L h_L \quad (4-29)$$

The gas side surface area is given by

$$S_g = \pi L h_g = \pi L (D - h_L) \quad (4-30)$$

The total surface area is given by

$$S_T = 2\pi RL \quad (4-31)$$

S_i, S_L, S_g are inserted in Eq. (4-17) to find τ_i

4.2.4.2 Annular Flow

Fig.4.3 for annular flow, the void fraction α is given by [Taitel and Dukler 1976, Ghajar 2004]:

$$\alpha = \frac{V_g}{V_g + V_L} \quad (4-9)$$

$$V_g = \pi(R - h_L)^2 L \quad \text{and} \quad V_g + V_L = \pi R^2 L$$

$$\alpha = \frac{(R - h_L)^2}{R^2}, \text{ Thus}$$

$$h_L = (1 - \sqrt{\alpha})R \quad (4-32)$$

The hydraulic diameter for liquid layer

$$d_{hL} = 4 \text{ Flow area/wetted perimeter}$$

$$d_{hL} = \frac{4(1 - \alpha) \frac{\pi}{4} d^2}{\pi d} = (1 - \alpha)d \quad (4-33)$$

$1 - \alpha = \text{liquid holdup}$

$$\text{Wall side liquid surface area } S_L = \pi d L \quad (4-34)$$

$$\text{Interfacial area, } S_i = \pi(d - 2h_L) L \quad (4-35)$$

The calculations are performed for pipe diameter of $d = 10 \text{ cm}$.

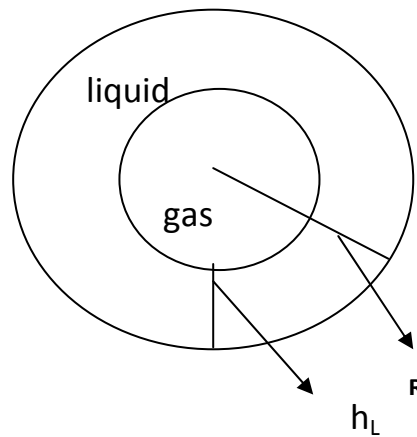
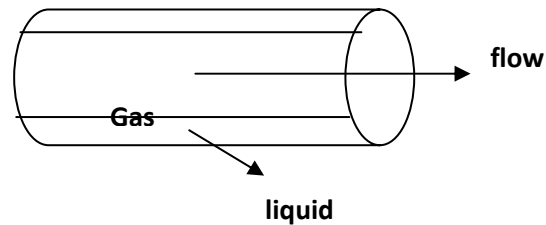


Fig. 4.3: Gas-Liquid Annular Flow

4.2.5 Mass Transfer Coefficient in Annular Flow

For annular flow in liquid phase the total flux is given by [Geankoplis 1995, Brodkey and Harshy 1989, Wang and Nestic 2003] as :-

$$N_A = k_L (C_b - C_w) = -(D_L + \varepsilon_{dL}) \frac{dC_L}{dy} \quad (4-36)$$

$$\int_0^{h_L} \frac{k_L dy}{D_L + \varepsilon_{dL}} = \frac{C_b}{C_w} \int_{C_b}^{C_w} \frac{dC_L}{C_b - C_w} \quad (4-37)$$

$$\frac{1}{k_L} = \int_0^{h_L} \frac{dy}{D_L + \varepsilon_{dL}} \quad (4-38)$$

where h_L is the liquid layer height adjacent to the surface.

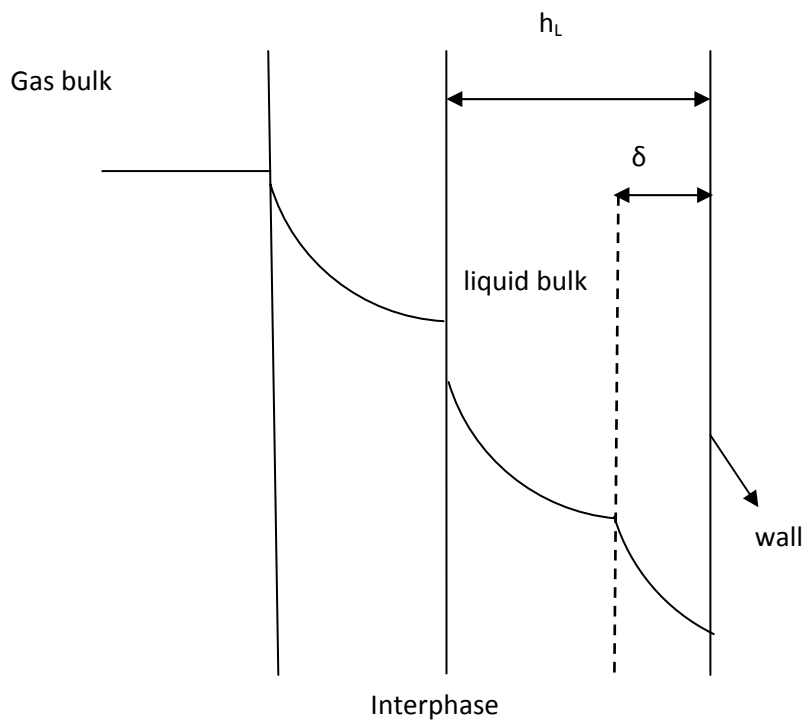


Fig. 4.4: Diffused Species Concentration Variation from Gas Bulk to the Wall

Figure 4.4 shows the diffused species concentration variation from gas bulk to the wall. In gas phase:

$$N_A = k_g(C_g - C_b) = -(D_g + \varepsilon_{dg}) \frac{dC_g}{dy} \quad (4-39)$$

$$\frac{1}{k_g} = \frac{R}{h_L} \int \frac{dy}{D_g + \varepsilon_{dg}} \quad (4-40)$$

The total flux at the surface:

$$N_{AT} = \frac{C_g - C_w}{R_T} \quad (4-41)$$

$$k = \frac{1}{R_T} \quad (4-42)$$

$$\text{or } k = \frac{1}{\frac{1}{k_L} + \frac{1}{k_g}} \quad (4-43)$$

Equation (4.55) represents a two layer resistance separated by interface similar to that proposed by Hughmark [1969] and Aravinth [2000]. Hence

$$k = \frac{1}{\int_0^{hL} \frac{dy}{D_L + \varepsilon_{dL}} + \frac{R}{h_L} \int \frac{dy}{D_g + \varepsilon_{dg}}} \quad (4-44)$$

Division by v_L

$$k/v_L = \frac{1}{\int_0^{hL} \frac{dy}{\left(\frac{D}{v_L} + \frac{\varepsilon_d}{v_L}\right)} + \frac{v_L}{v_g} \frac{R}{h_L} \int \frac{dy}{\left(\frac{D_g}{v_g} + \frac{\varepsilon_{dg}}{v_g}\right)}} \quad (4-45)$$

Since $v_L = Sc_L \cdot D_L$ and $Sh = kd_{hL}/D_L$

$$Sh = \frac{Sc_L d_{hL}}{\int_0^{hL} \frac{dy}{\left(\frac{D}{v_L} + \frac{\epsilon_d}{v_L}\right)} + \frac{v_L}{v_g} \frac{R}{hL} \int \frac{dy}{\left(\frac{D_g}{v_g} + \frac{\epsilon_{dg}}{v_g}\right)}} \quad (4-46)$$

Substituting $z = \frac{y}{R}$ yields

$$Sh = \frac{Sc_L d_{hL} / R}{\int_0^{z_L} \frac{dz}{\left(\frac{D}{v_L} + \frac{\epsilon_{dL}}{v_L}\right)} + \frac{v_L}{v_g} \frac{1}{z_L} \int \frac{dz}{\left(\frac{D_g}{v_g} + \frac{\epsilon_{dg}}{v_g}\right)}} \quad (4-47) \quad \text{where } z_L = h_L$$

/R.

If the Sherwood number (Sh) is based on the liquid phase, $Sh = kd_{hL}/D_L$, where d_{hL} is the hydraulic (equivalent) pipe diameter of the liquid phase. Since $v_L = D_L \cdot Sc_L$, thus

$$Sh = \frac{kd_{hL}}{D_L} = \frac{Sc_L d_{hL} / R}{\int_0^{z_L} \frac{dz}{\left(\frac{1}{Sc_L} + \frac{\epsilon_{dL}}{v_L}\right)} + \frac{v_L}{v_g} \frac{1}{z_L} \int \frac{dz}{\left(\frac{1}{Sc_g} + \frac{\epsilon_{dg}}{v_g}\right)}} \quad (4-48)$$

Knowing the variation of mass eddy diffusivity with y , Sh can be predicted for each value of Re_L , Re_g , Sc_L and α . h_L and d_{hL} vary with void fraction (or with liquid holdup). The variation of eddy diffusivity with y occurs in the two layers, liquid layer and gas layer [Sherwood, 1940].

a- Liquid Layer

1- Near Wall Region:

Most studies [Wasan and Wilke 1964, Deissler 1955, Hughmark 1969, Shaw and Hanraaty 1964, Mizushina et al 1971, Rosen and Tragrath 1995, Znad 1996, Aravinth 2000, Slaiman et al 2007] showed that in the near wall region the mass eddy diffusivity varies with y^3 . Thus in this region the eddy diffusivity varies as:

$$\epsilon_d / \nu_L = ay^3 \quad 0 < y < \delta \quad (4-49)$$

where a is independent of y and some studies showed that it is function of Re and/or Sc [[Mizushina et al 1971, Rosen and Tragrath 1995, Znad 1996, Slaiman et. al. 2007] and δ is the thickness of diffusion sublayer given by Eq. (3-49). For Annular flow it is more convenient to use the hydraulic diameter instead of liquid layer thickness in Eq. (3-49), hence

$$\delta = 25 Re_{sL}^{-7/8} d_{hL} \quad (4-50)$$

where d_{hL} the liquid layer hydraulic diameter.

2- Region with Linear Variation of Eddy Diffusivity:

Levitch [1962] and Sleicher et. al. [1972] showed that beyond the diffusion sublayer (δ) the eddy diffusivity varies linearly with y , i.e.:

$$\epsilon_{dL} / \nu_L = b y \quad \delta < y < h_L \quad (4-51)$$

where b is independent of y .

b- Gas Layer

3- Eddy Diffusivity at the Interface and Turbulent Core Region

Murphree [1932] determined the values of mass eddy diffusivity at the liquid-gas interface and found it to be function of the gas Reynolds number and independent of y [Sherwood 1940]. Best fit of Murphree data obtained for mass transfer between gas and liquid gives the following relation for mass eddy diffusivity.

Sato et al [1975] and Welle [1981] stated that the eddy diffusivity is independent of y in the core region of pipe. Hence the third region is

$$\epsilon_{dg}/v_g = 0.012Re_{sg}^{0.8} \quad h_L < y < R \quad (4-52)$$

It is convenient to write equations (4.49) and (4.51) and (4.52) in dimensionless form by using z instead of y where $z=y/R$, hence

$$\epsilon_{dL}/v_L = Az^3 \quad 0 < z < z_1 \quad (4-53a)$$

$$\epsilon_{dL}/v_L = Bz \quad z_1 < z < z_2 \quad (4-53b)$$

$$\epsilon_{dg}/v_g = 0.012Re_{sg}^{0.8} \quad z_2 < z < 1 \quad (4-53c)$$

where $z_1 = \delta/R$ and $z_2 = h_L/R$. To find values of A and B, Eq. (4.53b) is equal to Eq.(4.53c) at $z=z_2$ (interface), hence:

$$Bz_2 = 0.012Re_{sg}^{0.8}, \text{ or}$$

$$B = 0.012Re_{sg}^{0.8}/z_2 \quad (4-54)$$

Also Eq(4.53a) is Eq.(4.53b) at $z=z_1$, hence

$$A = B/z_1^2 = 0.012Re_{sg}^{0.8}/z_1^2 z_2 \quad (4-55)$$

Thus Eq. (4.48) becomes

$$Sh = \frac{Sc_L d_{hL}/R}{\int_0^{z_1} \frac{dz}{\left(\frac{1}{Sc_L} + Az^3\right)} + \int_{z_1}^{z_2} \frac{dz}{\left(\frac{1}{Sc_L} + Bz\right)} + \frac{v_L}{v_g} \int_{z_2}^1 \frac{dz}{\left(\frac{1}{Sc_g} + 0.012Re_{sg}^{0.8}\right)}} \quad (4-56)$$

In Eq. (4.48) the ratio of liquid to gas kinematic viscosity,

$$\frac{v_L}{v_g} = \frac{D_L Sc_L}{D_g Sc_g} \quad (4-57)$$

Accordingly, Eq. (4.56) becomes:

$$Sh = \frac{Sc_L d_{hL}/R}{\int_0^{z_1} \frac{dz}{\left(\frac{1}{Sc_L} + Az^3\right)} + \int_{z_1}^{z_2} \frac{dz}{\left(\frac{1}{Sc_L} + Bz\right)} + \int_{z_2}^1 \frac{\frac{D_L Sc_L}{D_g Sc_g} dz}{\left(\frac{1}{Sc_g} + 0.012Re_{sg}^{0.8}\right)}} \quad (4-58)$$

Therefore, Sh (or mass transfer coefficient or rate) is function of Re_{sL} , Re_{sg} , Sc_L , Sc_g , and h_L (or α). The liquid and gas velocities are taken according to Fig. 3.3

Diffusion coefficients of binary gas pair of A and B can be calculated using [Geankoplis 1993]:

$$D_{AB} = \frac{1.8583 \times 10^{-7} T^{3/2}}{P \sigma_{AB}^2 \Omega_{D,AB}} \left(\frac{1}{M_A} + \frac{1}{M_B}\right)^{1/2} \quad (4-59)$$

where M_A and M_B are molecular weights of A and B respectively, and P absolute pressure. Values of σ_{AB} and $\Omega_{D,AB}$ can be obtained from Bird et al [1960]. The Wilke and Chang [1955] correlation can be used to predict the diffusion coefficient in liquids:

$$D_{AB} = 1.173 \times 10^{-16} (\Psi \Psi_B)^{1/2} \frac{T}{\mu_B V_A^{0.6}} \quad (4-60)$$

where Ψ is associated parameter and is 2.6 for water, 1.9 for methanol, 1.5 for ethanol. V_A is molar volume of A and μ_B is viscosity of B [Geankoplis 1993]

4.2.6 Concentration Profile in Liquid Layer

For liquid layer

$$(D_L + \varepsilon_{dL}) \frac{dC}{dy} = k_L (C_b - C_w) \quad (4-36)$$

Hence,

$$\int_0^{h_L} \frac{dy}{D_L + \varepsilon_{dL}} = \int_{C_w}^{C_b} \frac{dC}{k_L (C_b - C_w)} \quad (4-37)$$

Performing the integration in the R.H.S yields

$$\frac{1}{k_L} = \int_0^{h_L} \frac{dy}{D_L + \varepsilon_{dL}} \quad (4-38)$$

From Eq. (4.37)

$$\int_{C_w}^C \frac{dC}{C_b - C_w} = k_L \int_0^y \frac{dy}{D_L + \varepsilon_d} \quad (4-61)$$

Substituting Eq. (4.38) in Eq. (4-61) yields

$$\int_{C_w}^C \frac{dC}{C_b - C_w} = \frac{\int_0^y \frac{dy}{D_L + \varepsilon_d}}{\int_0^{h_L} \frac{dy}{D_L + \varepsilon_{dL}}} \quad (4-62)$$

Performing the integration in the L.H.S., yields

$$C^* = \frac{C_L - C_w}{C_b - C_w} = \frac{\int_0^y \frac{dy}{D_L + \varepsilon_d}}{\int_0^{h_L} \frac{dy}{D_L + \varepsilon_{dL}}} \quad (4-63)$$

Multiplying both numerator and denominator by v_L/R , yields

$$C^* = \frac{C_{bL} - C_w}{C_{bL} - C_w} = \frac{\int_0^Z \frac{dz}{\text{Sc}_L + \varepsilon_{dL}/v_L}}{\int_0^{Z_2} \frac{dz}{\text{Sc}_L + \varepsilon_{dL}/v_L}} \quad (4-64)$$

Hence at a particular Re_L and Sc_L and by substituting the expression of ε_L/v_L and the value of Z , C^* is obtained.

To calculate the two phase mass transfer coefficient using Eq. (4.58), the following steps are followed :-

- 1- Specify Sc_L value
- 2- Specify the Re_{sL} and Re_{sg} .
- 3- Calculate void fraction α from Eq. (3.43).
- 4- Calculate the liquid layer height h_L using Eq.(4.32).
- 5- Calculate d_{hL} via Eq. (4.33).
- 6- Calculate D_g and D_L from Eqs. (4.59) and (4.60) respectively.
- 7- Calculate the thickness of diffusion layer (δ) from Eq. (4.50) and then calculate $Z_1 = \delta / R$ and $Z_2 = h_L/R$.
- 8- Calculate B and A from Eqs. (4.54) and (4.55).
- 9- By inserting the values of obtained from steps 1 to 7 in Eq. (4.58) and performing the integration using "MathCad" program, the Sh is obtained.
- 10- Use new values of Re_{sL} and Re_{sg} and repeat steps 2 through 9
- 11- Use new value of Sc_L and repeat steps 1 through 10.

Appendix D presents sample of calculations.

4.2.7 Mass Transfer Coefficient from Eddy Diffusivity in Two Phase

To examine the capability of the eddy diffusivity models proposed by other authors, these models are inserted in Eq. (4.48) to find Sh.

4.2.7.1 Wang and Nestic Model [2003]

Wang and Nestic [2003] developed the following model for eddy diffusivity by analyzing experimental results:

$$\varepsilon_d = 0.06\left(\frac{y}{\delta}\right)^3 \quad (3-58)$$

$$\text{with } \delta = 25 \text{Re}_{sL}^{-7/8} d_{hL} \quad (4-50)$$

The authors ignored the eddy diffusivity in the gas region. Hence, substituting Eqs. (3.58) and (3.50) in Eq. (4.48), yields

$$\text{Sh} = \frac{\text{Sc}_L d_{hL} / R}{\int_0^{\delta/R} \frac{1}{\text{Sc}_L + 0.06\left(\frac{y}{\delta}\right)^3} d(y/R)} \quad (4-65)$$

4.2.7.2 Sato et al-Welle [1981]

Sato et al [1981] developed the following expression of eddy diffusivity for two phase flow within the liquid layer

$$\varepsilon / \nu_L = \frac{0.4}{6} \text{Ru}_L^* (1 - (1 - z)^2)(1 + 2(1 - z)^2) \quad (3-16)$$

where $u_L^* = \sqrt{f_{wL} / 2} \text{Re}_{sL}$ with f_{wL} from Eq. (4.14).

Welle [1981] analyzed the experimental data of Sato et. al. [1981] and obtained the following correlation for eddy diffusivity at the interface to the pipe core:

$$\varepsilon / \nu_L = 0.0029 \alpha u_g \rho_L d / \mu_L \quad (3-17)$$

$$\text{or } \varepsilon = 0.0029 \alpha u_g d$$

$$\varepsilon = 0.0029 u_{sg} d$$

$$\text{since } \text{Re}_{sg} = \frac{du_{sg}}{v_g} \text{ hence,}$$

$$\varepsilon / v_g = 0.0029 \text{Re}_{sg} \quad (4-66)$$

Substituting Eqs. (3.15) and (4.78) in Eq. (4.57), yields

$$\text{Sh} = \frac{\text{Sc}_L d_{hL} / R}{\int_0^{z_3} \frac{dz}{\left(\frac{1}{\text{Sc}_L} + \frac{0.4}{6} R \sqrt{f_{wL}} / 2 \text{Re}_{sL} (1 - (1 - z)^2)(1 + 2(1 - z)^2)\right)} + \int_{z_2}^1 \frac{\frac{D_L \text{Sc}_L}{D_g \text{Sc}_g} dz}{z^2 \left(\frac{1}{\text{Sc}_g} + 0.0029 \text{Re}_{sg}\right)}} \quad (4-67)$$

4.2.7.3 Sato et al [1981]

They proposed the following expression based on the liquid later over entire cross section ignoring the gas phase eddy diffusivity

$$\frac{\varepsilon}{v_L} = [1 - \exp(-\frac{y^+}{A^+})]^2 \left\{ 1 - \frac{11}{6} \left(\frac{y^+}{R^+}\right) + \frac{4}{3} \left(\frac{y^+}{R^+}\right)^2 - \frac{1}{3} \left(\frac{y^+}{R^+}\right)^3 \right\} 0.4 y^+ \quad (3-13)$$

$R^+ = R u^* / v_L$, $A^+ = 16$, $y^+ = y u^* / v_L$ and $u^* = \sqrt{f_{wL}} / 2 \text{Re}_{sL}$, hence substitution in Eq. (4.48), yield:

$$\text{Sh} = \frac{\sqrt{\frac{f_{TP}}{2}} \text{Re}_{TP} \text{Sc}_L}{\int_0^{h^+} \frac{dy^+}{\left(\frac{1}{\text{Sc}_L} + [1 - \exp(-\frac{y^+}{A^+})]^2 \left\{ 1 - \frac{11}{6} \left(\frac{y^+}{R^+}\right) + \frac{4}{3} \left(\frac{y^+}{R^+}\right)^2 - \frac{1}{3} \left(\frac{y^+}{R^+}\right)^3 \right\} 0.4 y^+}\right)} \quad (4-68)$$

where

$$f_{TP} = (1-\alpha)f_{wL} + \alpha f_g \quad (4-69)$$

with f_{wL} and f_g from Eqs. (4.14) and (4.15) respectively. And the Re_{TP} is given by [Sato et al 1981]:

$$Re_{TP} = (1-\alpha)Re_L + \alpha Re_g = Re_{sL} + Re_{sg} \quad (4-70)$$

$$h_L^+ = \frac{h_L u^*}{v_L} \quad \text{and} \quad R^+ = \sqrt{\frac{f_{TP}}{8}} Re_{TP}$$

Chapter Five

Results and Discussion

The numerical values of theoretical results of single and two phase flow for the entire investigated range of Re , liquid temperature, Schmidt number, and void fraction are presented in appendices A, B, and C. The present chapter concerns the discussion and interpretation of the results.

5.1 Single Phase

Figure 5.1 shows the variation of eddy diffusivity with dimensionless distance from the smooth pipe wall (y^+) as obtained from various authors. It is evident that the eddy diffusivity increases with y^+ via increasing turbulence as the pipe bulk is approached.

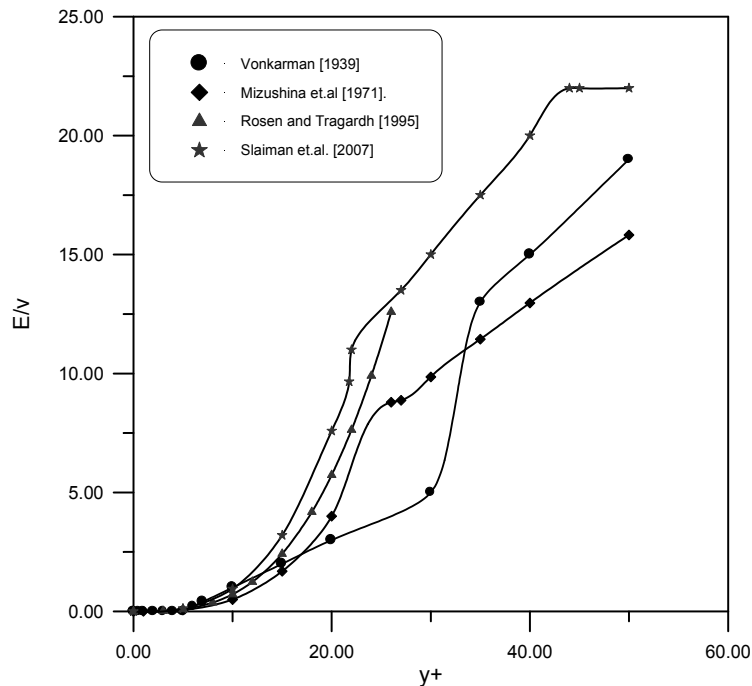
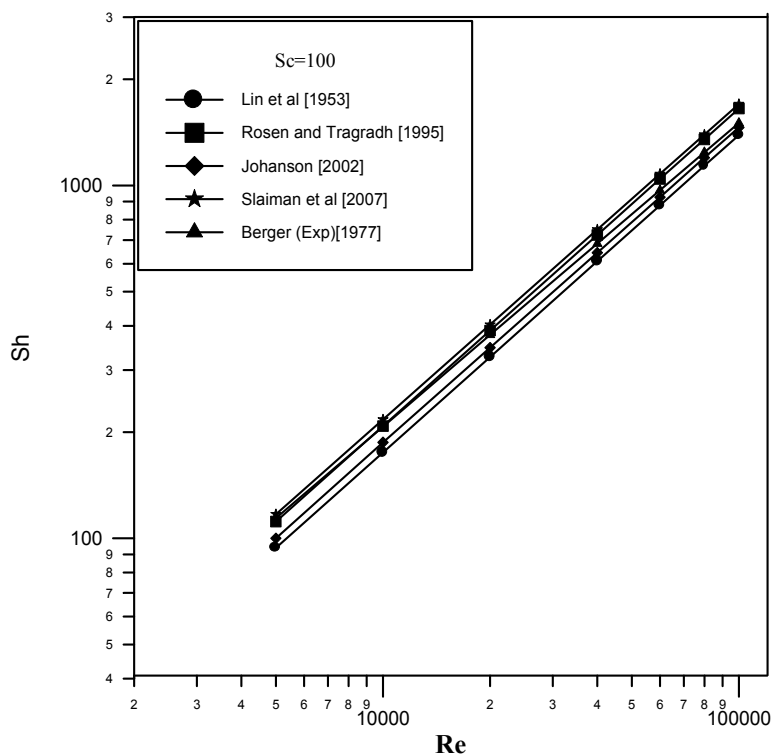
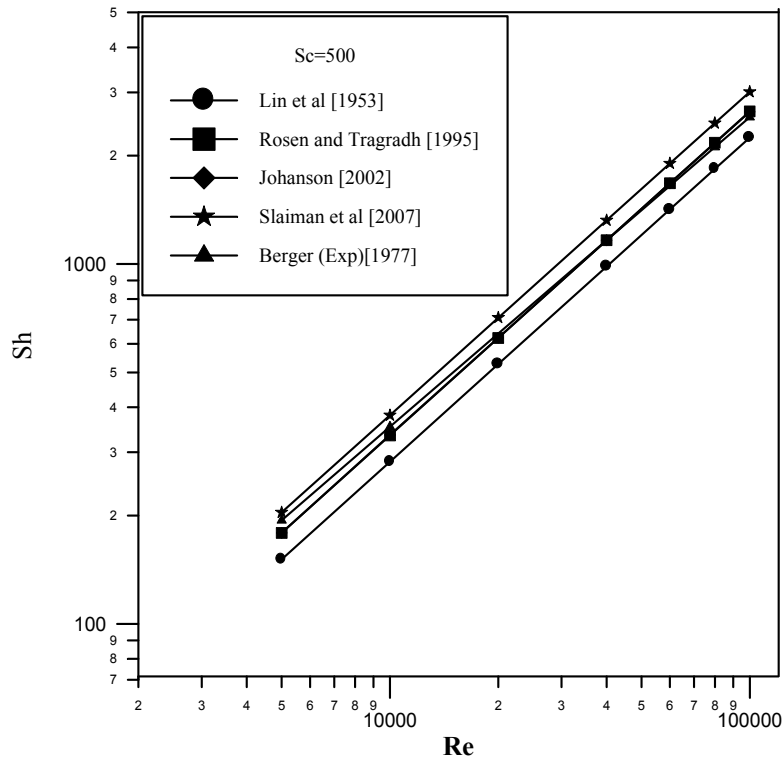


Fig. 5.1: Variation of Eddy Diffusivity with y^+ from Various Authors.

Figs. 5.2 to 5.4 show comparison of Sh obtained from various eddy diffusivity models, using Eqs. (4.1) to (4.4), with experimental correlation of Berger and Hau [1977] for wide range of Sc . The Fig. reveals that the Slaiman et. al. [2007] model and Rosen and Tragrath [1995] exhibit good agreement with experimental work of Berger and Hau [1977] for the whole range of Re and Sc . This close agreement indicates that the eddy diffusivity concept is an efficient way for predicting mass transfer coefficient in single phase turbulent mass transfer.

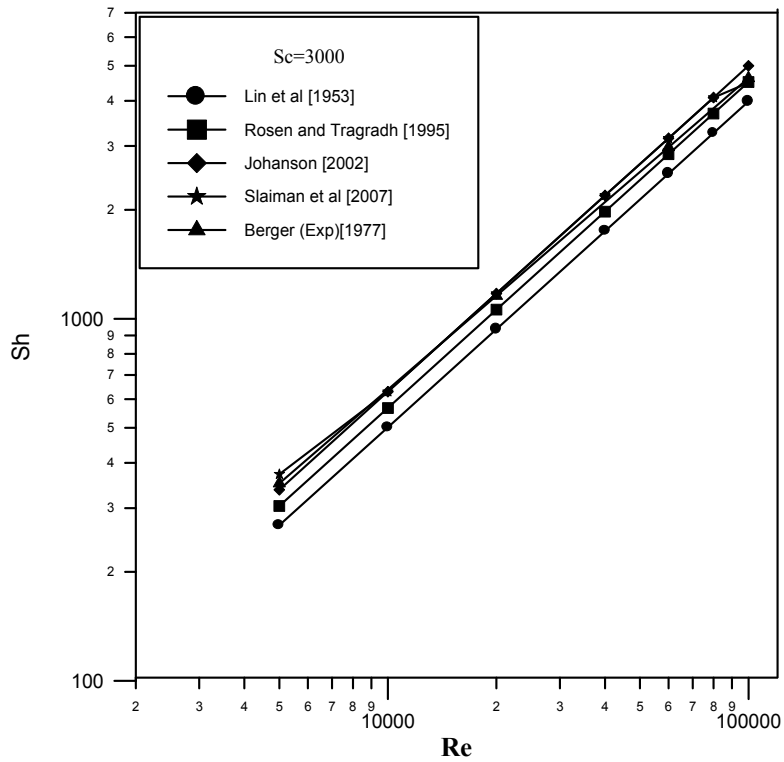


Figs. 5.2: Comparison of Sh obtained from Various Eddy Diffusivity Models for $Sc=100$.



Figs. 5.3: Comparison of Sh obtained from Various Eddy Diffusivity

Model for Sc=500.



Figs. 5.4: Comparison of Sh obtained from Various Eddy Diffusivity

Model for Sc=3000.

Figs. 5.5 through 5.7 show a comparison between the Sh for single phase mass transfer obtained from Berger and Hau [1977] correlation (Eq. (2.56)) and Sh for two phase mass transfer obtained from Wang and Nestic [2003] (Eq. (3.55)) and Wang et al. [2002] (Eq. (3.59)) for different values of Sc_L . It is evident that the two phase Sh is much higher than the single phase Sh . Wang and Nestic [2003] modified the Berger and Hau correlation (Eq. (2.56)) to predict the mass transfer coefficient in two phase by basing this correlation on the hydraulic diameter (equivalent diameter) of liquid phase, i.e. use of d_{HL} to calculate Re rather than pipe diameter. However this method failed to give accurate results for two phase mass transfer coefficient. Figs. 5.5 to 5.7 indicate that the mass transfer coefficient can not be obtained from the correlations that are proposed for single phase.

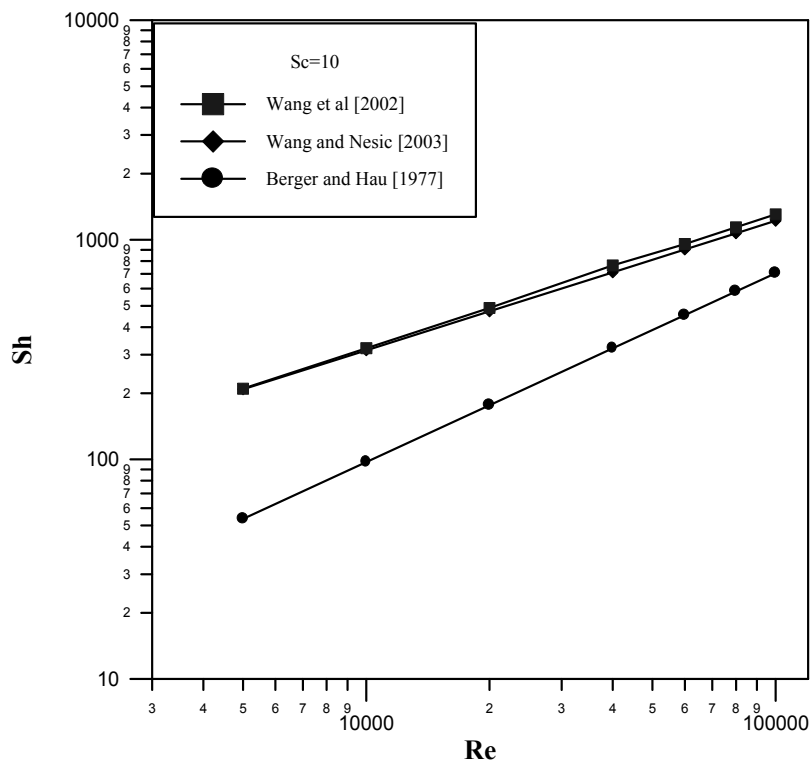


Fig. 5.5: Comparison between Single Phase Sh and Two phase Sh .

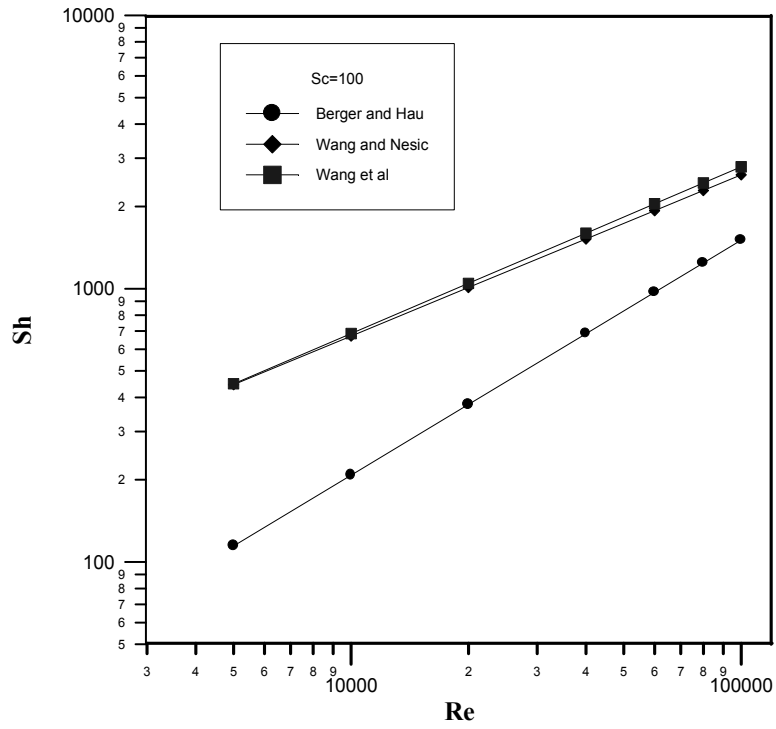


Fig. 5.6: Comparison between Single Phase Sh and Two phase Sh.

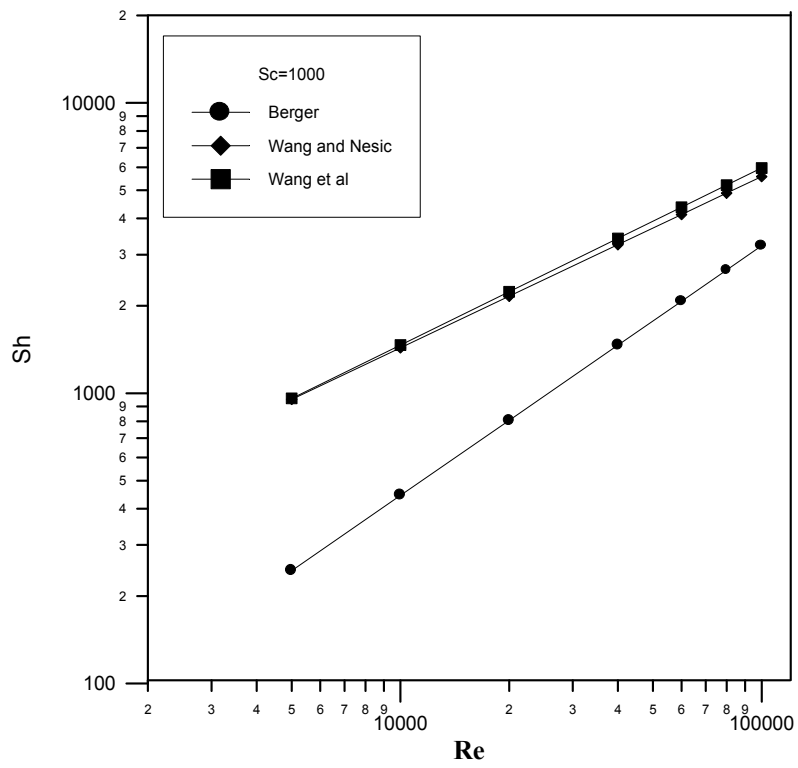


Fig. 5.7: Comparison between Single Phase Sh and Two phase Sh.

5.2 Two Phase

5.2.1 Void Fraction for Annular Flow

5.2.1.1 Effect of Re

Figs. 5.8 through 5.13 show the variation of void fraction (α) with superficial liquid Re (Re_{sL}) in annular flow as obtained from different authors, at different superficial gas Re (Re_{sG}) and various temperatures. The figures reveal that as superficial liquid Re (Re_{sL}) increases the void fraction decreases because the volume of liquid inside the pipe increased and this leads to decrease the volume of the gas, as a result the void fraction (α) decreases and vice versa. Also, it is evident that Zivi [1968] and Hart et al [1989] models are in harmony for the entire investigated range of Re_{sL} and temperatures.

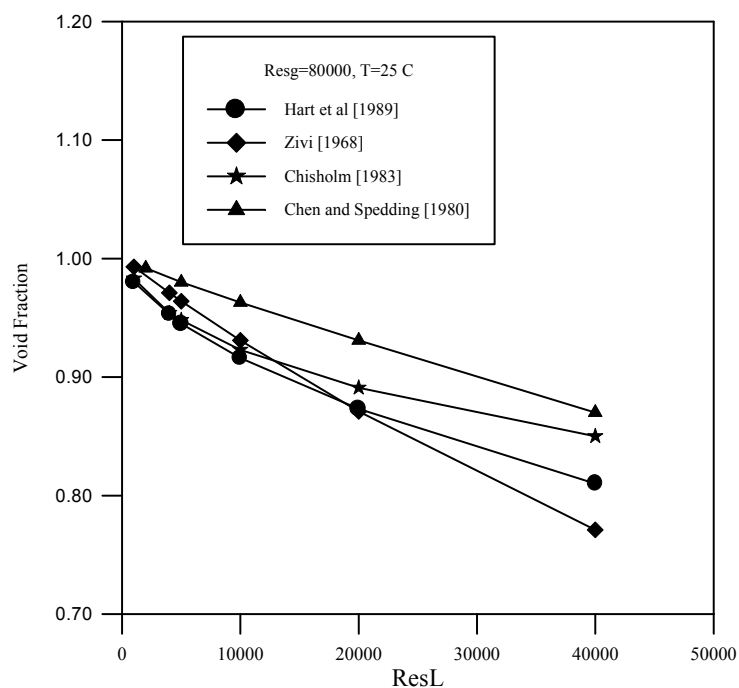


Fig. 5.8: Variation of Void Fraction with Re_{sL} at $Re_{sg}=80000$ and $T=25\text{ }^{\circ}\text{C}$

as Obtained from Various Authors.

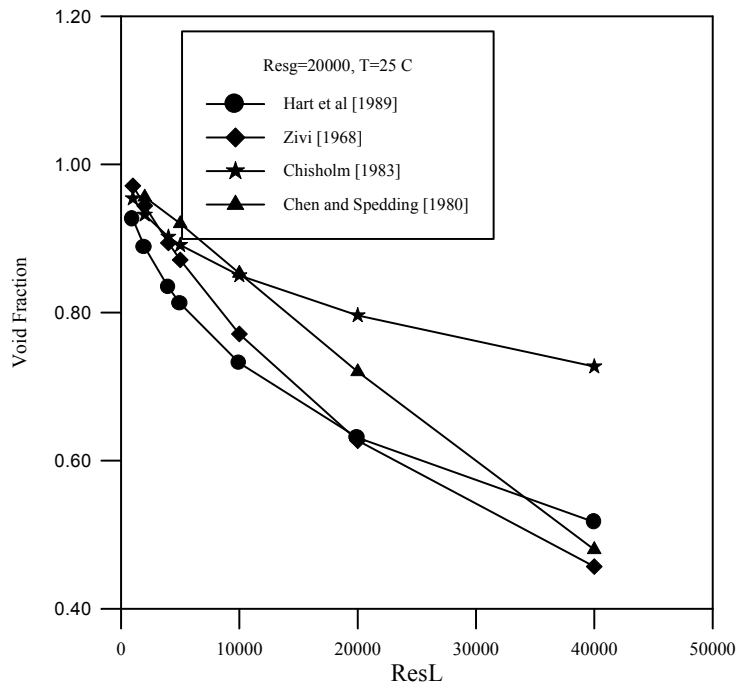


Fig. 5.9: Variation of Void Fraction with Re_{sL} at $Re_{sg} = 20000$ and $T = 25^\circ C$ as Obtained from Various Authors.

Obtained from Various

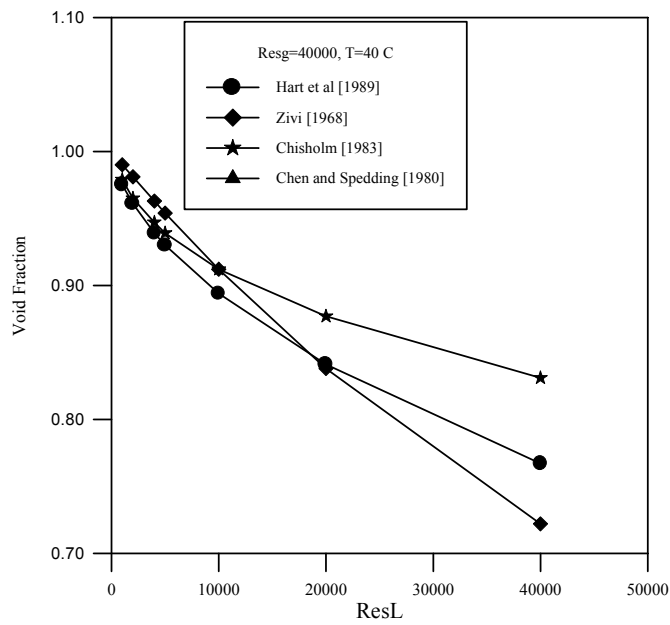


Fig. 5.10: Variation of Void Fraction with Re_{sL} at $Re_{sg} = 40000$ and $T = 40^\circ C$ as Obtained from Various Authors.

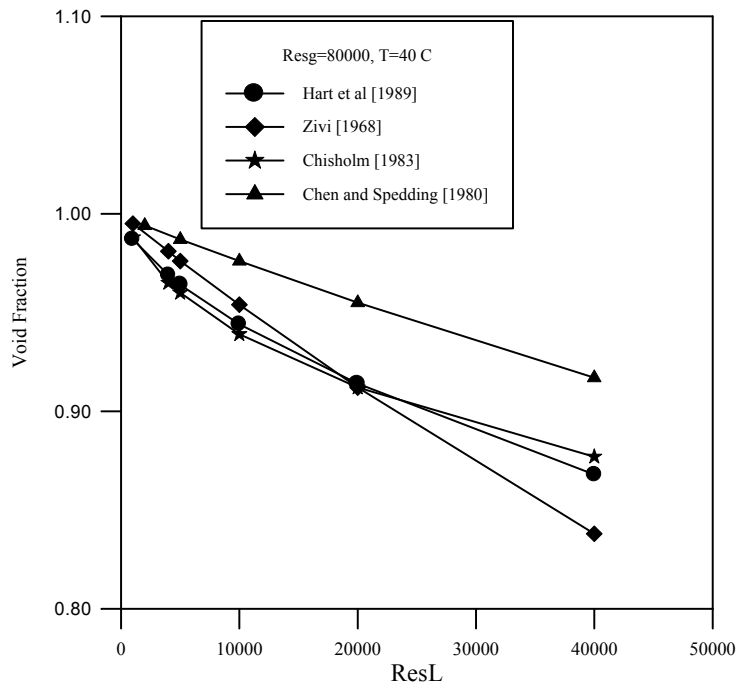


Fig.5.11: Variation of Void Fraction with Re_{sL} at $Re_{sg} = 80000$ and $T = 40^\circ C$ as Obtained from Various Authors.

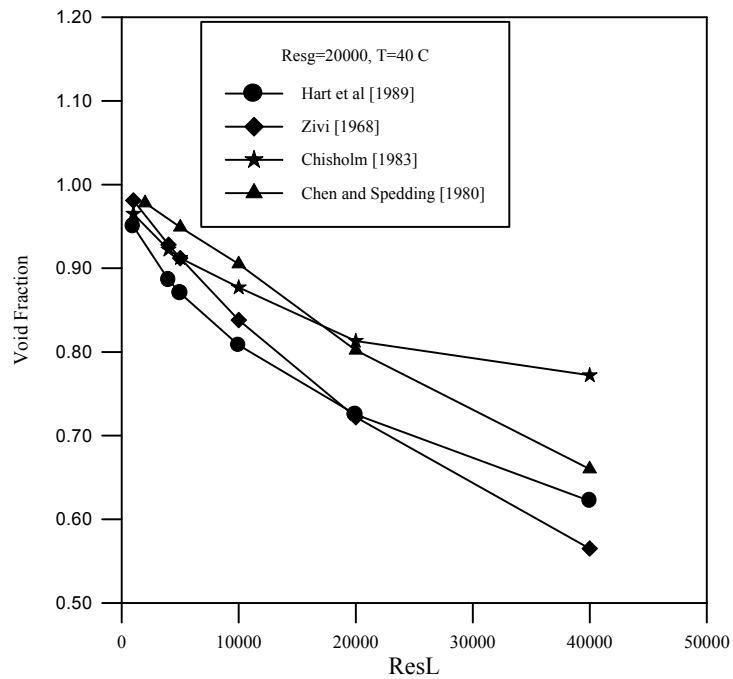


Fig. 5.12: Variation of Void Fraction with Re_{sL} at $Re_{sg} = 20000$ and $T = 40^\circ C$ as Obtained from Various Authors.

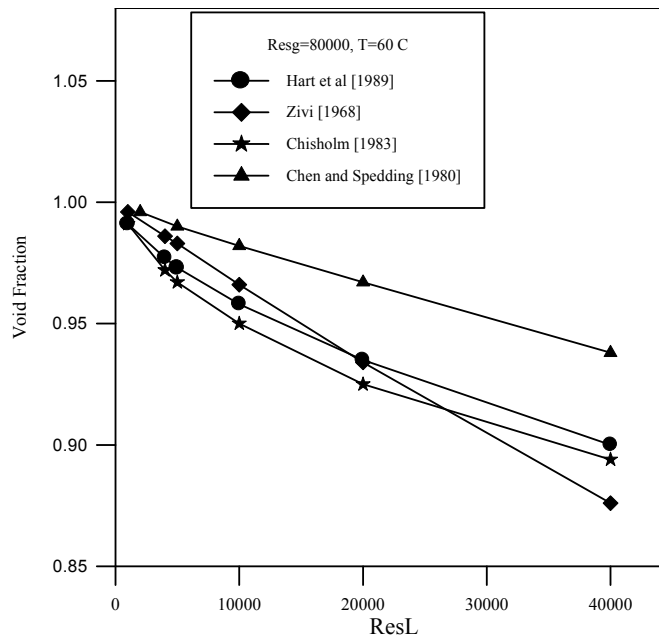


Fig. 5.13: Variation of Void Fraction with Re_{sL} at $Re_{sg} = 80000$ and $T = 60\text{ }^\circ\text{C}$ as Obtained from Various Authors.

Figure 5.14, for $Re_{sL} = 20000$ and $T = 25\text{ }^\circ\text{C}$, shows the variation of void fraction (α) with superficial gas Re (Re_{sg}) as obtained by different authors. It is clear that Hart et. al [1989] and Zivi [1968] are coincide with each other while Chisholm [1983] and Chen and Spedding [1980] exhibit some deviation. As the Re_{sg} increases the void fraction increases by increasing the gas volume in the pipe.

5.2.1.2 Effect of Liquid Temperature

The effect of liquid temperature on the void fraction is illustrated in Fig. 5.15. It is evident that the temperature increase leads to increase the void fraction. This behavior of void fraction with temperature is interpreted as follows; at a particular Re_{sL} when the temperature increases the liquid viscosity considerably decreases leading to decrease the liquid superficial velocity decreases causing an increase the void fraction (gas holdup).

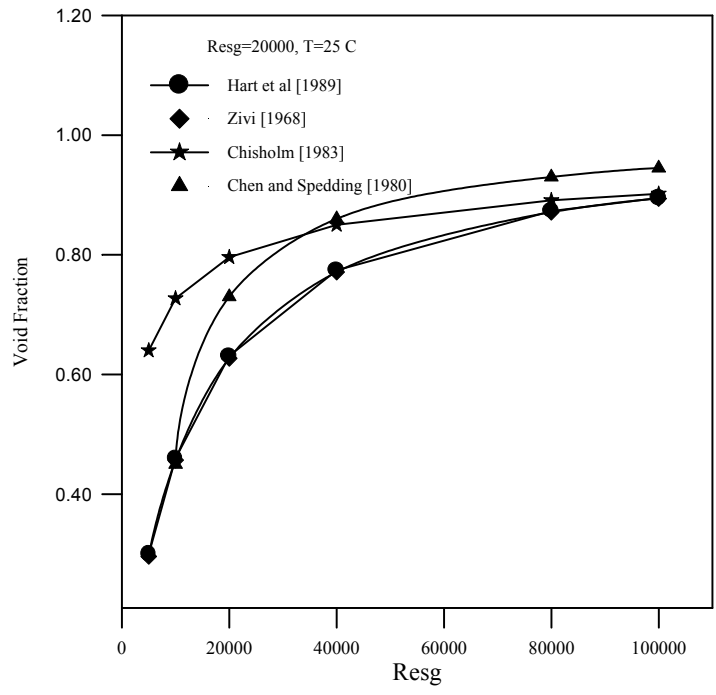


Fig. 5.14: Variation of Void Fraction with Re_{sg} at $Re_{sL} = 20000$ and $T = 25^\circ C$ as Obtained From Various Authors.

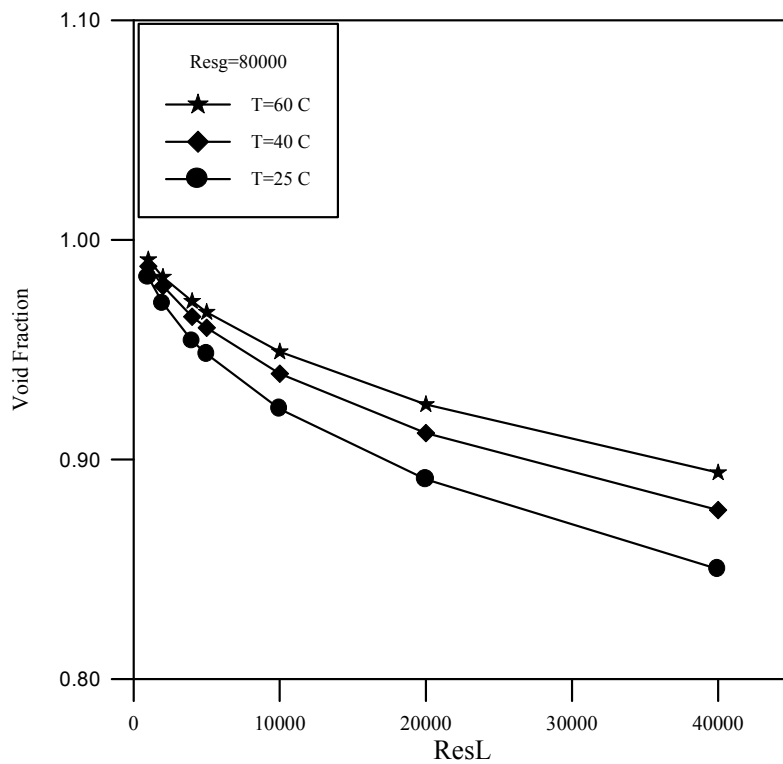


Fig. 5.15: Variation of Void Fraction with Re_{sL} for $Re_{sg} = 80000$ at Various Temperature.

5. 2. 2 Friction Factors

In present analysis for annular flow the friction factor between wall and liquid is estimated using equation (4.14) and the interfacial friction factor is estimated using equation (3.35).

5. 2. 2. 1 Effect of Liquid and Gas Reynolds Numbers

Figure 5.16 shows the effect of superficial liquid Re (Re_{sL}) on the friction factor at the wall (f_{wL}). It is evident that an increase in superficial liquid Re (Re_{sL}) leads to decrease the friction factor at the wall (f_{wL}), and this can be clearly seen from the Blasius relation Eq (4.14). This is in agreement with work of Wongwises and Naphon [2000] for annular flow.

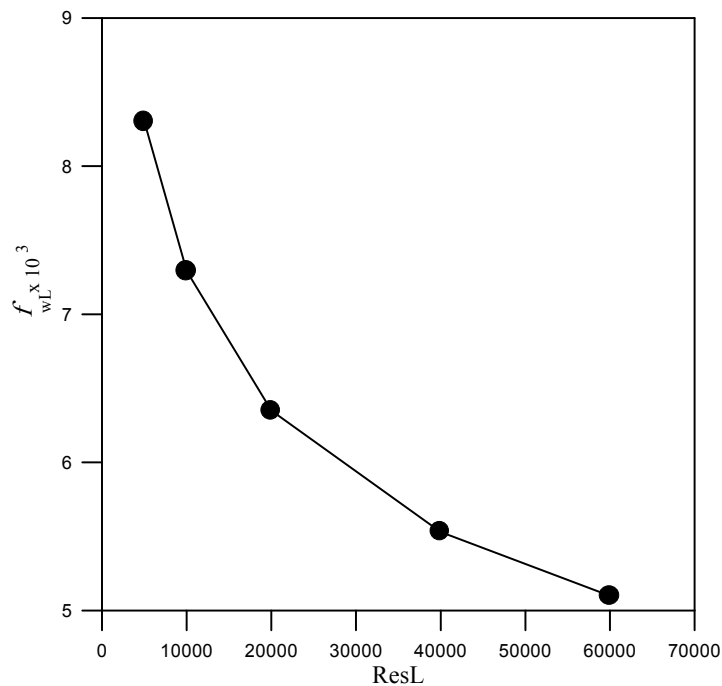


Fig. 5.16: Effect of Re_{sL} on the Friction Factor at the Wall.

The variation of interfacial friction factor with Re_{sL} at various superficial gas Re (Re_{sG}) at liquid temperature of 25 °C is shown in Fig. 5.17. The interfacial friction factor f_i results from drag exerted by the gas phase on

a rough surface, i.e. the rippling liquid phase [Sato et. al. 1981]. It is evident that as superficial liquid Re increased, the interfacial friction factor (f_i) increased. Also the figure reveals that the interfacial friction factor (f_i) decreases with increase superficial gas Re. It is to be noted from Figs 5.16 and 5.17 that the values of interfacial friction factor (f_i) are higher than the wall friction factor (f_{wL}). This is attributed to the presence of waves and ripples at gas liquid interface [Chen and Spedding 1983, Wongwises and Naphon 2000]. The presence of waves and ripples cause the f_i to increase with Re_{sg} as in case of the single phase flow on rough surface where for these surfaces the f increases as Re increases [Knudsen and Katz 1958, Dawson and Trass 1972]. Douglas and Matthews [1998] ascribed the increase in friction factor with Re on rough surfaces to the decrease in thickness of the momentum boundary layer eventually the projections penetrate the boundary layer and the behavior deviates from that of smooth pipe.

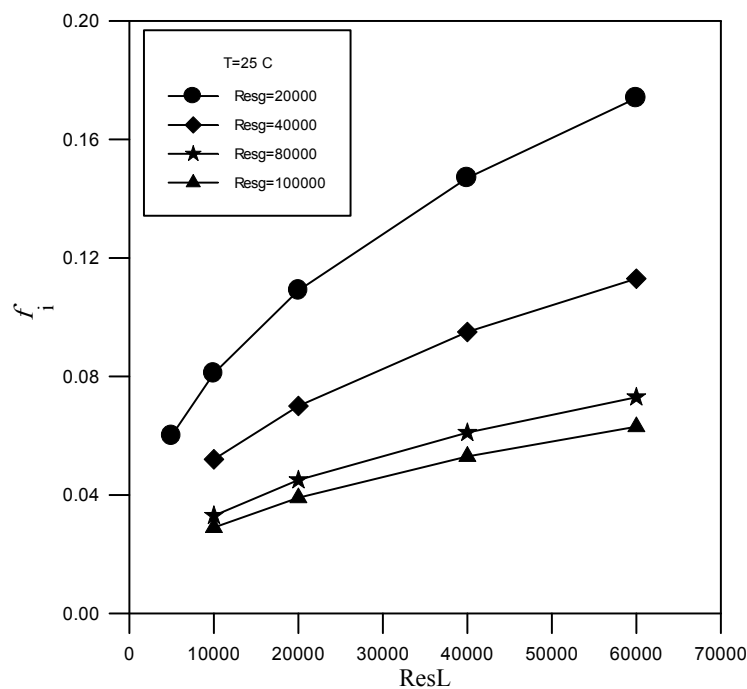


Fig. 5.17: Effect of Re_{sL} on the Interfacial Friction Factor at Different Re_{sg} .

5.2.2.2 Effect of Temperature

Figure 5.18 shows the effect of superficial liquid Re (Re_{sL}) on the interfacial friction factor (f_i) at various temperatures and $Re_{sG}=80000$. It is clear that as the liquid temperature increases the interfacial friction factor (f_i) decreased due to the decreases in the viscosity of the liquid which in turn leads to reduce the friction forces between the liquid and gas at the interface.

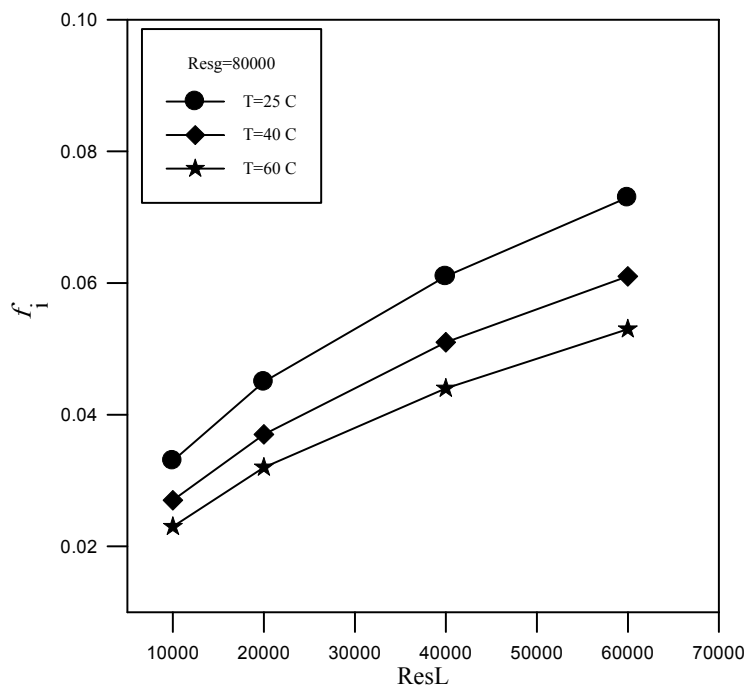


Fig. 5.18: Effect of Re_{sL} on the Interfacial Friction Factor at Different Temperatures.

5.2.3 Shear Stress

5.2.3.1 Effect of Liquid and Gas Reynolds Numbers

Figure 5.19 shows the variation of wall shear stress (τ_{wL}) with Re_{sL} at different Re_{sG} , for $T=25\text{ }^\circ\text{C}$. It indicates that as superficial liquid Re (Re_{sL}) increase, the wall shear stress (τ_{wL}) increases. This is due to the increase of the friction forces between the liquid layers and the pipe wall. It is also

evident that as Re_{sg} increases, the wall shear stress (τ_{wL}) increases due to the increase of the gas velocity which leads to increase the void fraction (α) and that cause a reduce in the liquid layer thickness causing to increase the momentum transfer from the gas to the liquid and then to the wall.

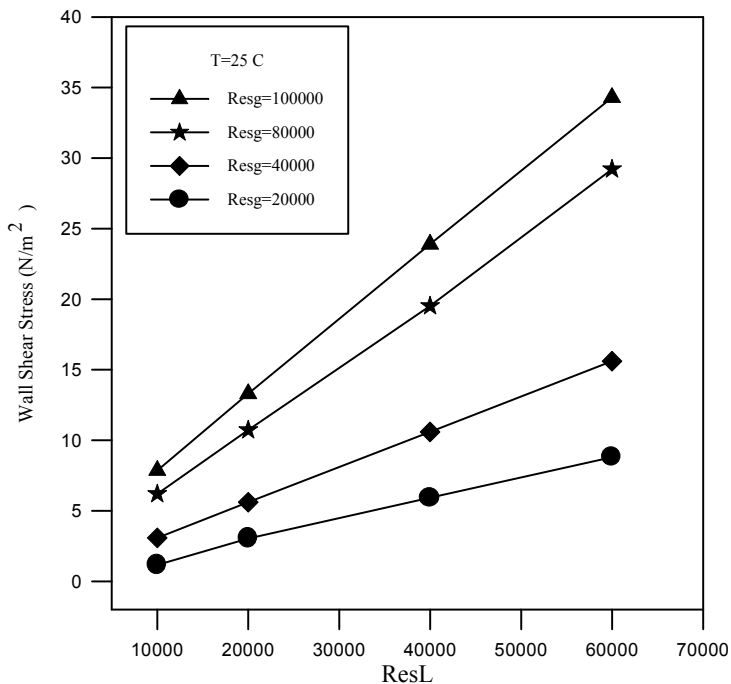


Fig. 5.19: Variation of τ_{wL} with Re_{sL} at various Re_{sg} and $T=25\text{ C}$

Figure 5.20 shows the variation of interfacial shear stress (τ_i) with superficial liquid Re at different superficial gas Re for $T=25\text{ }^\circ\text{C}$. The figure reveals that the increase of interfacial shear stress (τ_i) with increase of superficial gas Re . This increase is due to the increase of the gas velocity which leads to increase the friction forces between the gas and the liquid at the interface. Also the figure reveals that as superficial liquid Re increases, the interfacial shear stress (τ_i) increases and this can be attributed to the increased interaction between the liquid layer and the gas layer.

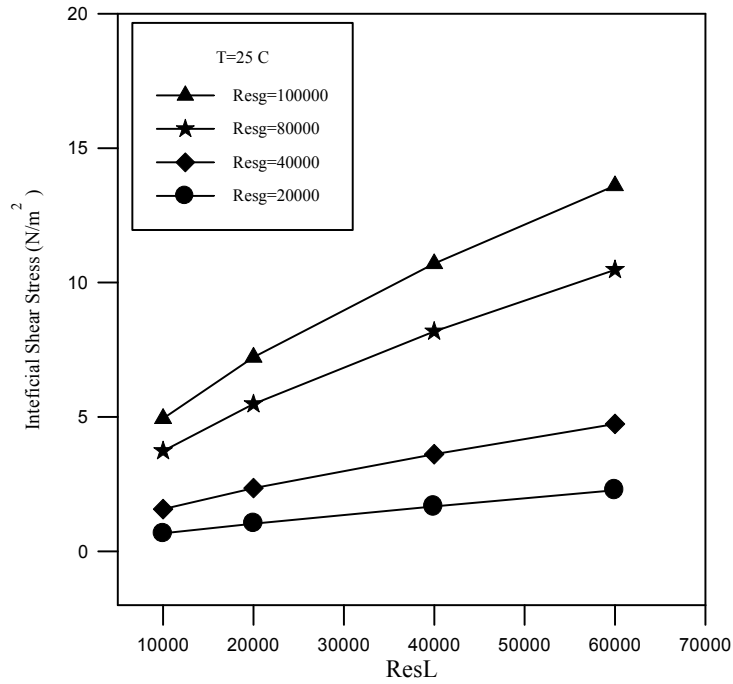


Fig. 5.20: Variation of τ_i with Re_{sL} at various Re_{sg} and $T=25\text{ C}$

5.2.3.2 Effect of Temperature

Figure 5.21 shows the variation of interfacial shear stress (τ_i) with superficial liquid Re (Re_{sL}) at various temperatures. It is clear that as the temperature increased the interfacial shear stress (τ_i) decreased. This decrease in the interfacial shear stress (τ_i) can be attributed to the fact that the temperature reduces the viscosity of the liquid and this leads to decrease the friction forces between liquid and gas at the interface.

For $Re_{sg}=80000$, Fig. 5.22 presents the variation of the wall shear stress (τ_{WL}) with superficial liquid Re at various temperatures. It is evident that as the temperature increased, the wall shear stress (τ_{WL}) decreased. This decrease in the wall shear stress (τ_{WL}) is due to the fact that the temperature increase reduces the viscosity of the liquid and this leads to decrease the friction forces between the liquid and the pipe wall.

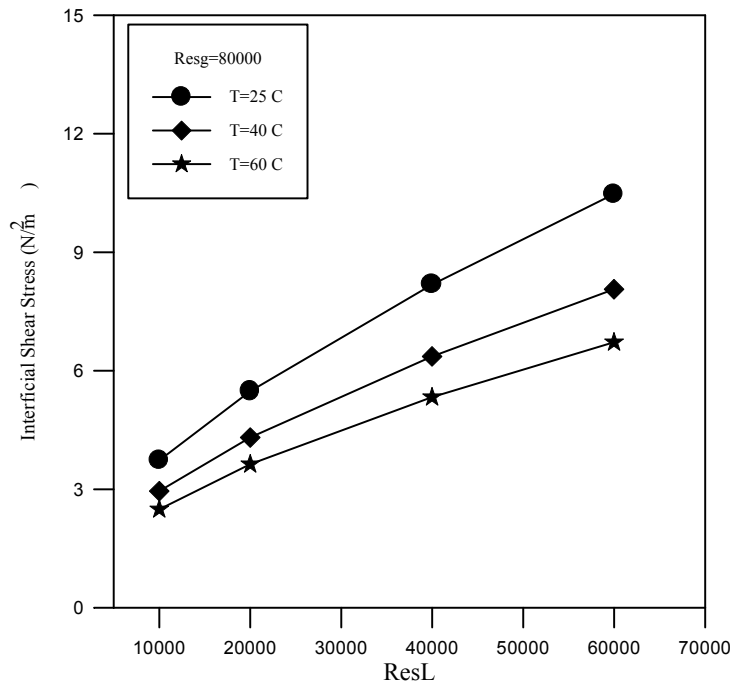


Fig. 5.21: Variation of τ_i with Re_{sL} at Different Temperatures

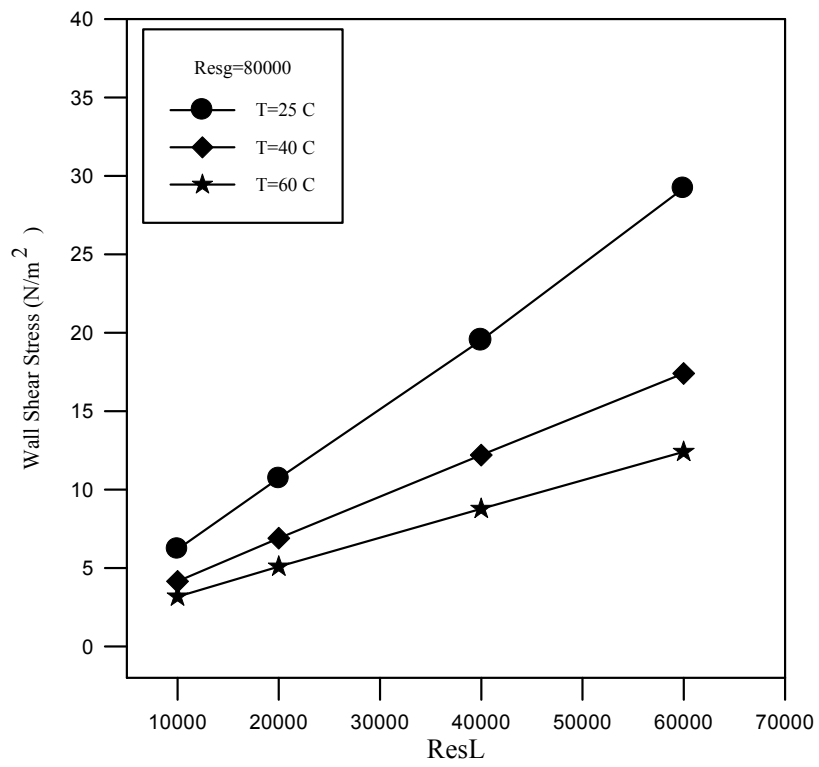


Fig. 5.22: Shows the Variation of τ_{wL} with Re_{sL} at Different Temperatures.

5.2.4 Mass Transfer Coefficient

Equation (4.58) is employed to predict the mass transfer coefficient for annular flow for wide range of Re_{sL} , Re_{sg} , and Sc_L . The calculations are carried out for $Sc_g=1$.

5.2.4.1 Comparison of Present Results with the Experimental Correlations

Figures 5.23 to 5.27 show the variation of Sh obtained from present analysis (using Eq.(4.58)) with Re_{sL} as compared with the proposed experimental correlations for two phase flow at different superficial gas Re and various temperatures and liquid (Sc_L) values. It is clear that the Sh predicted from present analysis is in excellent agreement with experimental work of Wang et. al [2002] for the whole range of temperature and liquid (Sc_L). It is to be noted that the Sh from Wang and Nescic model (stratified flow) coincides with Wang et al model (slug flow) despite the different flow regime indicating the similarity of mass transfer characteristics of these flow regimes.

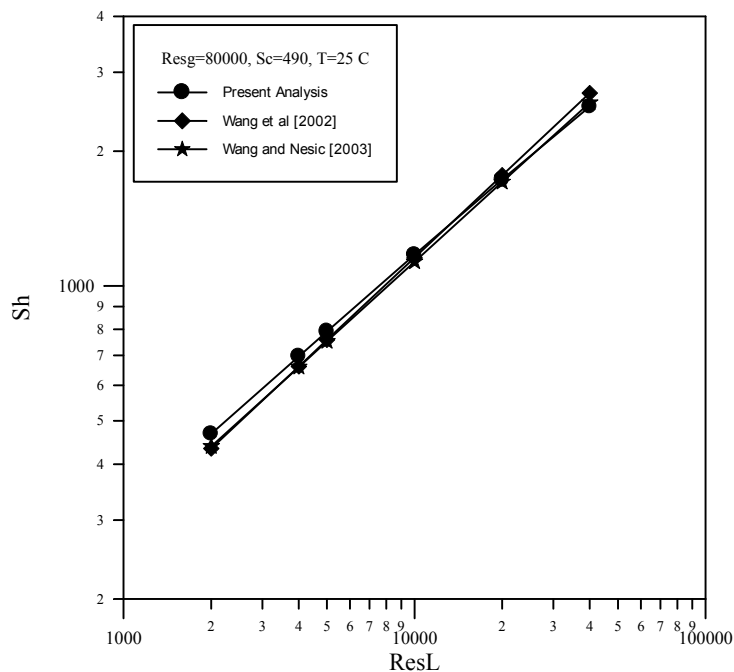


Fig. 5.23: Comparison of Sh of Present Analysis with Proposed Experimental Correlations at $Sc_L=490$.

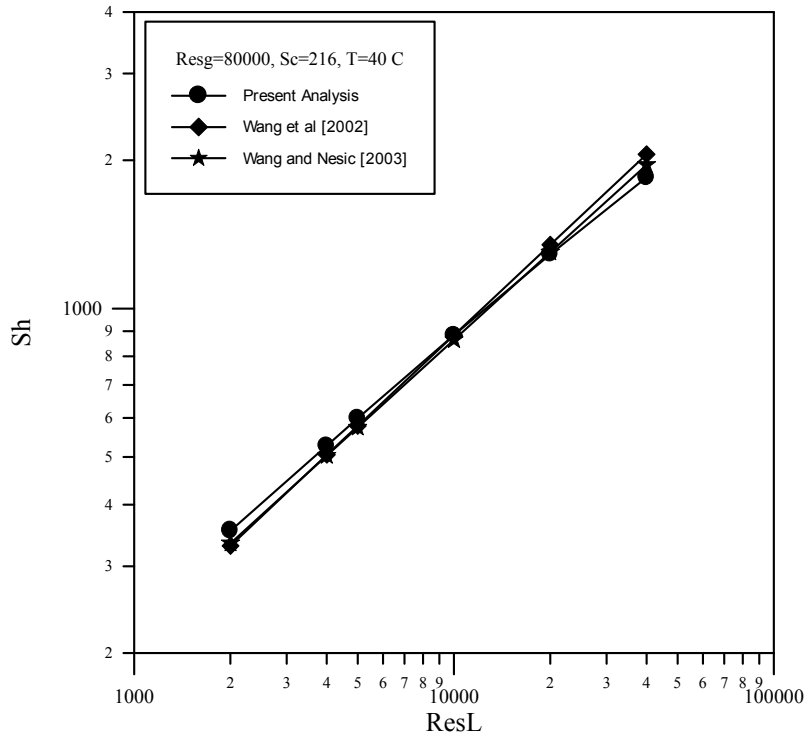


Fig. 5.24: Comparison of Sh of Present Analysis with Proposed Experimental Correlations at $Sc_L=216$.

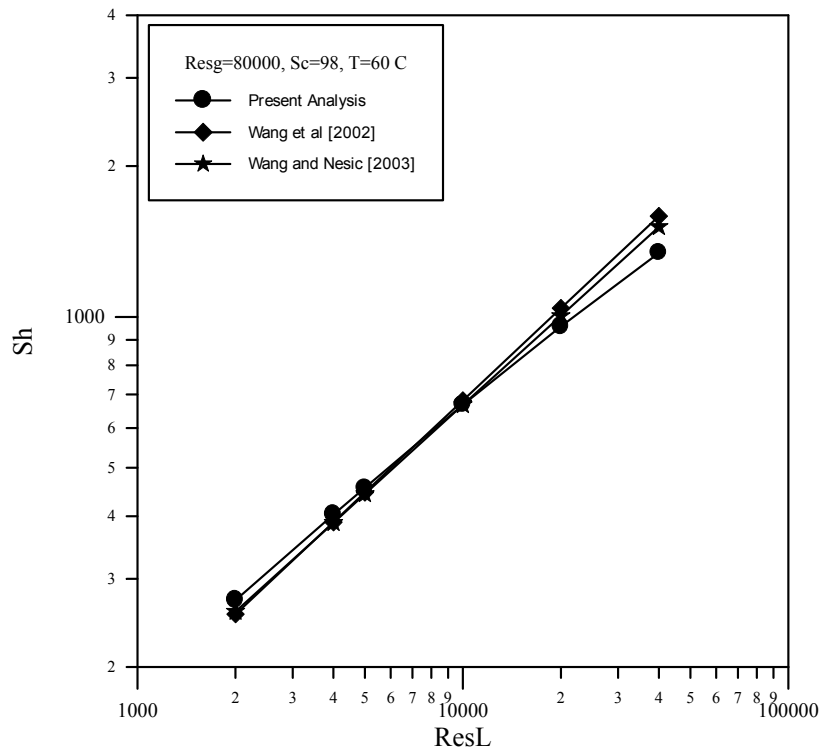


Fig. 5.25: Comparison of Sh of Present Analysis with Proposed Experimental Correlations at $Sc_L=98$.

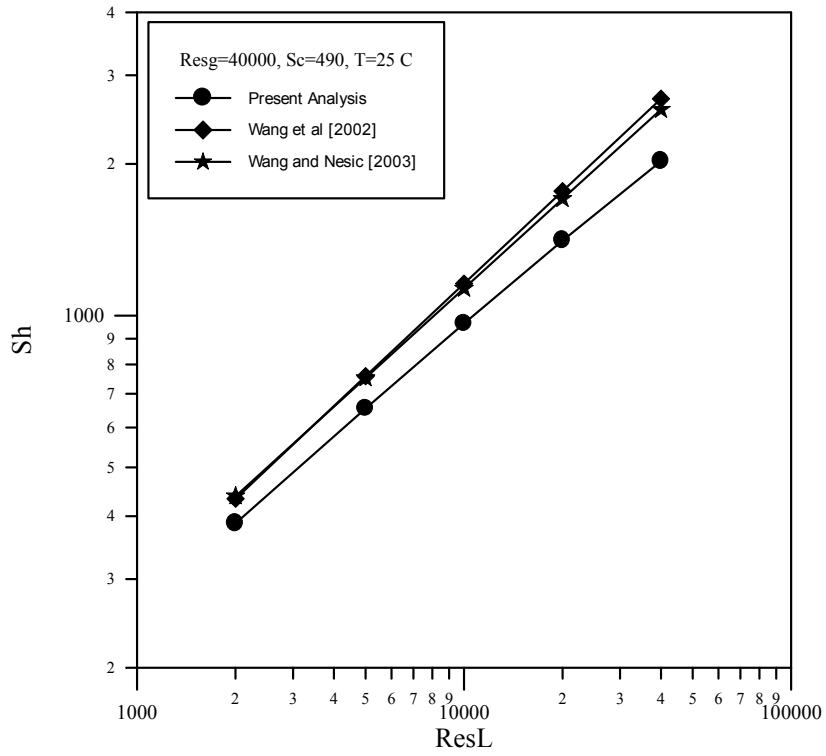


Fig. 5.26: Comparison of Sh of Present Analysis with Proposed Experimental Correlations at $Sc_L=490$.

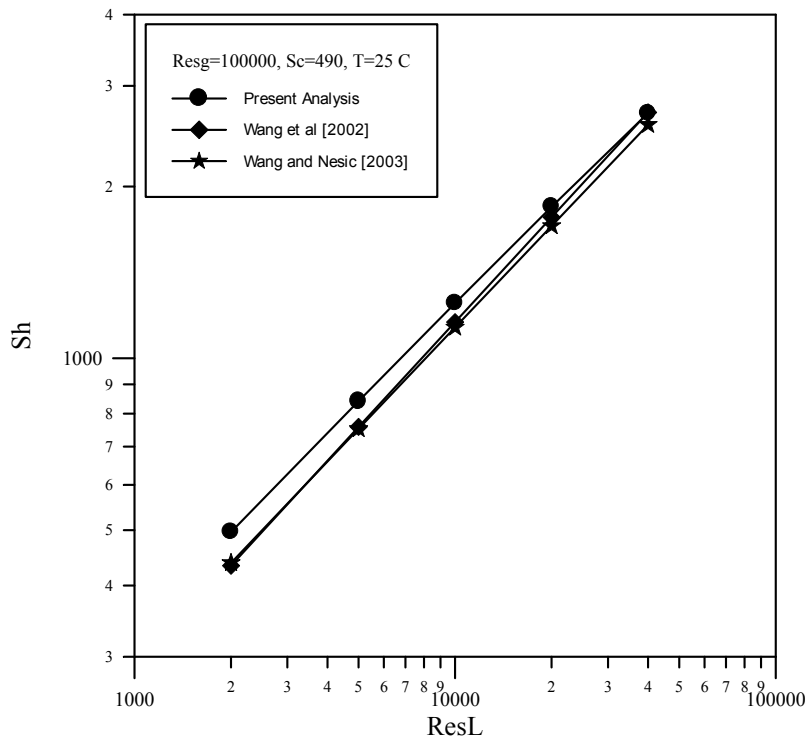


Fig. 5.27: Comparison of Sh of Present Analysis with Proposed Experimental Correlations at $Sc_L=490$.

5.2.4.2 Effect of Liquid Superficial Re

Figures 5.28 to 5.30 show the variation of Sh with superficial liquid (Re_{sL}) for various liquid (Sc_L) at different superficial gas (Re_{sg}). It is evident that Sh increased with increasing of superficial liquid (Re_{sL}), also these figures reveal that Sh increases with increasing of superficial gas (Re_{sg}). The increase of Sh with Re_{sL} is due to the increased eddy diffusion within the liquid layer reducing thickness of diffusion layer which represent the main resistance to mass transfer [Welty et. al. 2001, Brodkey and Harshy 1998, Poulson 1983] enhancing the transfer of active species (O_2) from the bulk to the wall leading to increase the mass transfer rate.

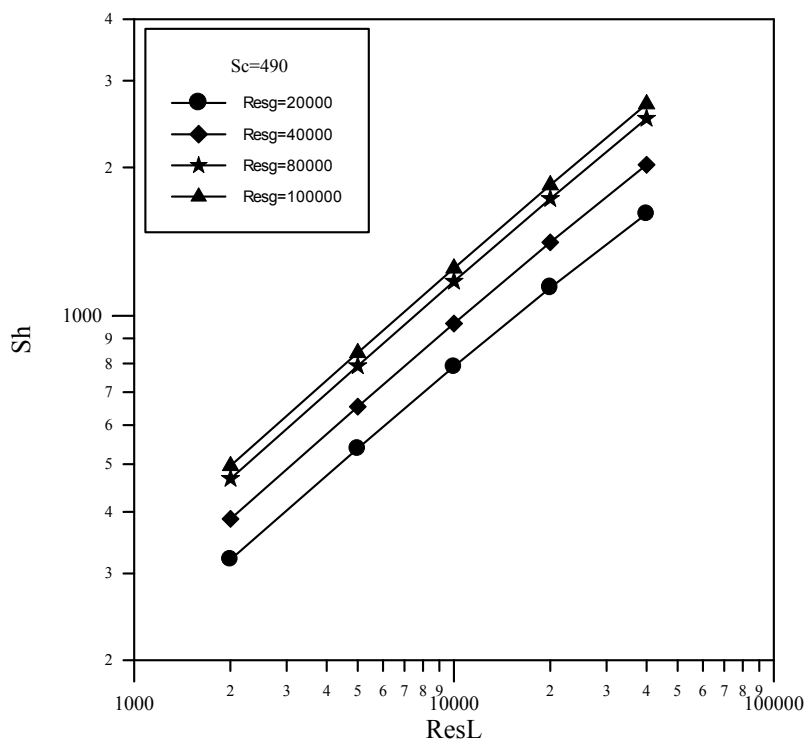


Fig. 5.28: Variation of Sh with Re_{sL} at Various Re_{sg} for $Sc_L=490$

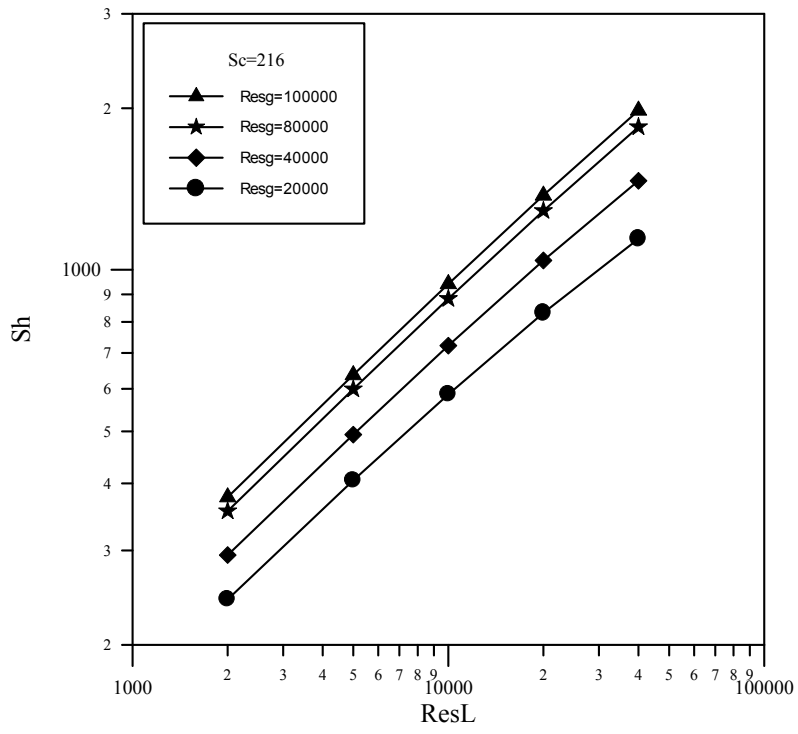


Fig. 5.29: Variation of Sh with Re_{sL} at Various Re_{sg} for $Sc_L=216$.

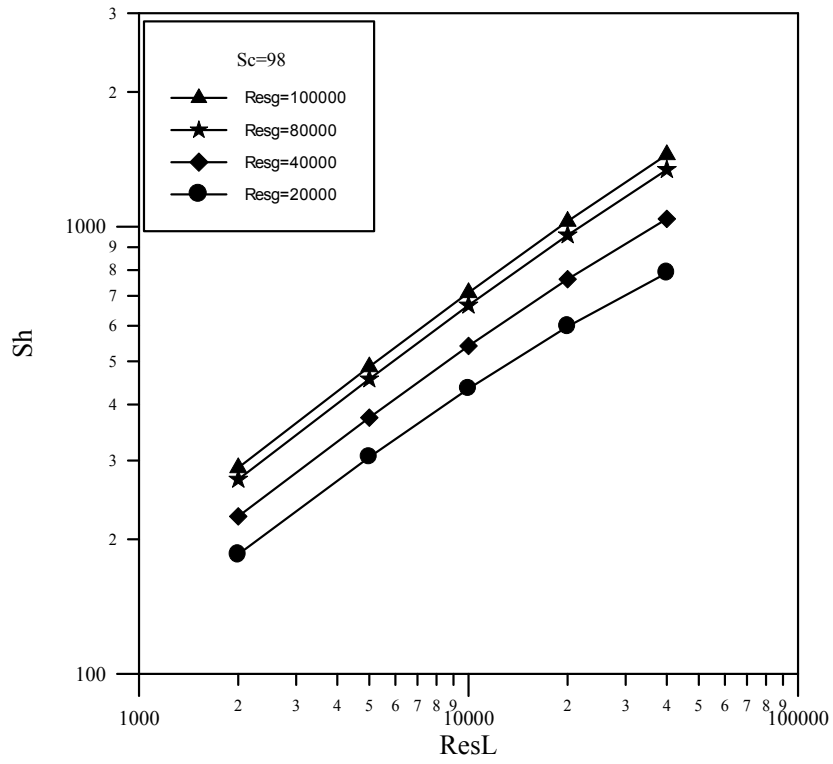


Fig.5.30: Variation of Sh with Re_{sL} at Various Re_{sg} for $Sc_L=98$.

5.2.4.3 Effect of Gas Superficial Re

To examine the capability of Eq. (4.58) to predict the influence of gas Re on the mass transfer coefficient, the results are compared with the experimental results of Langsholt et al [1997] in Fig. 5.31, where they determined Sh under stratified two phase flow at various gas velocities and various liquid holdup (or void fraction) in 0.1 m diameter pipe. Fig. 5.31 shows the variation of Sh with superficial gas Re at constant superficial liquid Re obtained from Eq. (4.58) as compared with the results of Langsholt et. al. It is evident that results obtained from present analysis agree well with experimental Langsholt et. al. data for the whole range of α . The difference may be ascribed to the difference in flow regime of present analysis (annular flow) and Langsholt et al (stratified flow). Fig. 5.31 reveals that increasing gas Re leads to increase Sh. This can be attributed to the increased eddy diffusion at the gas liquid interface increasing the transport of O₂ from air to water and hence to the pipe wall.

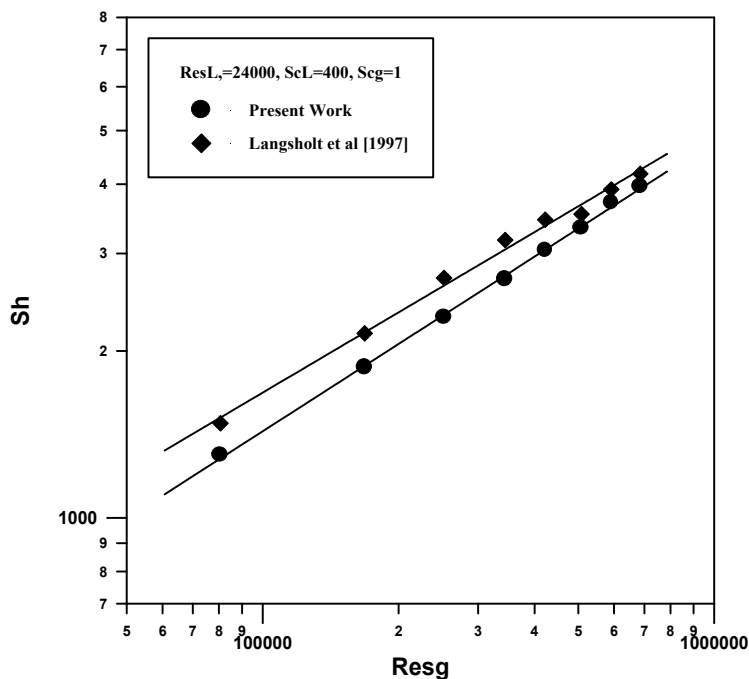


Fig. 5.31: Variation of Sh with Re_{sg} as Compared with Langsholt et al.

5.2.4.4 Effect of Liquid Schmidt Number and Temperature

Fig. 5.32 shows the effect of liquid Sc on the Sh for various values of liquid superficial Re . It can be noted that as the Sc_L increases, then Sh increases. This increase is ascribed to the fact that increasing Sc_L leads to decrease the thickness of diffusion layer (δ_d) [Harriot and Hamilton 1965, Brodkey and Harshy 1989, Geankoplis 1984] facilitating the passage of active species (O_2) to the pipe wall.

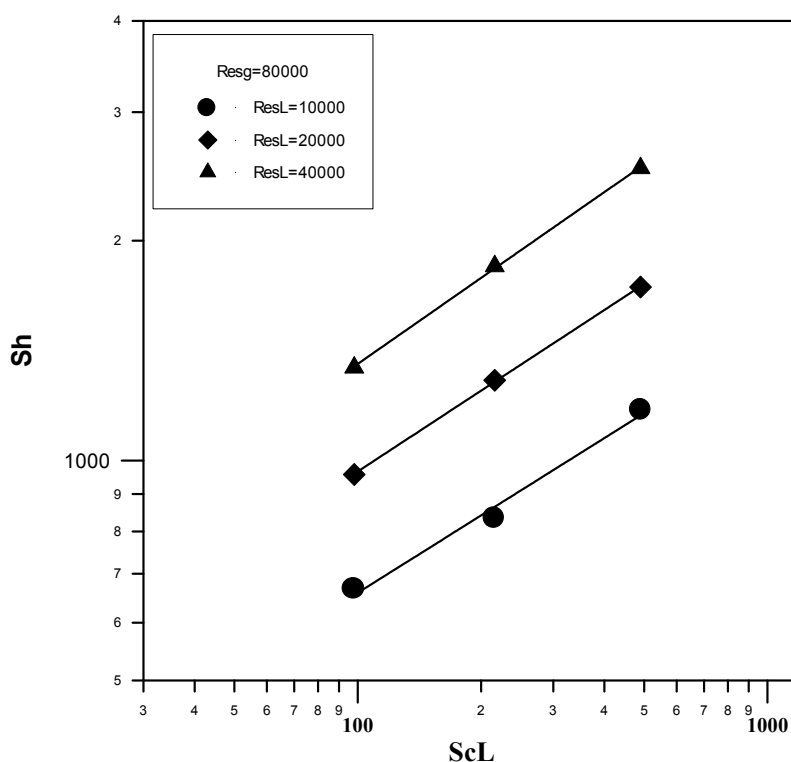


Fig. 5.32: Variation of Sh with Sc_L at Various Values of Re_{sL} .

5.2.4.5 Effect of Void Fraction

To investigate the effect of void fraction (α) on the friction factor and mass transfer coefficient, α is assumed to be independent on Re_L and Re_g . Fig. 5.33 shows the effect of α on the f_{wL} for stratified flow. It is clear that the f_{wL} decreases as Re_L increases. Also at a particular Re_L as the α increases, the friction factor increases via decreasing Re_{sL} leading to decrease of f_{wL} .

according to Eq. (4.14). Fig. 5.34 reveals that f_{wg} decreases as α increases because Re_{sg} increases leading to decrease f_{wg} according to Eq. (4.15). This trend is in accordance with the experimental results of Chun and Kim [1995], where they found experimentally that increasing Re_g leads to decrease f_{wg} .

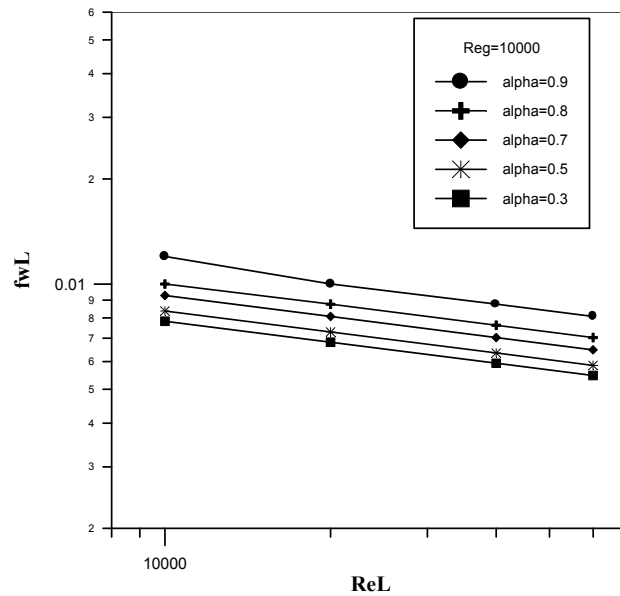


Fig. 5.33: Variation of f_{wL} with Reg at Various α .

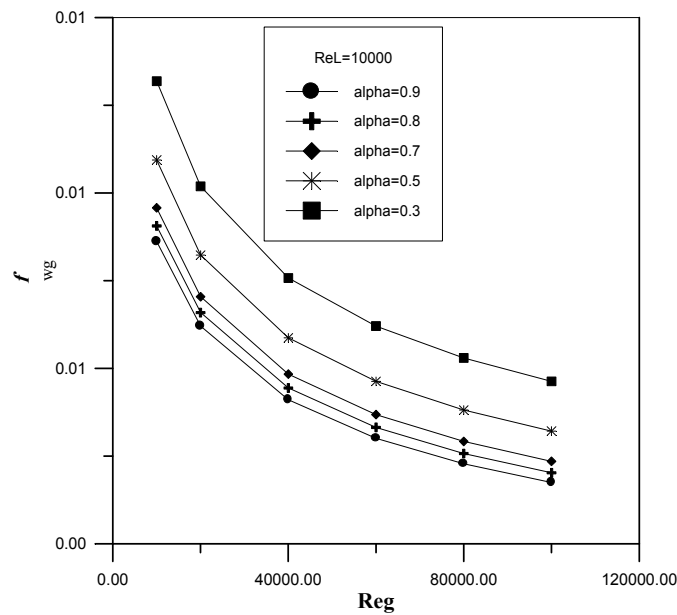


Fig. 5.34: Variation of f_{wg} with Reg at Various α .

Figure 5.35 shows the variation of Sh with Re_L at constant Re_g at $Sc_L=400$ and various α values. The Fig. indicates that Sh increases with

increasing Re_L for all α values. Also Sh exhibits unstable trend with α . The lower values of Sh are encountered at maximum α (0.9) and minimum α (0.1) indicating that Sh decreases as the system approaches the single phase. Hence the mass transfer rate increases at intermediate values of α (or liquid holdup). The void fraction of 0.1 is limited case in practice in annular flow since this type of two phase flow characterized by high void fraction [Tong 1975].

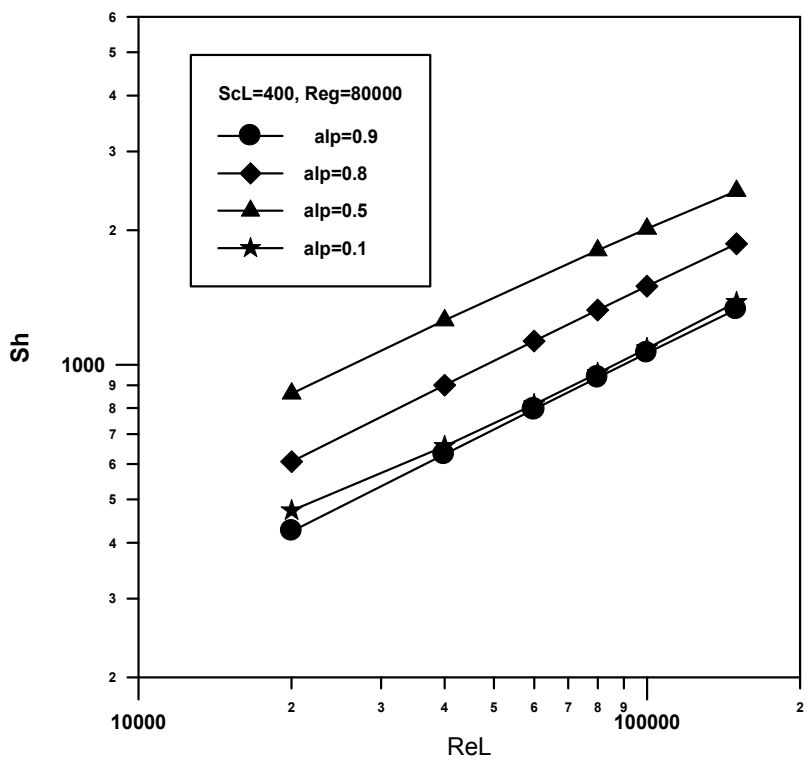


Fig. 5.35: Variation of Sh with Re_L at Various α Values.

Fig. 5.36 shows the variation of Sh with superficial liquid Re at constant superficial gas Re and various α values at Sc_L of 400. It is evident that at a particular Re_{sL} , α has slight effect on Sh indicating that Re_{sL} is the effective rather than Re_L .

Using statistical analysis, the following correlation is obtained for the investigated range of Re_{sg} , Re_{sL} and Sc_L with 5% error:

$$Sh=0.032Re_{sL}^{0.54}Re_{sg}^{0.299}Sc_L^{0.344} \quad c.c=0.99 \quad (5.1)$$

It is to be noticed that the dependence of Sh on Sc_L is in harmony with the previous findings concerning the effect of Sc on Sh in single phase turbulent mass transfer [Lin and Sherwood 1950, Harriot and Hamilton 1965, Hubard and Lightfoot 1966, Dawson and Trass 1972, Rosen and Tragrath 1995, Aravinth 2000]. Also Eq. (5.1) indicates that the dependence of Sh on Re_{sL} is higher than that of Re_{sg} indicating that the effect of liquid Re on mass transfer rate is higher than that of gas Re .

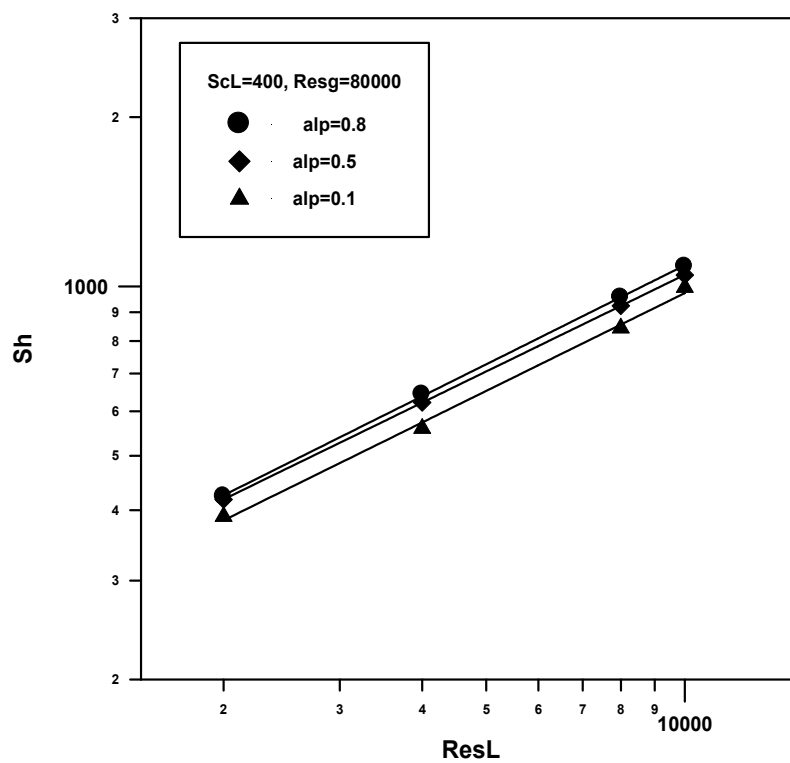


Fig. 5.36: Variation of Sh with Re_{sL} at Various α Values.

5.2.5 Mass Transfer Coefficient from Eddy Diffusivity in Two Phase

Eqs. (4.65), (4.67), and (4.68) are employed to obtain Sh based on various two phase eddy diffusivity models. Figures 5.37 and 5.38 show a comparison of Sh obtained from various eddy diffusivity models proposed by different authors for two phase flow, for $Re_{sg} = 80000$ and various Sc_L as compared with experimental correlation of Wang and Nesic [2003]. The trend reveals that Sato and Welle [1981] and Wang and Nesic [2003] models exhibit fair agreement with experimental correlation of Wang and Nesic [2003], while, Sato et al [1981] model exhibits considerable deviation. This poor agreement with experimental results shown in Figs. 5.37 and 5.38 reveals the complexity of two phase flow and the unpredictability of eddies turbulence in two phase flow. Accordingly, no one of the proposed eddy diffusivity models agree well with the experimental data. It is worthy to note that the eddy diffusivity expressions developed in present analysis (Eqs. (4.53)) give more accurate results (Figs. 5.23 to 5.27) than those presented in Figs. 5.37 and 5.38.

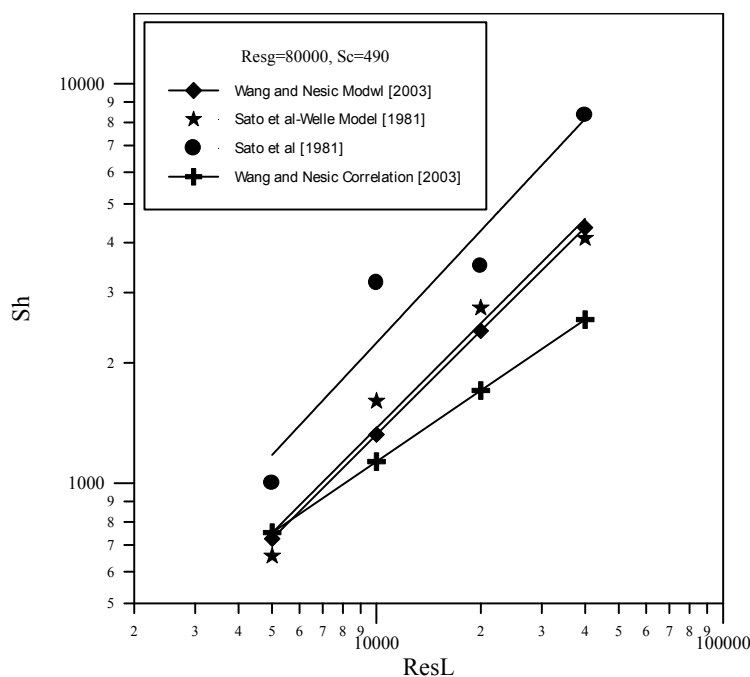


Fig. 5.37: Comparison of Sh Obtained from Eddy Diffusivity Models Proposed by Various Authors.

5. 2. 6 Concentration Profile

The concentration profile in the liquid layer is obtained by inserting the eddy diffusivity expressions (Eqs. (4.53)) developed in present analysis in Eq. (4.64) and performing the integration for each value of z . The numerical values of C^* are presented in tables B. 24 to B.27 in appendix B.

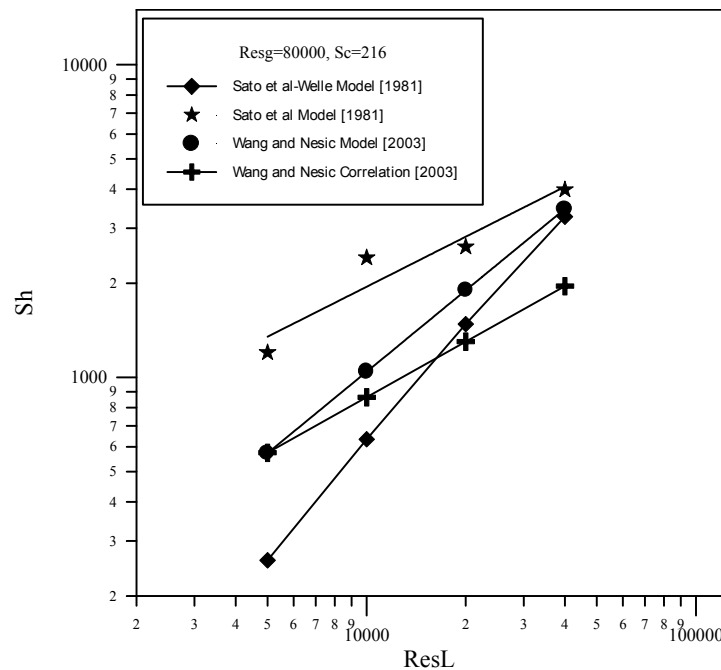


Fig. 5.38: Comparison of Sh Obtained from Eddy Diffusivity Models Proposed by Various Authors

5. 2. 6. 1 Effect of Liquid Superficial Re

Figure 5.39 and 5.40 show concentration profile in the liquid layer. The concentration profile increases from the wall surface where $C=C_w$, which is nearly zero, to the liquid bulk. As the bulk is approached the C increases and hence C^* increases according to Eq. (5.2). Beyond the diffusion layer the concentration C approaches C_{bL} and this leads to make C^* is constant and eventually one. Figs 5.39 and 5.40 illustrates the effect of Re_{sL} , for $Re_{sg}=40000$ and $Re_{sg}=80000$ at constant liquid Sc ($Sc_L=490$). The

linear part of the curves represents the concentration profile occurring within the diffusion layer adjacent to the wall [Brodkey and Harshy 1998, Geankoplis 1984, Welty et al 2001]. Fig. 5.39 indicates that in the diffusion layer (linear part of the curve), the superficial liquid Re (Re_{SL}) has negligible effect on C^* . This is because the turbulent eddies resulting from the increased liquid velocity can not penetrate the diffusion layer. Out of the diffusion layer, the increase in the superficial liquid Re (Re_{SL}) leads to decrease C^* . As superficial liquid Re (Re_{SL}) increased, the concentration (C) at a particular Z in the liquid layer approached C_{bl} , because of the high turbulence. As C approaches C_{bl} , the C^* decreases according to:

$$C^* = \frac{C_{bl} - C_w}{C_{bl} - C_w}$$

As the liquid superficial Re increases the random motion of the eddies which move irregularly in all direction in the liquid layer enhanced and as a result the turbulence increases in this layer reducing in the thickness of the diffusion layer adjacent to the wall by reducing the concentration gradient (dC/dy).

5. 2.6. 2 Effect of Gas Superficial Re

For $Re_{SL} = 10000$ and $Sc_L = 490$, Fig.5.41 shows the variation of C^* with the dimensionless distance (Z) at various values of Re_{sg} . The Fig. indicates that increasing Re_{sg} slightly increases C^* beyond the diffusion layer. In addition, as superficial gas Re (Re_{sg}) is increased, the steepness of the concentration profile increase indicating a decrease in the thickness of the diffusion layer.

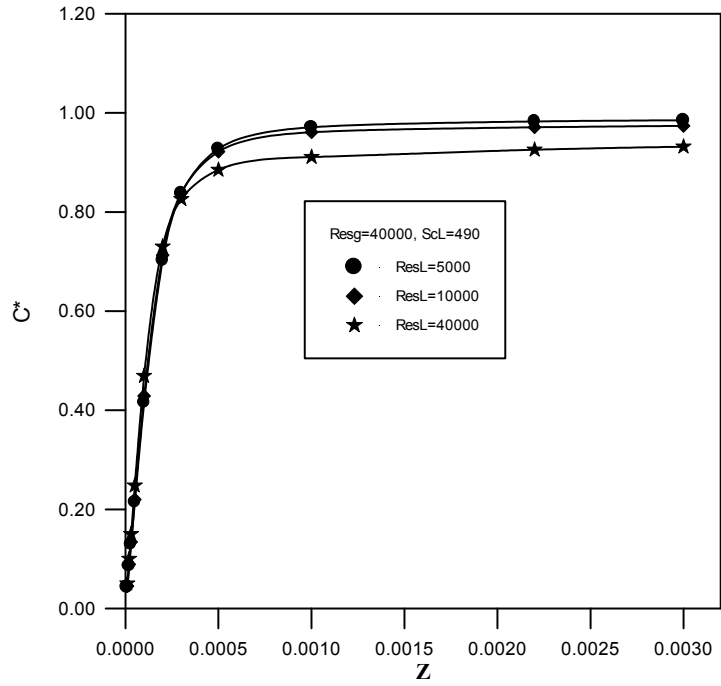


Fig. 5.39: Concentration Profile in the Liquid Layer and The Effect of Re_{sL} .

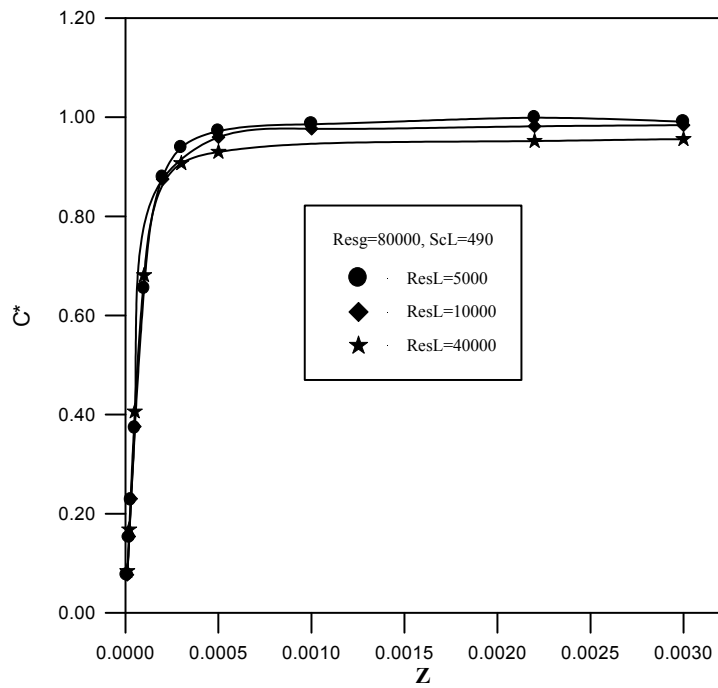


Fig. 5.40: Concentration Profile in the Liquid Layer and The Effect of Re_{sL} .

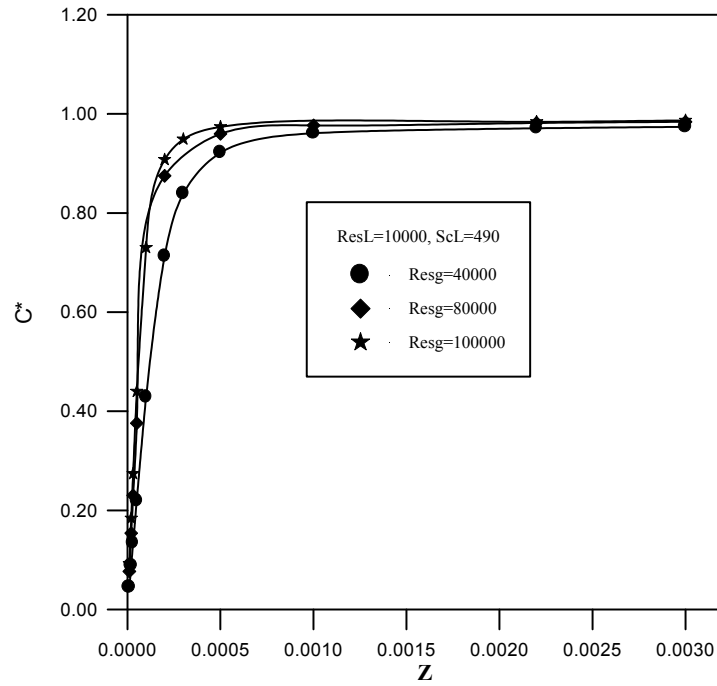


Fig. 5. 41: Concentration Profile in the Liquid Layer and the Effect of Re_{sg} .

5. 2.6.3 Effect of Liquid Schmidt Number

Figure 5.42 shows the effect of Sc_L on the dimensionless concentration (C^*) profile for $Re_{sL}=20000$ and $Re_{sg}=80000$ at various values of liquid. It indicates that a high mass transfer resistance is associated with a high concentration gradient, so that, Fig 5.42 serves to show the location of the principal resistance to mass transfer as a function of Sc_L . At low Sc_L the resistance is evidently distributed throughout the liquid, while at high Sc_L the resistance to mass transfer is progressively narrower and nearer to the wall in dimensionless terms. At high Sc_L the major resistance is concentrated near the wall. This findings is in agreement with experimental results of Hubber and Lightfoot [1966], Znad [1996] and Hasan [2003].

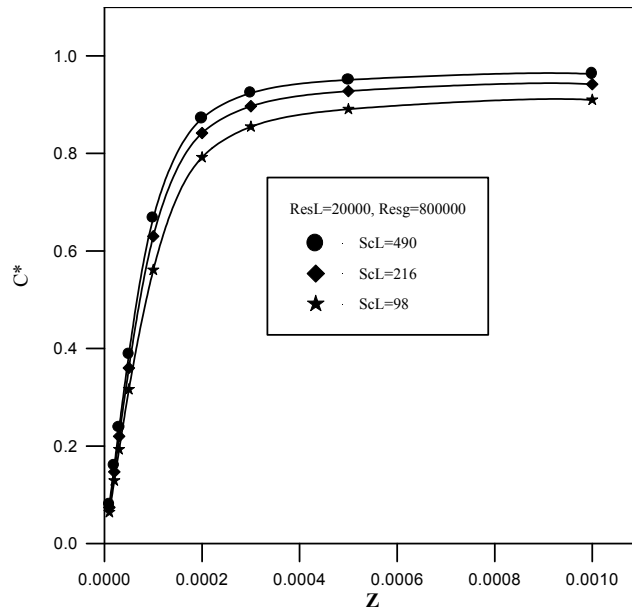


Fig. 5.42: Effect of Sc_L on the Concentration Profile in the Liquid Layer.

Chapter Six

Conclusions and Recommendations

6.1 Conclusions

For the present investigation the following points may be concluded:

- 1- The eddy diffusivity concept can be used successfully to predict mass transfer coefficient between pipe wall and fluid bulk under annular two phase flow conditions. The previously proposed models for eddy diffusivity in two-phase failed to fit the experimental results in two phase flow mass transfer. The eddy diffusivity expression obtained from present analysis exhibits good agreement with experimental results.
- 2- Both liquid Re and gas Re affect the mass transfer coefficient but the effect of liquid Re is higher than the gas Re .
- 3- The liquid layer plays the major role in determining the mass transfer coefficient since it consists the diffusion boundary layer in the wall vicinity which represents the major resistance to mass transfer.
- 4- The mass transfer coefficient is strongly affected by liquid Sc and slightly by gas Sc . The void fraction affects the mass transfer coefficient with unstable trend.
- 5- The void fraction increases with increasing gas Re and decreasing liquid Re . It increases with liquid temperature increase.
- 6- The interfacial friction factor increases with increasing liquid superficial Re and decreases with increasing gas superficial Re . It decreases with liquid temperature increase.
- 7- Both wall shear stress and interfacial shear stress increased with Re_{sL} and Re_{sg} . They decrease with increasing liquid temperature.

8- Both liquid superficial Re and gas superficial Re have slight effects on concentration profile within the diffusion layer. Beyond diffusion layer, Re_{sL} and Re_{sg} affect concentration profile.

9- The single phase eddy diffusivity models failed in expressing the mass transfer coefficient in two phase flow conditions. The mass transfer coefficient based on eddy diffusivity models of Slaiman et. al. [2007] model and Rosen and Tragradh [1995] is found to agree well with experimental results.

6.2 Recommendations

For future work the following suggestions are recommended:

1. It is interesting to perform theoretical analysis for the case of vertical pipe instead of horizontal pipe.
2. Investigation of other flow regimes such slug flow, stratified flow, and bubble flo, is worthwhile.
3. A study the effect of the presence of heat flux through pipe wall on the two phase mass transfer coefficient is recommended.
4. A study of the effect of pipe wall roughness on the friction factors, and mass transfer is interesting.

References

- Ansari M., D. Sylvister, C. Sariea, O. Shahom, and J. P. Brill, 1994, " Comprehensive Mechanistic Model for Upward Two Phase Flow in Well Bores", SPE, Production and Facilities, May, 143-151.
- Aravinth S., "Prediction of Heat and Mass Transfer for Fully Developed Turbulent Fluid Flow in Tubes", Int. J. Heat Mass Trans., 43, 1399-1408, 2000.
- Berger F. B. and K. F. Hau, Int. J. heat Mass Trans, Vol.20, P. 1185, 1977.
- Blusius H., Mitt, Forchung Surbocit. VDI BI, 131, P.1, 1913 (cited in 13).
- Brodkey R. S. and H. C. Hershey, Transport Phenomena, 2nd Printing, Mc Graw Hill, New York, 1989.
- Butterworth D. , A Comparison of Some Void .Fraction Relationships for Gas-Liquid Flow .Int .J.Multiphase Flow ,Vol.1 ,P-845-850 ,1975.
- Butterworth D., Air-water annular flow in a horizontal tube, Prog. Heat Mass Transfer , Vol.6 ,P-235-251, 1972.
- Chen J.J. and P.L. Spedding, " An Analysis of Holdup in Horizontal Gas-Liquid Flow" Int. J. Multiphase Flow, Vol.9 ,P-147-159, 1983.
- Chen J.J.J., Int. Comm. Heat Mass Trans., Vol. 12, P.219, 1985.
- Chilton T.H. and A. P. Colburn, Ind. Eng. Chem., Vol. 26, No.11, P. 1183, 1934.
- Chisholm, D., 1983, Two phase flow in pipelines and heat exchangers, Int. George Godwin (Ed.), London and New York in association and Institution of Chemical Engineers, New York.
- Chun, M. H. and Y. S. Kim, "A Semi empirical correlation for adiabatic interfacial friction factor in horizontal air water countercurrent stratified flow", Int. Comm. Heat Mass Transfer, Vol. 22, No. 5, pp. 617-628, 1995.

- Coulson J. M. and J. F. Richardson, Chemical engineering, 5th Edition, Butter Worth Heinemann, Britain, 1998.
- Danckwerts, P.V., (1951) "Significance of Liquid Film Coefficient in Gas Absorption"; Ind. and Eng. Chem., 43, 1460.
- Davies J.T., Turbulence Phenomena, Academic Press ,1972.
- Dawson D. A. and O. Trass, Int. J. Heat Mass Trans., Vol.15, P.1317, 1972.
- Deissler, G., "Analysis of turbulent heat transfer, mass transfer and friction in smooth tubes at high Prandtl and Schmidt numbers", NASA technical report, 1955.
- Douglas J.F and R.D. Matthews, Solving Problems in fluid Mechanics, Vol.2, 3rd Ed., Longman, England, 1998.
- Drew T.B, E .C. Koo, and W. H. McAdams, Trans. AIChE, Vol. 28, P. 56,1932.**
- Dukler et al, "Gas –Liquid Flow at Microgravity Conditions" Int. J. Multiphase flow, Vol.14, No.4, pp. 389-400,1989.
- Eisenberg M., C. W. Tobias, and C.R. Wike, J. Electrochem. Soc., Vol. 101, P.306, 1954.
- Fage A. and H.C. Townend, Proc. Roy. Soc., London, 135A,P.646, 1932.
- Fossa, M., " A Simple Model to Evaluate Direct Contact Heat Transfer and Flow Characteristics in Annular Two Phase Flow", In. J. Heat and Fluid Flow, 16, 272-279, 1995.
- Gay B., N. V. Mackley and J. D. Jenkins, , Int. J. Heat Mass Transfer, Vol. 19, P. 995, 1976.**
- Geankoplis C. J., 1984, "Mass Transport Phenomena", Ohio State University, Ohio.
- Gilliland F.R. and T.K. Sherwood, , Indus. And Eng. Chemistry, Vol. 26, P. 105, 1934.

- Gurniki F, K. Fukagata, S. Zahrai, and F.H. Bark, (2000)" LES of turbulent Channel Flow of Binary Electrolyte", J. Appl. Electrochem., 30, 1335-1343.
- Gutfinger G., "Topics in Transport Phenomena", Mech. Eng. Dept., Israel Institute of Technology, Hemisphere Publishing Corporation, John Wiley and Sons, Washongton, 1975.
- Haland S.E., Trans. ASME, JFE, Vol. 105, P. 89, 1983.
- Harriott, P. and R. M. Hamilton, Chem. Eng. Sci., Vol. 20, P. 1073, 1965.**
- Hart J., P. J. Hamerma and J. M. Fortuin, "Correlations Predicting Fractional Pressure Drop and Liquid Holdup During Horizontal Gas-Liquid Pipe Flow with a Small Liquid Holdup", Int. J. Multiphase Flow, Vol. 15, No. 6. pp. 947-984, 1989.
- Hasan B. O., Ph. D. Thesis, Chem. Eng. Dept., Nahrain University, Baghdad, Iraq, 2003.
- Hinze J.O. , Turbulance Phenomena, 2nd Edition., McGraw-Hill, USA, 1975.
- Hu, G. H. and C. Zhang, 2006," A Modified k- ϵ turbulence model for the simulation of two phase flow and heat transfer in condensers" Int. J. of Heat and Mass transfer,
- Hubbard D. W. and E. N. Lightfoot, Ind. Eng. Chem., Vol.5, P.370, 1966,
- Hughmark G. H., Ind. Eng. Chem. Fund., Vol. 8,No.1, P. 31, 1969.**
- Ibrahim, S.H. ,AICh EMI ,Modular Instruction ,Series c ,Transport ,Vol. 5, Mass Transport , 1984, P-31.
- Isakoff S. E. and T.B. Drew, Preceeding of the General Disscusion of heat Transfer, Inst. Mech. Eng. (London) and ASME, New York,1951
- Jaralla A. A., Ph. D. Thesis, UMIST, 1984.
- Kim J. Y. and A. J. Ghajar (2006), A General heat transfer correlation for non boiling gas-liquid flow with different flow patterns in horizontal pipes, Int. J. of Multiphase flow, 32, 447-465.

- Knudsen J. G. and D. L. Katz, Fluid Dynamics and Heat Transfer, Mc Graw Hill, New York, 1958.
- Langsholt. M., M. Nordsveen, K.Lunde, S.Nesic, and J.Enerhaug , "Wall Shear Stress And Mass Transfer Rates- Important Parameters In CO₂ Corrosion", BHR Group ,1997.
- Levich W. G., Physicochemical Hydrodynamics, New Jersey, Prentice Hall,P. 689, 1962 (cited in 14).
- Lin C.S., E.B. Denton, H.S. Gaskill, and G.L. Putnam, Ind. Eng. Chem., Vol.43, P. 2136, 1951.
- Lin W.H. and T.K. Sherwood, Chem. Eng. Progr., May, P. 258, 1950.
- Lin, C.S., R.W Moulton, and G. L. Putnam, (1953) " Mass Transfer between Solid Wall and Fluid Streams", Ind. Eng. Chem. 43,636
- Lockhart R.W. and R.C. Martinelli ,proposed correlations for isothermal two-phase flow in pipes, chem.Engng.Prog. Vol.45,P-39-48,1949.
Mc Graw Hill, New York, 1989.
- Meyerink E.S.C. and S.K. Friedlander, , Chem. Eng. Sc., Vol. 17 P. 121, 1962
- Michell J.E. and T. J. Hanratty, J. Fluid Mech. Vol.26, Part 1, P.199, 1966.
- Mizushima T. and F. Ogino, J. Chem. Eng. Japan, Vol.3, No.2, P. 166, 1970.
- Mizushima T., F. Ogino, Y. Oka and H. Fukuda, Int. J. Heat Mass Trans.,Vol. 14, P. 1705, 1971.
- Murphee E.V., 1932, Ind. Eng. Chem., 24 ,726.
- Nikurdse J. , VDI- Forschungsheft, 356, 1932.
- Nikurdse J., VDI- Forschungsheft, 361, 1933 (cited in 13).
- Notter R.H. and C.A.Sliecher ,Chem. Eng. Sci. Vol.27, P.2073, 1972.
- Oliemans R.V.A., Modeling of gas-condensate flow in horizontal and inclined pipes paper presented at the 1987 ETCE Conf.(6th A. Pipeline Engineering symp.),Dallas,Tex.,1987.

Page F., W.G. Schinger, D.K., Breaux, and B.H. Sage, Ind. Eng. Chem., Vol.44, No.2, P.424, 1952.

Perry, R.H. and C.H. Chilton, " Chem. Eng. Hand-Book", 6th Ed., Mc Graw Hill, USA, 1997.

Philip J.W., Robert, and R.Webester, Turbulent Diffusion, School of Civil and Environmental Engineering, Georgia Institute of Technology, Atlanta, 2002.

Pots B.F.M., Mechanistic Models for the Prediction of CO₂ Corrosion Rates under Multiphase Flow Conditions ,NACE International ,P-137 ,1995.

Poulson B. and R. Robinson, Corr. Sci., Vol. 26, No.4, P. 265, 1986.

Poulson, B., Corrosion Science, Vol. 23, No. 1, P. 391, 1983.

Richrdit H., NACA TM, 1047, 1943

Roberts, P.J. and Webster, D.R., Turbulent Diffusion in Environmental Fluid Mechanics – Theories and Application (ASCE), 2001.

Rosen C., C. Tragardh ,The Chemical Engineering Journal ,Vol.59, P-153, 1995

Rosén, C. and Trägårdh, C. 1993, Computer simulations of mass transfer in the concentration boundary layer over ultrafiltration membranes, Journal of Membrane Science, Volume 85, Issue 2, 11 November 1993, Pages 139-156.

Samh S. A., Ph. D. Thesis, Dept. of Chem. Eng., University of Technology, Baghdad, 1994.

Sato Y., M. Sadatomi, and Sekoguchi, " Momentum and Heat Transfer Analysis in Two Phase Bubble Flow", Int. Multiphase Flow J., Vol. 7, pp.167-177, 1981.

Shaw D. A. and T. J. Hanratty, AIChE. J., Vol. 23, No. 1, P. 28, 1977.

Shaw P. V. and T. J. Hanratty, A.I.Ch.E. J., Vol. 13, P. 689, 1964.

Sherwood T.K. , K.A. Smith, and P.E. Fowlest, Chem. Eng. Sci., Vol.23, P.1225, 1968.

- Sherwood.T .K, 1940, Mass Transfer And Friction In Turbulent Flow, AICHE, pp.817.
- Sirker K. K. and T. J. Hanratty, Ind. Eng. Chem. Fund. Vol. 8, P189, 1969.
- Slaiman Q. J., M. Abu-Khader, and Basim O. Hasan, "Prediction of Heat Transfer Coefficient Based on Eddy Diffusivity Concept", Trans. IChemE, Part A, Chemical Engineering Research and Design, 85(A4): 455-464, 2007.
- Sleicher, C.A. and J.R. and Calif, Trans. ASME, P.693, 1958.
- Son J. S. and T. J. Hanratty, AICHE, Vol. 13, P. 689, 1967.
- Spalding D. B. . Int. Developments in Heat Transfer, ASME, Vol.11,P.439, 1961. (cited in 14).
- Spedding P.L. and J.J.J. Chen , Correlation and estimation of holdup in two-phase flow ,proc.N.Z. Geothermal Workshop, P.180-199, 1979b.
- Spedding P.L. and J.J.J. Chen ,Correlation of holdup in two-phase flow .ANZAAS,Vol.49 ,Auckland, 1979 a.
- Stripantrapan W. and S. Wongwises, 2005, "Two phase Flow of refrigerants during evaporation under constant heat flux", Int. Communications in Heat and Mass Transfer, 32, 386-402.
- Taitel Y. and A.E. Dukler, A.E., A model for predicting flow regime transitions in horizontal and near horizontal gas-liquid flow. AIChE.JI,Vol.22.P-47-55,1976.
- Thomson W. J. , Introduction to Transport Phenomena, 1st Edition, Prentice Hall PTR, New Jersey, 2000.
- Sherwood, T.K., Woertz ,W.L, and L.A. Seder , Ind. Eng. Chem. , 31,457, 462 (1939).
- Townsend A.A., J. Fluid Mech., Vol. 11, P. 97, 1961.
- Van Driest E. R., J. aero. Sci. Vol. 23, P. 1007, 1956.
- Von Karman T., NACH, TM. 611, 1931.

- Wallis G.B., "Annular two-phase flow ,part I,A simple theory , part II, additional effects ,Trans .ASME , J.Basic Engng P-59-72, P-73-81, 1970.
- Wang H, 2005, Application Of Electrochemical Noise Technique In Multiphase Flow, Corrosion, Paper No. 05368.
- Wang H, T. Hong, J.Y.Cai, W.P.Jepson, and Ch.Bosch, Enhanced Mass Transfer And Wall Shear Stress In Multiphase Slug Flow, Corrosion, Paper No. 02501, 2002.
- Wang H.W., CO₂ Corrosion Mechanistic Modeling in Horizontal Stug Flow ,Ph.D. Thesis ,Ohio University ,2001.
- Wang S. and S.Nesic, On Coupling CO₂ Corrosion And Multiphase Flow Models, Corrosion 03631, paper Np. 03631, 2003.
- Wangises, S, W. Khankaew, and, W. Vetchsupakhun, "Prediction of Liquid Holdup in Horizontal Stratified Two-Phase Flow", Thammasat Int. Tech, vol.3, No. 2, July 1998.
- Wasan D.T., R.W. Charles, J. Heat Mass Tr., Vol.7, P.87, 1964.
- Wasan, T and C. R. Wike, Int. J. Heat Mass Trans.,Vol. 7, P. 87, 1964.
- Welle Van Der R, 1981, Turbulence Viscosity In Vertical Adiabatic Gas-Liquid Flow, Int. J. Multiphase Flow. Vol. 7.pp 461-473.
- Welty J. R., C. E. Wicks, and G. Rorrer, Fundamentals of Momentum, Heat, and Mass Transfer, 4th Edition, John Wiley and Sons, United States of America, 2001
- Welty J. R., C. E. Wicks, and G. Rorrer, Fundamentals of Momentum, Heat, and Mass Transfer, 4th Edition, John Wiley and Sons, United States of America, 2001.
- Whalley, P. B. and Hewitt, G. F., "The Correlation of Liquid entrainment Fraction and entrainment rate in Annular Flow", AERE-R9187, 1978.

Wongwises, S. and P. Naphon, "Heat transfer and flow characteristics in vertical annular two phase two component flow" *Thammasat. Int. J. Sc. Tech.* Vol.5, No. 1, January, April, 2000.

Zivi S. M., (1968) *J. Heat Transfer*, 90, 267.

Znad H. T., *Analysis of Mass Transfer Coefficient under Turbulent flow Conditions Using LCDT*, M.Sc. Thesis, Saddam University, Baghdad, 1996.

Appendix A

Results Single Phase

Table A.1: Values of Sh obtained From Various Eddy Diffusivity Models, Sc=100

Re	Sh Lin et al [1953]	Sh Johanson [1991]	Sh Rosen and Tragradh [1995]	Sh Slaiman et al [2007]
5000	93.89	100.707	111.526	117.042
10000	175.205	187.018	208.114	217.424
20000	326.944	347.31	388.355	403.909
40000	610.099	645.003	724.696	750.362
60000	878.784	926.467	1.044*10 ³	1.078*10 ³
80000	1.138*10 ³	1.198*10 ³	1.352*10 ³	1.394*10 ³
100000	1.392*10 ³	1.462*10 ³	1.653*10 ³	1.702*10 ³

Table A.2 : Values of Sh obtained From Various Eddy Diffusivity Models,

Sc=500

Re	Sh Lin et al [1953]	Sh Johanson [1991]	Sh Rosen and Tragradh [1995]	Sh Slaiman et al [2007]
5000	151.464	179.951	179.193	204.388
10000	282.642	335.219	334.387	380.801
20000	527.428	624.459	623.988	709.483
40000	984.216	1.163*10 ³	1.164*10 ³	1.322*10 ³
60000	1.418*10 ³	1.674*10 ³	1.677*10 ³	1.902*10 ³
80000	1.837*10 ³	2.167*10 ³	2.173*10 ³	2.463*10 ³
100000	2.245*10 ³	2.648*10 ³	2.656*10 ³	3.009*10 ³

Table A.3: Values of Sh obtained From Various Eddy Diffusivity Models, Sc=1000

Re	Sh Lin et al [1953]	Sh Johanson [1991]	Sh Rosen and Tragradh [1995]	Sh Slaiman et al [2007]
5000	188.504	230.082	219.901	258.187
10000	351.76	428.872	410.349	481.315
20000	656.408	799.419	765.739	897.272
40000	1.225*10 ³	1.49*10 ³	1.429*10 ³	1.673*10 ³
60000	1.764*10 ³	2.145*10 ³	2.058*10 ³	2.408*10 ³
80000	2.286*10 ³	2.778*10 ³	2.666*10 ³	3.118*10 ³
100000	2.794*10 ³	3.394*10 ³	3.26*10 ³	3.811*10 ³

Table A.4: Values of Sh obtained From Various Eddy Diffusivity Models, Sc=3000

Re	Sh Lin et al [1953]	Sh Johanson [1991]	Sh Rosen and Tragrahd [1995]	Sh Slaiman et al [2007]
5000	268.888	337.614	304.275	372.532
10000	501.764	629.668	567.797	694.837
20000	936.324	1.174*10 ³	1.06*10 ³	1.296*10 ³
40000	1.747*10 ³	2.19*10 ³	1.977*10 ³	2.417*10 ³
60000	2.517*10 ³	3.154*10 ³	2.848*10 ³	3.481*10 ³
80000	3.26*10 ³	4.085*10 ³	3.69*10 ³	4.509*10 ³
100000	3.986*10 ³	4.993*10 ³	4.51*10 ³	5.511*10 ³

Appendix B

Results of Two Phase Calculations

Table B-1: Values of Void Fraction at different Re_{sL} and Re_{sg} From Various Authors, $T_L=25$.

ResL	Resg	Hart et al 1989	Zivi [1968]	Chisholm[1983]
1000	5000	0.757	0.894	0.902
2000	5000	0.664	0.808	0.864
3000	5000	0.602	0.737	0.837
4000	5000	0.556	0.678	0.815
5000	5000	0.52	0.627	0.796
6000	5000	0.49	0.584	0.779
10000	5000	0.406	0.457	0.727
20000	5000	0.3	0.296	0.641

Table B.2: Values of Void Fraction at different Re_{sL} and Re_{sg} From Various Authors, $T_L=25$.

ResL	Resg	Hart et al 1989	Zivi [1968]	Chisholm[1983]
1000	10000	0.861	0.944	0.932
2000	10000	0.798	0.894	0.902
3000	10000	0.752	0.849	0.881
4000	10000	0.715	0.808	0.864
5000	10000	0.684	0.771	0.85
6000	10000	0.657	0.737	0.837
10000	10000	0.577	0.624	0.796
20000	10000	0.461	0.457	0.727
40000	10000	0.384	0.296	0.64

Table B.3: Values of Void Fraction at different Re_{sL} and Re_{sg} From Various Authors, $T_L=25$.

ResL	Resg	Hart et al 1989	Zivi [1968]	Chisholm[1983]	Chen and Spedding 1980
1000	20000	0.926	0.971	0.954	
2000	20000	0.888	0.944	0.932	0.956
3000	20000	0.858	0.918	0.916	
4000	20000	0.834	0.894	0.902	
5000	20000	0.812	0.871	0.891	0.92
6000	20000	0.793	0.849	0.881	
10000	20000	0.732	0.771	0.85	0.853
20000	20000	0.631	0.627	0.796	0.72
40000	20000	0.517	0.457	0.727	0.48

Table B.4: Values of Void Fraction at different Re_{sL} and Re_{sg} From Various Authors, $T_L=40$ C.

ResL	Resg	Hart et al 1989	Zivi [1968]	Chisholm[1983]
1000	10000	0.906	0.963	0.947
2000	10000	0.859	0.928	0.922
4000	10000	0.795	0.886	0.889
5000	10000	0.77	0.838	0.877
10000	10000	0.678	0.722	0.831
20000	10000	0.569	0.565	0.771
40000	10000	0.452	0.393	0.696

Table B.5: Values of Void Fraction at different Re_{sL} and Re_{sg} From Various Authors, $T_L=40$ C.

ResL	Resg	Hart et al 1989	Zivi [1968]	Chisholm[1983]	Dukler
1000	20000	0.95	0.981	0.965	
2000	20000	0.924	0.963	0.947	0.978
4000	20000	0.886	0.928	0.922	
5000	20000	0.87	0.912	0.912	0.949
10000	20000	0.808	0.838	0.877	0.905
20000	20000	0.725	0.722	0.831	0.802
40000	20000	0.622	0.565	0.772	0.663

Table B.6: Values of Void Fraction at different Re_{sL} and Re_{sg} From Various Authors, $T_L=40$ C.

ResL	Resg	Hart et al 1989	Zivi [1968]	Chisholm[1983]
1000	40000	0.975	0.99	0.979
2000	40000	0.961	0.981	0.965
4000	40000	0.939	0.963	0.947
5000	40000	0.93	0.954	0.939
10000	40000	0.894	0.912	0.912
20000	40000	0.841	0.838	0.877
40000	40000	0.767	0.722	0.831

Table B.7: Values of Void Fraction at different Re_{sL} and Re_{sg} From Various Authors, $T_L=60$ C.

ResL	Resg	Hart et al 1989	Zivi [1968]	Chisholm[1983]
1000	10000	0.929	0.973	0.956
2000	10000	0.893	0.947	0.934
4000	10000	0.841	0.899	0.905
5000	10000	0.82	0.87	0.894
10000	10000	0.742	0.78	0.853
20000	10000	0.644	0.639	0.80
40000	10000	0.53	0.47	0.732

Table B.8: Values of Void Fraction at different Re_{sL} and Re_{sg} From Various Authors, $T_L=60$ C.

ResL	Resg	Hart et al 1989	Zivi [1968]	Chisholm[1983]	Chen and Spedding 1980
1000	20000	0.963	0.986	0.972	
2000	20000	0.944	0.973	0.96	0.984
4000	20000	0.914	0.947	0.934	
5000	20000	0.901	0.934	0.925	0.963
10000	20000	0.852	0.876	0.894	0.93
20000	20000	0.783	0.78	0.853	0.869
40000	20000	0.693	0.639	0.80	0.754

Table B.9: Values of Void Fraction at different Re_{sL} and Re_{sg} From Various Authors, $T_L=60$ C.

ResL	Resg	Hart et al 1989	Zivi [1968]	Chisholm[1983]	Chen and Spedding 1980
1000	80000	0.991	0.996	0.991	
2000	80000	0.985	0.993	0.983	0.996
4000	80000	0.977	0.986	0.972	
5000	80000	0.973	0.983	0.967	0.99
10000	80000	0.958	0.966	0.949	0.982
20000	80000	0.935	0.934	0.925	0.967
40000	80000	0.9	0.876	0.894	0.938

Table B.10: Values of f_{wL} , f_i , τ_w , and τ_i at various Re_{sL} for $Re_{sg}=20000$ and $T_L=25$ C.

Re_{sL}	(Chisholm 1983)	$fwL \times 10^3$	f_i	τ_w N/m ²	τ_i N/m ²
10000	0.85	7.291	0.081	1.161	0.67
20000	0.79	6.35	0.109	3.04	1.03
40000	0.727	5.53	0.147	5.93	1.669
60000	0.679	5.1	0.174	8.88	2.27

Table B.10 Values of f_{wL} , f_i , τ_w , and τ_i at various Re_{sL} for $Re_{sg}=80000$, $T=25$,

ResL	(Chisholm 1983)	$fwL \times 10^3$	$fg \times 10^3$	f_i	τ_w N/m ²	τ_i N/m ²
5000						
10000	0.923	7.291	4.81	0.033	6.191	3.732
20000	0.891	6.347	4.81	0.045	10.722	5.478
40000	0.85	5.525	4.81	0.061	19.516	8.179
60000	0.82	5.095	4.81	0.073	28.208	10.471

Table B.11: Values of f_{wL} , f_i , τ_w , and τ_i at various Re_{sL} $Re_{sg}=80000$ and $T=40$ C

ResL	(Chisholm 1983)	$fwL \times 10^3$	$fg \times 10^3$	f_i	τ_w N/m ²	τ_i N/m ²
10000	0.939	7.291	4.81	0.027	4.15	2.952
20000	0.912	6.347	4.81	0.037	6.9	4.31
40000	0.877	5.525	4.81	0.051	12.2	6.36
60000	0.851	5.095	4.81	0.061	17.4	8.06

Table B.12 Values of f_{wL} , f_i , τ_w , and τ_i at various Re_{sL} $Re_{sg}=100000$, $T=25$,

ResL	(Chisholm 1983)	$fwL \times 10^3$	$fg \times 10^3$	f_i	τ_w N/m ²	τ_i N/m ²
10000	0.932	7.291	4.6	0.029	7.86	4.938
20000	0.902	6.347	4.6	0.039	13.3	7.22
40000	0.864	5.525	4.6	0.053	23.9	10.7
60000	0.837	5.095	4.6	0.063	34.3	13.6

Table B.13: Values of Sh at various Re_{sL} and Re_{sg} for $Scl=490$ as Compared with other Correlations

ResL	Resg	(Chisholm 1983)	Sh (present)	Sh Wang et al (2002)	Sh Wang and Nestic (2003)
1000	80000	0.983	312.7	284.1	291.1
2000	80000	0.971	467.5	433.6	438.1
4000	80000	0.948	696.9	661.7	659.5
5000	80000	0.923	791.8	758.2	752.3
10000	80000	0.983	1174	1157	1132
20000	80000	0.891	1728	1766	1705
40000	80000	0.85	2515	2696	2566

Table B.14: Values of Sh at various Re_{sL} and Re_{sg} for $Scl=490$ as Compared with other Correlations

ResL	Resg	(Chisholm 1983)	Sh Present	Sh Wang et al (2002)	Sh Wang and Nestic (2003)
2000	20000	0.932	320.9	433	438
5000	20000	0.891	538	758	752
10000	20000	0.85	789	1157	1132
20000	20000	0.796	1140	1766	1705
40000	20000	0.727	1611	2696	2566

Table B.15: Values of Sh at various Re_{sL} and Re_{sg} for $Scl=490$ as Compared with other Correlations.

ResL	Resg	Kim and Ghajar 2006	Sh Present	Sh Wang et al (2002)	Sh Wang and Nestic (2003)
2000	40000	0.945	387	433	438
5000	40000	0.923	654	758	752
10000	40000	0.891	964	1157	1132
20000	40000	0.85	1409	1766	1705
40000	40000	0.796	2026	2696	2566

Table B.16: Values of Sh at various Re_{sL} and Re_{sg} for $Scl=490$ as Compared with other Correlations

ResL	Resg	Kim and Ghajar 2006	Sh present	Sh Wang et al (2002)	Sh Wang and Nestic (2003)
2000	100000	0.975	496	433	438
5000	100000	0.954	841	758	752
10000	100000	0.932	1249	1157	1132
20000	100000	0.902	1842	1766	1705
40000	100000	0.864	2690	2696	2566

Table B.17: Values of Sh at various Re_{sL} and Re_{sg} for $Sc_L=216$ as Compared with other Correlations

ResL	Resg		Sh (present)	Sh Wang et al (2002)	Sh Wang and Nestic (2003)
1000	80000	0.988	237.6	216.8	222.1
2000	80000	0.979	354.9	330.9	334.4
4000	80000	0.965	527.9	505	503.3
5000	80000	0.96	599.2	578.7	574.1
10000	80000	0.939	883.3	883.1	864.2
20000	80000	0.912	1288	1348	1301
40000	80000	0.877	1846	2057	1958

Table B.18: Values of Sh at various Re_{sL} and Re_{sg} for $Sc_L=216$ as Compared with other Correlations

ResL	Resg	Kim and Ghajar 2006	Sh present
2000	20000	0.947	243
5000	20000	0.912	405
10000	20000	0.877	586
20000	20000	0.831	831
40000	20000	0.772	1142

Table B.19: Values of Sh at various Re_{sL} and Re_{sg} for $Sc_L=216$ as Compared with other Correlations

ResL	Resg	Kim and Ghajar 2006	Sh present
2000	40000	0.965	294
5000	40000	0.939	493
10000	40000	0.912	722
20000	40000	0.877	1041
40000	40000	0.831	1465

Table B.20: Values of Sh at various Re_{sL} and Re_{sg} for $Sc_L=216$ as Compared with other Correlations.

ResL	Resg	Kim and Ghajar 2006	Sh present
2000	100000	0.982	377
5000	100000	0.965	637
10000	100000	0.947	941
20000	100000	0.922	1376
40000	100000	0.889	1982

Table B.21: Values of Sh at various Re_{sL} and Re_{sg} for $Sc_L=98$ as Compared with other Correlations

ResL	Resg		Sh (present)	Sh Wang et al (2002)	Sh Wang and Nestic (2003)
1000	80000	0.991	182.7	167.4	171.5
2000	80000	0.983	272.2	255.4	258.1
4000	80000	0.972	403.2	389	388.5
5000	80000	0.967	456.7	446.7	443.2
10000	80000	0.949	667.1	681	667
20000	80000	0.925	957.9	1041	1004
40000	80000	0.894	1341	1589	1512

Table B.22: Values of Sh at various Re_{sL} and Re_{sg} for $Sc_L=98$ as Compared with other Correlations

ResL	Resg	Kim and Ghajar 2006	Sh Present Work
2000			185
5000	20000	0.925	305
10000	20000	0.894	434
20000	20000	0.853	598
40000	20000	0.80	788

Table B.23: Values of Sh at various Re_{sL} and Re_{sg} for $Sc_L=98$ as Compared with other Correlations.

ResL	Resg	Kim and Ghajar 2006	Sh (present)
2000	100000	0.986	289
5000	100000	0.972	486
10000	100000	0.956	712
20000	100000	0.934	1028
40000	100000	0.905	1449

Table B.24: Variation of Concentration with Z at Resg=40000 and SCL=490

Z	C* ResL=5000	C* ResL=10000	C* ResL=20000	C* ResL=40000
0.00001	0.043	0.045	0.047	0.05
0.00002	0.086	0.089	0.094	0.1
0.00003	0.129	0.134	0.144	0.15
0.00005	0.214	0.22	0.234	0.248
0.0001	0.415	0.429	0.449	0.469
0.0002	0.702	0.713	0.726	0.73
0.0003	0.837	0.839	0.838	0.826
0.0005	0.928	0.922	0.91	0.885
0.001	0.971	0.961	0.942	0.911
0.0022	0.983	0.971	0.953	0.926
0.003	0.985	0.974	0.957	0.932
0.005	0.988		0.963	0.941
0.008	0.991	0.983	0.97	0.95
0.01	0.992	0.985	0.973	0.955
0.03			0.987	0.976
0.05		0.999	0.994	0.985
0.1				0.999

Table B.25: Variation of Concentration with Z at Resg=80000 and SCL=490

Z	C* ResL=5000	C* ResL=10000	C* ResL=20000	C* ResL=40000
0.00001	0.076	0.077	0.08	0.084
0.00002	0.152	0.154	0.16	0.168
0.00003	0.228	0.23	0.238	0.25
0.00005	0.373	0.376	0.388	0.406
0.0001	0.655	0.657	0.668	0.681
0.0002	0.879	0.875	0.872	0.681
0.0003	0.939	0.933	0.924	0.907
0.0005	0.972	0.964	0.951	0.93
0.001	0.986	0.977	0.963	0.942
0.0022	0.99	0.982	0.097	0.952
0.003	0.991	0.984	0.0973	0.956
0.005	0.993	0.987	0.0978	0.963
0.008				
0.01	0.996	0.992	0.984	0.972
0.03		0.998	0.994	0.987
0.05			0.999	0.994
0.1				

Table B.26: Variation of Concentration with Z at $Re_{sg}=100000$ and $Sc_L=490$

Z	C^* ResL=10000
0.00001	0.092
0.00002	0.184
0.00003	0.274
0.00005	0.445
0.0001	0.73
0.0002	0.908
0.0003	0.949
0.0005	0.974
0.001	0.981
0.0022	0.984
0.003	0.987
0.005	0.989

Table B.27: Variation of Concentration with Z at $Re_{sl}=20000$ and $Re_{sg}=80000$,

Z	C^* ScL=490	C^* ScL=216	C^* ScL=98
0.00001	0.08	0.074	0.064
0.00002	0.16	0.147	0.129
0.00003	0.238	0.22	0.193
0.00005	0.388	0.36	0.316
0.0001	0.668	0.63	0.561
0.0002	0.872	0.842	0.792
0.0003	0.924	0.897	0.855
0.0005	0.951	0.928	0.891
0.001	0.963	0.942	0.91
0.0022	0.97	0.954	0.929
0.003	0.973	0.959	0.937
0.005	0.978	0.966	0.95
0.008		0.974	0.961
0.01		0.977	0.967
0.03		0.994	0.994

Table B.27 : Values of Sh As obtained From Two Phase eddy Diffusivity Model

at Resg=40000 and Sc=490

ResL	Present	Wang and Nestic Model2003	Sato el[1981] – Welle [1981]	Sato et al [1981]	Wang Correlation	Wang and Nestic Correlaion
5000	654	721	916	1725	758	752
10000	964	1312	2111	1868	1157	1132
20000	1409	2375	4511	2303	1766	1795
40000	2026	4294	9426	2877	2696	2566

Table B.28 :Values of Sh As obtained From Two Phase eddy Diffusivity Model

at Resg=80000, Sc=490

ResL	Present	Wang and Nestic Model2003	Sato el[1981] – Welle [1981]	Sato et al [1981]	Wang Correlation	Wang and Nestic Correlaion
5000	791.8	726	657	-	758	752
10000	1174	1323	1604	3175	1157	1132
20000	1727	2406	2745	3491	1427	1705
40000	2515	4361	4102	8344	2696	2566

Table B.29 :Values of Sh As obtained From Two Phase eddy Diffusivity Model

at Resg=40000, Sc=216

ResL	Present	Wang and Nestic Model2003	Sato el[1981] – Welle [1981]	Sato et al [1981]	Wang Correlation	Wang and Nestic Correlaion
5000	493.2	569	365	1399	578	574
10000	722	1036	836	1413	883	864
20000	1041	1882	1809	1658	1348	1301
40000	1465	3408	3654	2168	2057	1958

Table B.30 :Values of Sh As obtained From Two Phase eddy Diffusivity Model

Resg=80000, Sc=216

ResL	Present model	Wang and Nestic Model2003	Sato el[1981] – Welle [1981]	Sato et al [1981]	Wang Correlation	Wang and Nestic Correlaion [2003]
5000	599.2	572	260	1500	578.7	574
10000	883	1044	634	2413	883.1	864
20000	1288	1901	1480	2615	1348	1301
40000	1846	3452	3267	3983	2057	1958

Table B.31 :Values of Sh As obtained From Two Phase eddy Diffusivity Model

at Resg=40000, Sc=98

ResL	Present model	Wang and Nesic Model2003	Sato et al [1981] – Welle [1981]	Sato et al [1981]	Wang Correlation	Wang and Nesic Correlaion [2003]
5000	374	462	160	1085	446	443
10000	541	842	361.9	1084	681	667
20000	763	1532	772	1260	1041	1005
40000	1041	2779	1538	1638	1589	1512

Table B.32: Values os Sh at Resg=80000 and Sc=98

ResL	Present model	Wang and Nesic Model2003	Sato et al [1981] – Welle [1981]	Sato et al [1981]	Wang Correlation	Wang and Nesic Correlaion [2003]
5000	456.8	464	114	-	446.8	443.5
10000	667	847	275	1874	681.9	667.4
20000	958.2	1545	637	1990	1041	1005
40000	1341	2334	1391	2334	1598	1512

Appendix C

Flow Independent Void Fraction (Stratified flow)

Table C.1: Value of Friction Factor for Various Values of Re_{sL} and Re_{sg} at $\alpha=0.9$

Re_L	Re_g	Re_{sL}	Re_{sg}	f_{wL}	f_{wg}
10000	10000	1000	9×10^3	0.012	7.446×10^{-3}
10000	20000	1000	1.8×10^4	0.012	6.482×10^{-3}
10000	40000	1000	3.6×10^4	0.012	5.643×10^{-3}
10000	60000	1000	5.4×10^4	0.012	5.203×10^{-3}
10000	80000	1000	7.2×10^4	0.012	$10^{-3} \times 4.912$
10000	100000	1000	9×10^4	0.012	4.698×10^{-3}

Table C.2: Value of Friction Factor for Various Values of Re_{sL} and Re_{sg} at $\alpha=0.9$

Re_L	Re_g	Re_{sL}	Re_{sg}	f_{wL}	f_{wg}
20000	10000	2000	9×10^3	0.01	7.446×10^{-3}
20000	20000	2000	1.8×10^4	0.01	6.482×10^{-3}
20000	40000	2000	3.6×10^4	0.01	5.643×10^{-3}
20000	60000	2000	5.4×10^4	0.01	5.203×10^{-3}
20000	80000	2000	7.2×10^4	0.01	$10^{-3} \times 4.912$
20000	100000	2000	9×10^4	0.01	4.698×10^{-3}

Table C.3: Value of Friction Factor for Various Values of Re_{sL} and Re_{sg} at $\alpha=0.9$

Re_L	Re_g	Re_{sL}	Re_{sg}	f_{wL}	f_{wg}
40000	10000	4000	9×10^3	8.757×10^{-3}	7.446×10^{-3}
40000	20000	4000	1.8×10^4	8.757×10^{-3}	6.482×10^{-3}
40000	40000	4000	3.6×10^4	8.757×10^{-3}	5.643×10^{-3}
40000	60000	4000	5.4×10^4	8.757×10^{-3}	5.203×10^{-3}
40000	80000	4000	7.2×10^4	8.757×10^{-3}	$10^{-3} \times 4.912$
40000	100000	4000	9×10^4	8.757×10^{-3}	4.698×10^{-3}

Table C.4: Value of Friction Factor for Various Values of Re_{sL} and Re_{sg} at $\alpha=0.9$

Re_L	Re_g	Re_{sL}	Re_{sg}	f_{wL}	f_{wg}
60000	10000	6000	9×10^3	8.075×10^{-3}	7.446×10^{-3}
60000	20000	6000	1.8×10^4	8.075×10^{-3}	6.482×10^{-3}
60000	40000	6000	3.6×10^4	8.075×10^{-3}	5.643×10^{-3}
60000	60000	6000	5.4×10^4	8.075×10^{-3}	5.203×10^{-3}
60000	80000	6000	7.2×10^4	8.075×10^{-3}	$10^{-3} \times 4.912$
60000	100000	6000	9×10^4	8.075×10^{-3}	4.698×10^{-3}

Table C.5: Value of Friction Factor for Various Values of Re_{sL} and Re_{sg} at $\alpha=0.8$

Re_L	Re_g	Re_{sL}	Re_{sg}	f_{wL}	f_{wg}
10000	10000	2000	8×10^3	0.01	7.623×10^{-3}
10000	20000	2000	1.6×10^4	0.01	6.636×10^{-3}
10000	40000	2000	3.2×10^4	0.01	5.777×10^{-3}
10000	60000	2000	4.8×10^4	0.01	5.327×10^{-3}
10000	80000	2000	6.4×10^4	0.01	$10^{-3} \times 5.029$
10000	100000	2000	8×10^4	0.01	4.81×10^{-3}

Table C.5: Value of Friction Factor for Various Values of Re_{sL} and Re_{sg} at $\alpha=0.8$

Re_L	Re_g	Re_{sL}	Re_{sg}	f_{wL}	f_{wg}
20000	10000	4000	8×10^3	8.757×10^{-3}	7.623×10^{-3}
20000	20000	4000	1.6×10^4	8.757×10^{-3}	6.636×10^{-3}
20000	40000	4000	3.2×10^4	8.757×10^{-3}	5.777×10^{-3}
20000	60000	4000	4.8×10^4	8.757×10^{-3}	5.327×10^{-3}
20000	80000	4000	6.4×10^4	8.757×10^{-3}	$10^{-3} \times 5.029$
20000	100000	4000	8×10^4	8.757×10^{-3}	4.81×10^{-3}

Table C.6: Value of Friction Factor for Various Values of Re_{sL} and Re_{sg} at $\alpha=0.8$

Re_L	Re_g	Re_{sL}	Re_{sg}	f_{wL}	f_{wg}
40000	10000	8000	8×10^3	7.623×10^{-3}	7.623×10^{-3}
40000	20000	8000	1.6×10^4	7.623×10^{-3}	6.636×10^{-3}
40000	40000	8000	3.2×10^4	7.623×10^{-3}	5.777×10^{-3}
40000	60000	8000	4.8×10^4	7.623×10^{-3}	5.327×10^{-3}
40000	80000	8000	6.4×10^4	7.623×10^{-3}	$10^{-3} \times 5.029$
40000	100000	8000	8×10^4	7.623×10^{-3}	4.81×10^{-3}

Table C.7: Value of Friction Factor for Various Values of Re_{sL} and Re_{sg} at $\alpha=0.8$

Re_L	Re_g	Re_{sL}	Re_{sg}	f_{wL}	f_{wg}
60000	10000	12000	8×10^3	7.029×10^{-3}	7.623×10^{-3}
60000	20000	12000	1.6×10^4	7.029×10^{-3}	6.636×10^{-3}
60000	40000	12000	3.2×10^4	7.029×10^{-3}	5.777×10^{-3}
60000	60000	12000	4.8×10^4	7.029×10^{-3}	5.327×10^{-3}
60000	80000	12000	6.4×10^4	7.029×10^{-3}	$10^{-3} \times 5.029$
60000	100000	12000	8×10^4	7.029×10^{-3}	4.81×10^{-3}

Table C.8: Value of Friction Factor for Various Values of Re_{sL} and Re_{sg} at $\alpha=0.7$

Re_L	Re_g	Re_{sL}	Re_{sg}	f_{wL}	f_{wg}
10000	10000	3000	7×10^3	9.275×10^{-3}	7.83×10^{-3}
10000	20000	3000	1.4×10^4	9.275×10^{-3}	6.816×10^{-3}
10000	40000	3000	2.8×10^4	9.275×10^{-3}	5.934×10^{-3}
10000	60000	3000	4.2×10^4	9.275×10^{-3}	5.472×10^{-3}
10000	80000	3000	5.6×10^4	9.275×10^{-3}	$10^{-3} \times 5.166$
10000	100000	3000	7×10^4	9.275×10^{-3}	4.94×10^{-3}

Table C.9: Value of Friction Factor for Various Values of Re_{sL} and Re_{sg} at $\alpha=0.7$

Re_L	Re_g	Re_{sL}	Re_{sg}	f_{wL}	f_{wg}
20000	10000	6000	7×10^3	8.075×10^{-3}	7.83×10^{-3}
20000	20000	6000	1.4×10^4	8.075×10^{-3}	6.816×10^{-3}
20000	40000	6000	2.8×10^4	8.075×10^{-3}	5.934×10^{-3}
20000	60000	6000	4.2×10^4	8.075×10^{-3}	5.472×10^{-3}
20000	80000	6000	5.6×10^4	8.075×10^{-3}	$10^{-3} \times 5.166$
20000	100000	6000	7×10^4	8.075×10^{-3}	4.94×10^{-3}

Table C.10: Value of Friction Factor for Various Values of Re_{sL} and Re_{sg} at $\alpha=0.7$.

Re_{eL}	Re_{cg}	Re_{sL}	Re_{sg}	f_{wL}	f_{wg}
40000	10000	12000	7×10^3	7.029×10^{-3}	7.83×10^{-3}
40000	20000	12000	1.4×10^4	7.029×10^{-3}	6.816×10^{-3}
40000	40000	12000	2.8×10^4	7.029×10^{-3}	5.934×10^{-3}
40000	60000	12000	4.2×10^4	7.029×10^{-3}	5.472×10^{-3}
40000	80000	12000	5.6×10^4	7.029×10^{-3}	$10^{-3} \times 5.166$
40000	100000	12000	7×10^4	7.029×10^{-3}	4.94×10^{-3}

Table C.11: Value of Friction Factor for Various Values of Re_{sL} and Re_{sg} at $\alpha=0.7$

Re_{eL}	Re_{cg}	Re_{sL}	Re_{sg}	f_{wL}	f_{wg}
60000	10000	18000	7×10^3	6.482×10^{-3}	7.83×10^{-3}
60000	20000	18000	1.4×10^4	6.482×10^{-3}	6.816×10^{-3}
60000	40000	18000	2.8×10^4	6.482×10^{-3}	5.934×10^{-3}
60000	60000	18000	4.2×10^4	6.482×10^{-3}	5.472×10^{-3}
60000	80000	18000	5.6×10^4	6.482×10^{-3}	$10^{-3} \times 5.166$
60000	100000	18000	7×10^4	6.482×10^{-3}	4.94×10^{-3}

Table C.12: Value of Shear Stress and interfacial Friction Factor for Various Values of Re_{sL} and Re_{sg} at $\alpha=0.9$

Re_{eL}	Re_{cg}	τ_{wL}	τ_{wg}	τ_i	f_i
10000	10000	0.058	3.139×10^{-3}	0.055	0.167
10000	20000	0.058	0.011	0.053	0.036
10000	40000	0.058	0.038	0.047	7.361×10^{-3}
10000	60000	0.058	0.079	0.037	2.558×10^{-3}
10000	80000	0.058	0.133	0.025	$10^{-4} \times 9.519$
10000	100000	0.058	0.198	9.796×10^{-3}	2.379×10^{-4}

Table C.13: Value of Shear Stress and interfacial Friction Factor for Various Values of Re_{sL} and Re_{sg} at $\alpha=0.9$

Re_{eL}	Re_{cg}	τ_{wL}	τ_{wg}	τ_i	f_i
20000	10000	0.201	3.139×10^{-3}	0.193	0.786
20000	20000	0.201	0.011	0.191	0.146
20000	40000	0.201	0.038	0.185	0.031
20000	60000	0.201	0.079	0.175	0.013
20000	80000	0.201	0.133	0.163	$10^{-3} \times 6.408$
20000	100000	0.201	0.198	0.148	3.675×10^{-3}

Table C.14: Value of Shear Stress and interfacial Friction Factor for Various Values of Re_{sL} and Re_{sg} at $\alpha=0.9$

Re_{eL}	Re_{cg}	τ_{wL}	τ_{wg}	τ_i	f_i
40000	10000	0.701	3.139×10^{-3}	0.673	5.777
40000	20000	0.701	0.011	0.671	0.684
40000	40000	0.701	0.038	0.665	0.127
40000	60000	0.701	0.079	0.655	0.051
40000	80000	0.701	0.133	0.643	0.027
40000	100000	0.701	0.198	0.628	0.016

Table C.15: Value of Shear Stress and interfacial Friction Factor for Various Values of Re_{sL} and Re_{sg} at $\alpha=0.9$

Re_{eL}	Re_{eg}	τ_{wL}	τ_{wg}	τ_I	f_I
60000	10000	1.453	3.139×10^{-3}	1.397	39.83
60000	20000	1.453	0.011	1.395	1.993
60000	40000	1.453	0.038	1.389	0.305
60000	60000	1.453	0.079	1.379	0.117
60000	80000	1.453	0.133	1.367	0.061
60000	100000	1.453	0.198	1.352	0.037

Table C.16: Value of Shear Stress and interfacial Friction Factor for Various Values of Re_{sL} and Re_{sg} at $\alpha=0.8$

Re_{eL}	Re_{eg}	τ_{wL}	τ_{wg}	τ_I	f_I
10000	10000	0.05	3.214×10^{-3}	0.056	0.171
10000	20000	0.05	0.011	0.053	0.035
10000	40000	0.05	0.039	0.043	6.807×10^{-3}
10000	60000	0.05	0.081	0.029	1.962×10^{-3}
10000	80000	0.05	0.136	9.45×10^{-3}	$10^{-4} \times 3.608$
10000	100000	0.05	0.203	-0.014	-3.396×10^{-4}

Table C.17: Value of Shear Stress and interfacial Friction Factor for Various Values of Re_{sL} and Re_{sg} at $\alpha=0.8$.

Re_{eL}	Re_{eg}	τ_{wL}	τ_{wg}	τ_I	f_I
20000	10000	0.175	3.214×10^{-3}	0.197	0.802
20000	20000	0.175	0.011	0.194	0.148
20000	40000	0.175	0.039	0.184	0.031
20000	60000	0.175	0.081	0.17	0.012
20000	80000	0.175	0.136	0.151	$10^{-3} \times 5.926$
20000	100000	0.175	0.203	0.127	3.164×10^{-3}

Table C.18: Value of Shear Stress and interfacial Friction Factor for Various Values of Re_{sL} and Re_{sg} at $\alpha=0.8$

Re_{eL}	Re_{eg}	τ_{wL}	τ_{wg}	τ_I	f_I
40000	10000	0.61	3.214×10^{-3}	0.688	5.909
40000	20000	0.61	0.011	0.685	0.699
40000	40000	0.61	0.039	0.676	0.129
40000	60000	0.61	0.081	0.661	0.051
40000	80000	0.61	0.136	0.642	0.027
40000	100000	0.61	0.203	0.618	0.016

Table C.19: Value of Shear Stress and interfacial Friction Factor for Various Values of Re_{sL} and Re_{sg} at $\alpha=0.8$.

Re_{eL}	Re_{eg}	τ_{wL}	τ_{wg}	τ_I	f_I
60000	10000	1.265	3.214×10^{-3}	1.429	40.754
60000	20000	1.265	0.011	1.426	2.038
60000	40000	1.265	0.039	1.417	0.311
60000	60000	1.265	0.081	1.402	0.119
60000	80000	1.265	0.136	1.383	0.062
60000	100000	1.265	0.203	1.359	0.037

Table C.20: Value of Shear Stress and interfacial Friction Factor for Various Values of Re_{sL} and Re_{sg} at $\alpha=0.7$.

Re_L	Re_{eg}	τ_{wL}	τ_{wg}	τ_l	f_l
10000	10000	0.046	3.301×10^{-3}	0.055	0.167
10000	20000	0.046	0.011	0.051	0.034
10000	40000	0.046	0.04	0.039	6.137×10^{-3}
10000	60000	0.046	0.083	0.021	1.41×10^{-3}
10000	80000	0.046	0.139	-3.565×10^{-3}	$10^{-4} \times -1.361$
10000	100000	0.046	0.208	-0.033	-8.033×10^{-4}

Table C.21: Value of Shear Stress and interfacial Friction Factor for Various Values of Re_{sL} and Re_{sg} at $\alpha=0.7$

Re_L	Re_{eg}	τ_{wL}	τ_{wg}	τ_l	f_l
20000	10000	0.161	3.301×10^{-3}	0.194	0.791
20000	20000	0.161	0.011	0.19	0.145
20000	40000	0.161	0.04	0.178	0.03
20000	60000	0.161	0.083	0.16	0.011
20000	80000	0.161	0.139	0.136	$10^{-3} \times 5.343$
20000	100000	0.161	0.208	0.106	2.644×10^{-3}

Table C.22: Value of Shear Stress and interfacial Friction Factor for Various Values of Re_{sL} and Re_{sg} at $\alpha=0.7$.

Re_L	Re_{eg}	τ_{wL}	τ_{wg}	τ_l	f_l
40000	10000	0.562	3.301×10^{-3}	0.679	5.831
40000	20000	0.562	0.011	0.676	0.688
40000	40000	0.562	0.04	0.663	0.127
40000	60000	0.562	0.083	0.645	0.05
40000	80000	0.562	0.139	0.621	0.026
40000	100000	0.562	0.208	0.591	0.015

Table C.23: Value of Shear Stress and interfacial Friction Factor for Various Values of Re_{sL} and Re_{sg} at $\alpha=0.7$.

Re_L	Re_{eg}	τ_{wL}	τ_{wg}	τ_l	f_l
60000	10000	1.167	3.301×10^{-3}	1.41	40.222
60000	20000	1.167	0.011	1.407	2.01
60000	40000	1.167	0.04	1.395	0.306
60000	60000	1.167	0.083	1.376	0.117
60000	80000	1.167	0.139	1.352	0.06
60000	100000	1.167	0.208	1.323	0.036

Appendix D

Sample of Calculations

To estimate Sh at $Re_{sL}=20000$ and $Re_{sg}=20000$ at $40\text{ }^\circ\text{C}$ using Eq. (4.58).

The physical properties of air and water are taken from Perry and Chilton [1997].

At $40\text{ }^\circ\text{C}$

$$\rho_L \text{ of water} = 991.5 \text{ kg/m}^3$$

$$\rho_g \text{ of air} = 1.2 \text{ kg/m}^3$$

$$\mu_L \text{ of water} = 0.645 \times 10^{-3} \text{ kg/m.s}$$

$$\mu_g \text{ of air} = 1.9 \times 10^{-5} \text{ kg/m.s}$$

$$\text{Diffusivity of O}_2 \text{ in water (D}_L) = 3 \times 10^{-9} \text{ m}^2/\text{s}$$

$$\text{Diffusivity of O}_2 \text{ in air (D}_g) = 3 \times 10^{-5} \text{ m}^2/\text{s}$$

$$Sc_L = \frac{\mu_L}{\rho_L D_L} = 216.1$$

$$u_{sL} = \frac{Re_{sL} \mu_L}{\rho_L d} = 0.13 \text{ m/s}$$

$$u_{sL} = \frac{Re_{sL} \mu_L}{\rho_L d} = 3.167$$

The void fraction is obtained from Eq. (3.43)

$$\alpha = \left[1 + \left(\frac{1-x}{x} \right) \left(\frac{\rho_g}{\rho_L} \right) \left(\frac{\rho_L}{\rho_m} \right)^{0.5} \right]^{-1} \quad (3.43)$$

with

$$x = \frac{\rho_g u_{sg}}{\rho_g u_{sg} + \rho_g u_{sg}} \quad (4.11)$$

$$= 0.029$$

$$\rho_m = \frac{1}{\frac{1-x}{\rho_L} + \frac{x}{\rho_g}} \quad (4.10)$$

$$= 40.28 \text{ kg/m}^3$$

Hence from Eq. (3.43)

$$\alpha = 0.831$$

The liquid layer height is

$$h_L = (1 - \sqrt{\alpha})R \quad (4.32)$$

$$h_L = (1 - \sqrt{0.831}) \times 0.05 = 0.00443 \text{ m} = 0.443 \text{ cm}$$

The hydraulic diameter

$$d_{hL} = \frac{4(1-\alpha)\frac{\pi d^2}{4}}{\pi d} = (1-\alpha)d \quad (4.33)$$

$$= (1-0.831) \times 0.1 = 0.017 \text{ m} = 1.7 \text{ cm}$$

The thickness of diffusion layer

$$\delta = 25 \text{Re}_{sL}^{-7/8} d_{hL} \quad (4.50)$$

$$\delta = 7.299 \times 10^{-5} \text{ m}$$

$$Z_2 = h_L/R = 0.089$$

$$Z_1 = \delta/R = 1.46 \times 10^{-4}$$

$$B = 0.012 \text{Re}_{sg}^{0.8} / z_2 \quad (4.54)$$

$$B = 0.012(20000)^{0.8} / 0.089 = 373$$

$$A = B/z_1^2 = 0.012 \text{Re}_{sg}^{0.8} / z_1^2 z_2 \quad (4.55)$$

$$A = 1.754 \times 10^8$$

By substitution of above values in Eq. (4.67):

D-2

$$Sh = \frac{Sc_L d_{hL}/R}{\int_0^{z_1} \frac{dz}{\left(\frac{1}{Sc_L} + Az^3\right)} + \int_{z_1}^{z_2} \frac{dz}{\left(\frac{1}{Sc_L} + Bz\right)} + \int_{z_2}^1 \frac{\frac{D_L Sc_L}{D_g Sc_g} dz}{\left(\frac{1}{Sc_g} + 0.012 Re_{sg}^{0.8}\right)}}$$

and performing the integration, Sh= 813.

الخلاصة

تم اجراء دراسة نظرية لتحليل انتقال الكتلة والاجهاد القصي لجريان اضطرابي ثنائي الطور غاز سائل (هواء- ماء) باتجاه واحد في انبوب افقي باستخدام مفهوم الانتشارية الدوامية. تم حساب ومناقشة معامل انتقال الكتلة لمديات واسعة من عدد رينولدز الظاهري للسائل والغاز وعدد شممت للسائل ودرجة الحرارة. كذلك تمت دراسة وحساب الاجهادات القصية ومعاملات الاحتكاك عند الجدار وعند اسطح البيني للسائل والغاز باستخدام علاقات عملية ونظرية مقترحة للجريان الثنائي الطور. تم تقسيم تغير الانتشارية الدوامية الى منطقتين رئيسيتين الاولى في السائل والثانية في الغاز. كما تم الحصول على نموذج جديد للانتشارية الدوامية باستخدام مبدأ ثلاث مقاوات لانتقال الكتلة على التوالي. تمت دراسة ومناقشة تأثير عدد رينولدز الظاهري للسائل والغاز وعدد شممت للسائل ودرجة الحرارة على معامل انتقال الكتلة. اثبتت صحة النتائج عن طريق مقارنتها بنتائج عملية لباحثين آخرين مستحصلة من دراسة التاكل تحت ظروف جريان اضطرابي ثنائي الطور.

دللت النتائج على ان الانتشارية الدوامية هي طريقة كفوءة للتنبؤ بمعامل انتقال الكتلة. كذلك زيادة عدد رينولدز الظاهري للسائل والغاز يؤدي الى زيادة معامل انتقال الكتلة وزيادة عدد شممت للسائل يؤدي الى زيادة معامل انتقال الكتلة ويكون تأثير عدد شممت للسائل اكبر من تأثير الغاز. كذلك زيادة عدد رينولدز الظاهري للسائل والغاز ودرجة الحرارة يؤثر على الاجهادات القصية ومعامل الاحتكاك.

شكر وتقدير

اولا وقبل كل شيء الحمد والشكر لله على تمام الصحة وقوة الإيمان التي ساعدتني على تخطي جميع الصعاب التي واجهتها طيلة فترة البحث.

اود ان اعبر عن خالص شكري وتقديري وعرفاني بالجميل للمشرف ا.م. د. باسم عبيد حسن لما قدمه لي من اهتمام كبير وجهد بالغ ولما ابداه من توجيهات قيمة ساعدت على انجاز هذا العمل.

لا انسى ان اشكر من رباني على طريق الخير و المعرفة من شرفني بحمل اسمه ابي.

ولا انسى ان اتقدم بجزيل الشكر والتقدير الى رفيق دربي الى من ساندني و وقف الى جانبي طوال فترة البحث زوجي.

ولا انسى اعز من في الوجود امي و اخوتي.

م. عشتار زكي صادق

التنبؤ بمعامل انتقال الكتلة تحت ظروف جريان ثنائي الطور باستخدام نظريات
الانتشار الاضطرابي

رسالة

مقدمة الى كلية الهندسة في جامعة النهريين وهي جزء من متطلبات نيل درجة ماجستير
علوم في الهندسة الكيمياوية

من قبل

عشتار زكي صادق

(بكالوريوس علوم في الهندسة الكيمياوية ٢٠٠٤)

١٤٢٨

ذو الحجة

٢٠٠٨

كانون الثاني